Formation of gene expression patterns in growing tissues

Marcin Zagórski

JAGIELLONIAN UNIVERSITY
IN KRAKÓW

National Science Centre Poland

NAWA
NARODOWA AGENCJA WYMIANY AKADEMICKIEJ

Ministry of Science and Higher Education
Republic of Poland

CSRC

RESEARCH UNIVERSITY
EXCELLENCE INITIATIVE

Development of mouse embryo

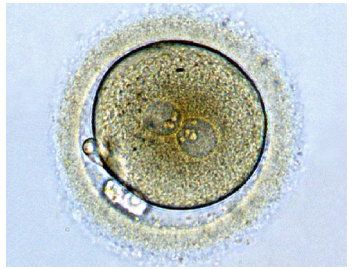

@wikipedia.org

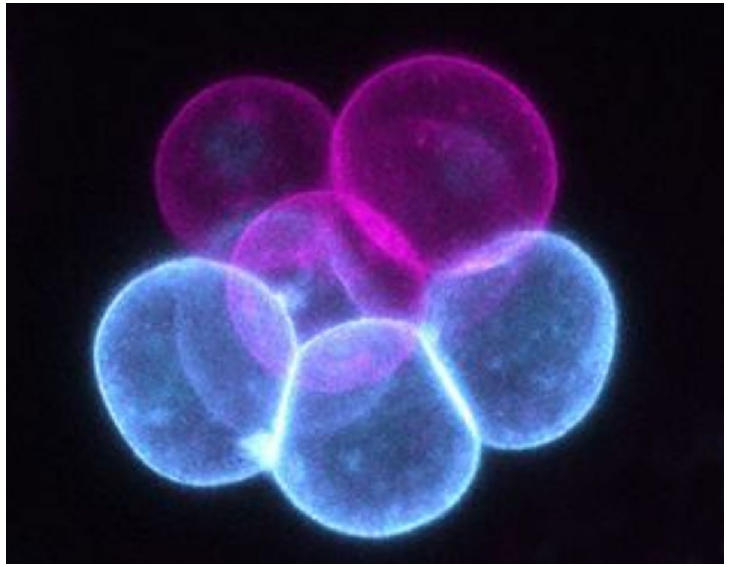

@Recher, et al.., University of Cambridge

@Petersen, Miller. Marine Biological Laboratory in Woods Hole

Morphogen gradients through gene regulatory network specify cell fates

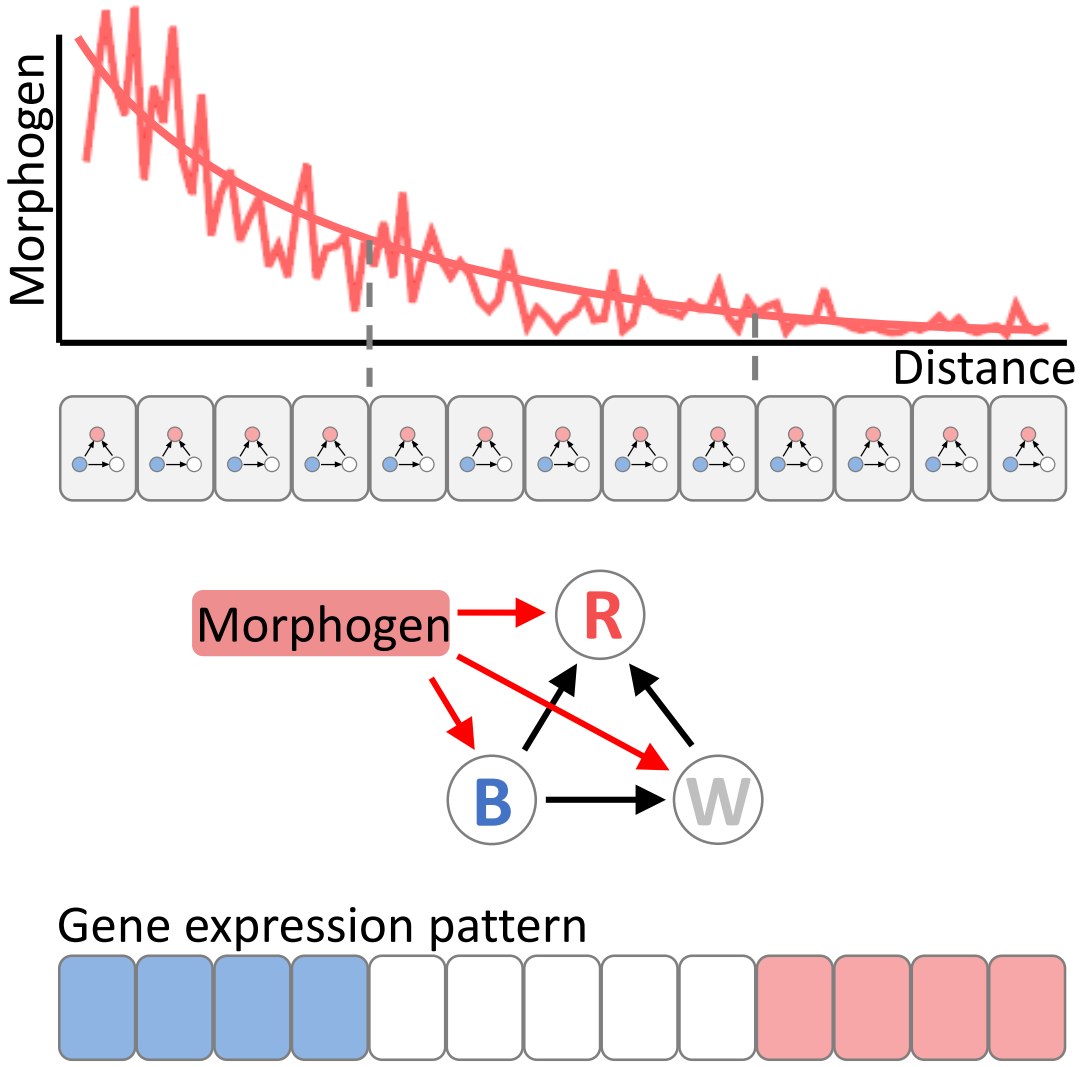

The GRN acts as an information decoder that specifies target pattern

Input signal

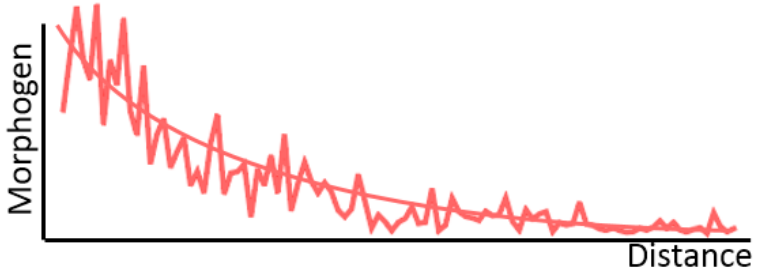

Information decoder

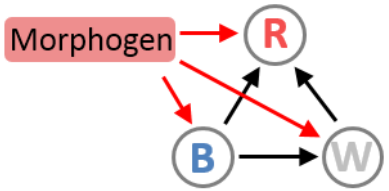

Output signal

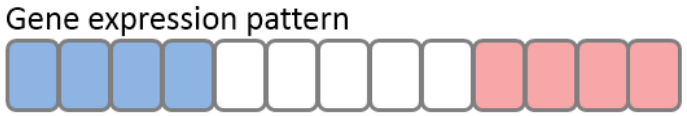

Zagorski et al., Science, 2017
Petkova et al., Cell, 2019
Tkacik & Gregor, Development, 2021

Neural tissue in spinal cord undergoes changes in size and shape over time

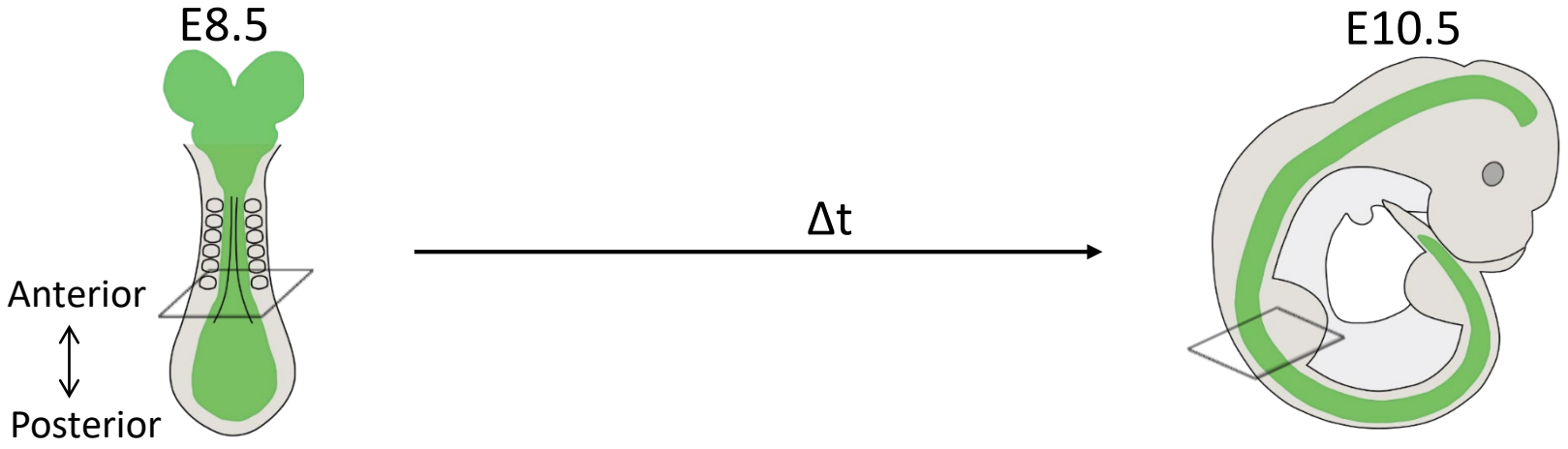

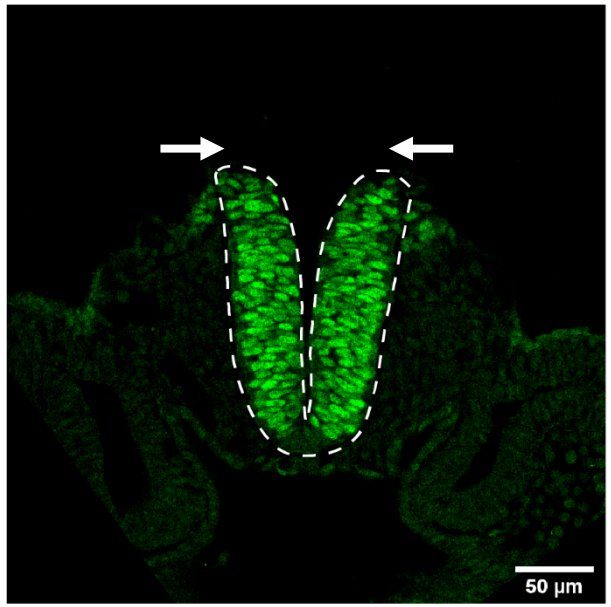

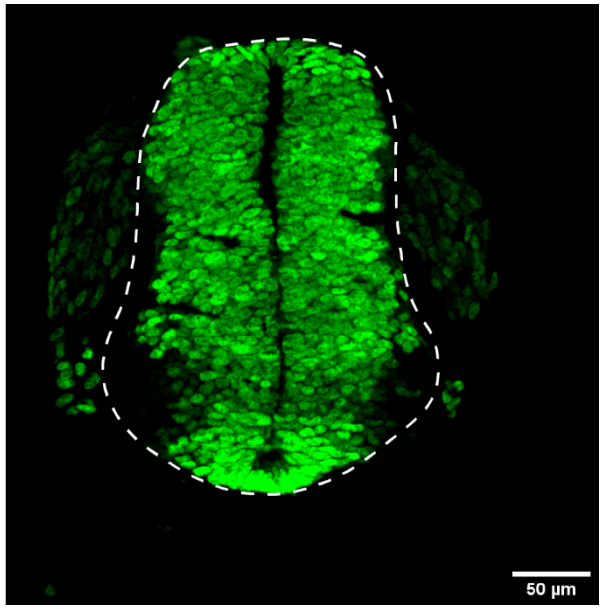

Dorsal

Ventral

@Kicheva Lab

Morphogen signaling gradients establish a striped pattern of neural progenitors

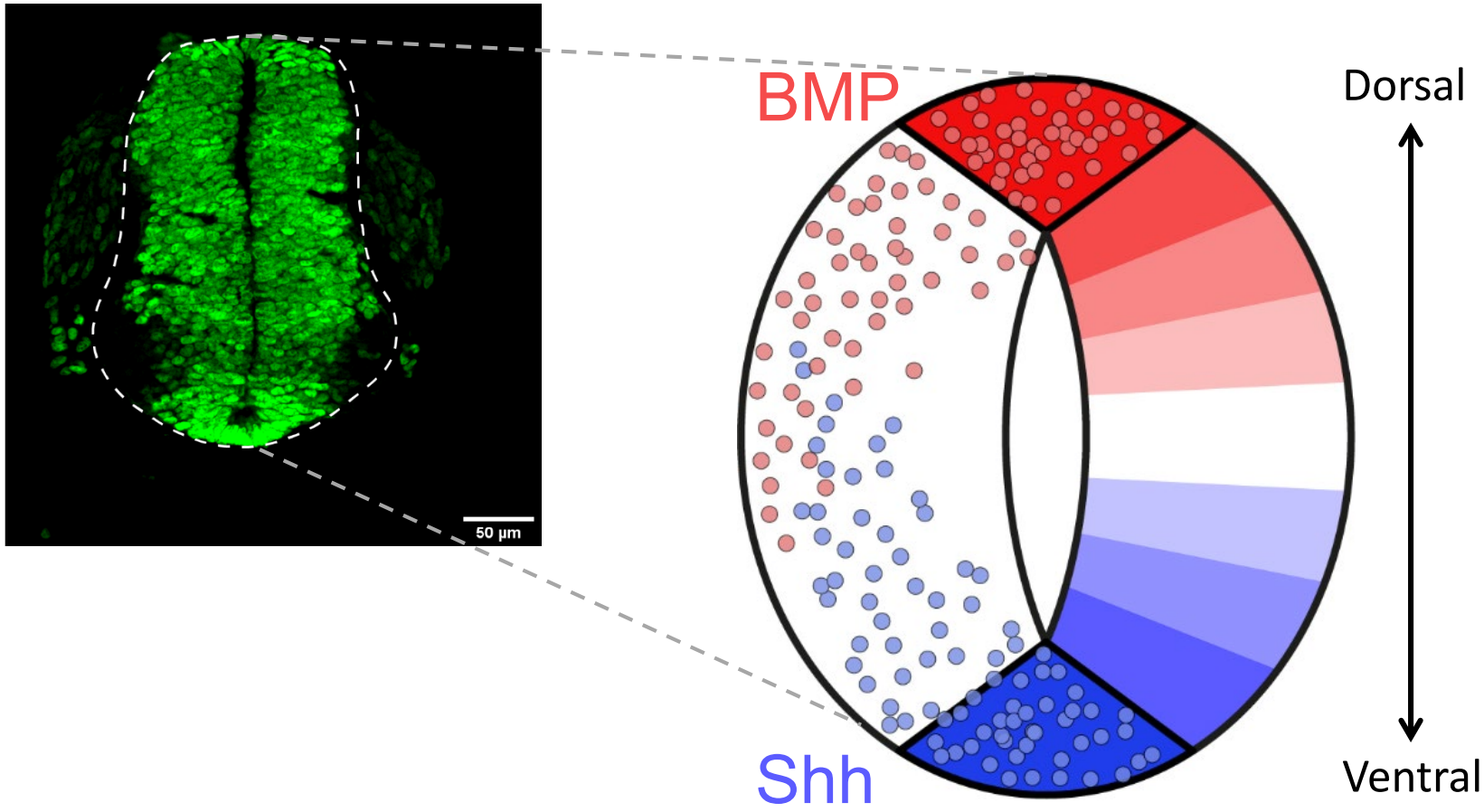

The striped pattern of gene expression domains is formed progressively

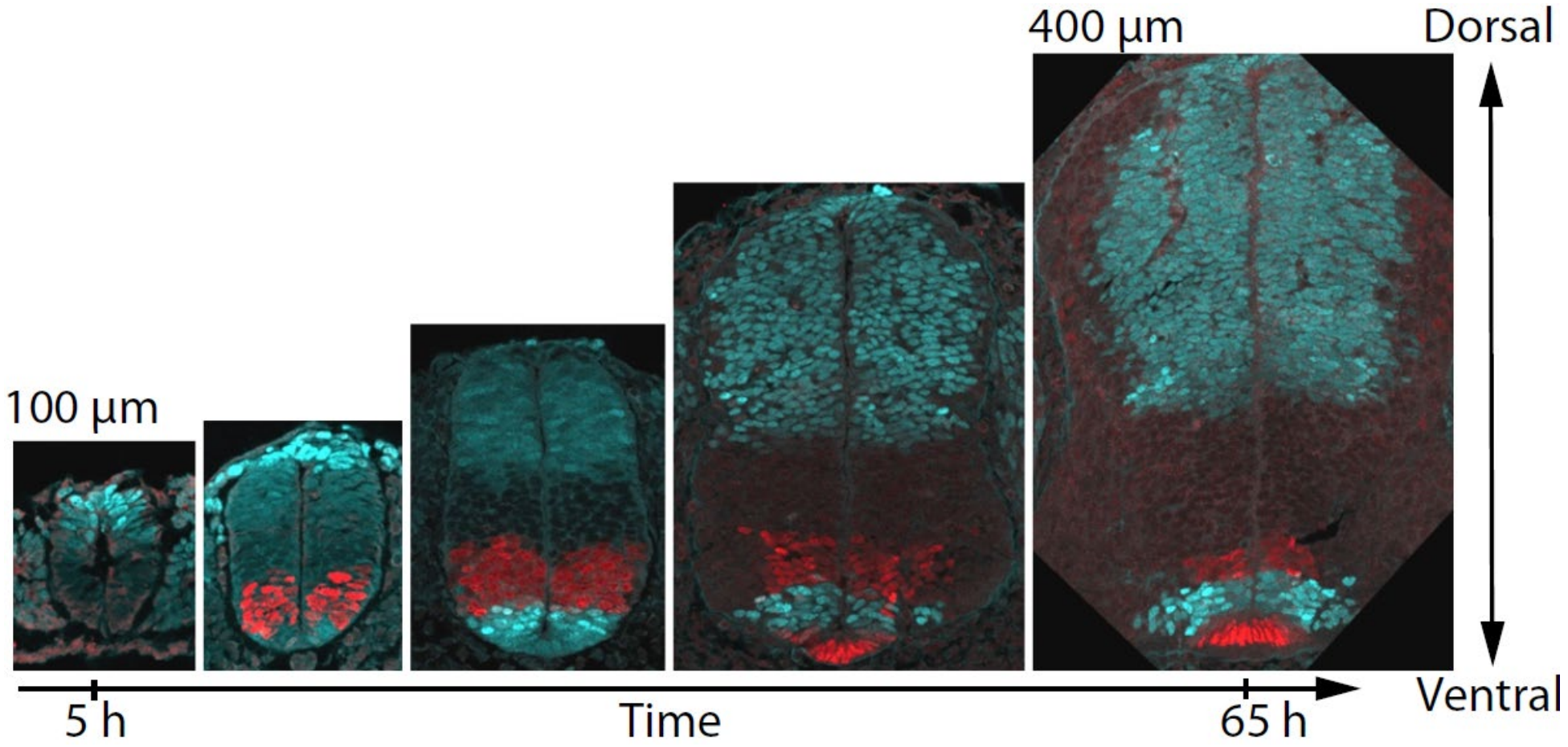

Zagorski et al., Science, 2017

Research questions

- How are morphogens interpreted to result in precise and reproducible patterns?
- How is pattern formation affected by tissue mechanical properties, cellular dynamics, and growth?
- How is morphogen source formed in a growing tissue?
- What are conditions for emergence of stable patterns in tissues?

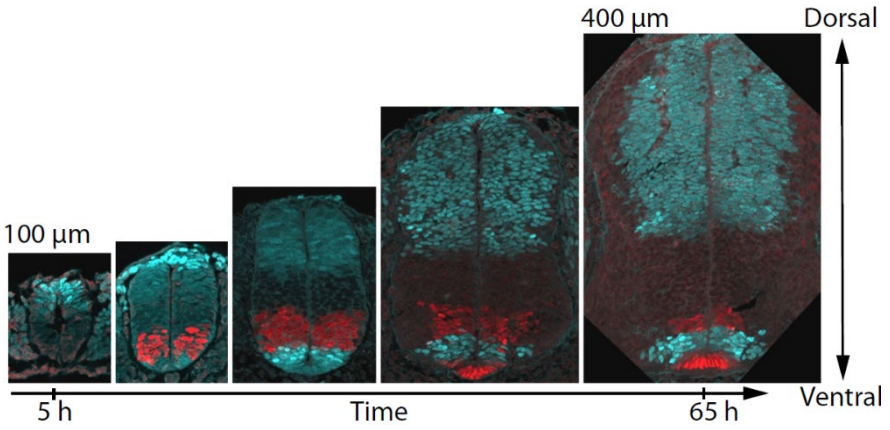

Research questions

- How are morphogens interpreted to result in precise and reproducible patterns?
- How is pattern formation affected by tissue mechanical properties, cellular dynamics, and growth?
- How is morphogen source formed in a growing tissue?
- What are conditions for emergence of stable patterns in tissues?

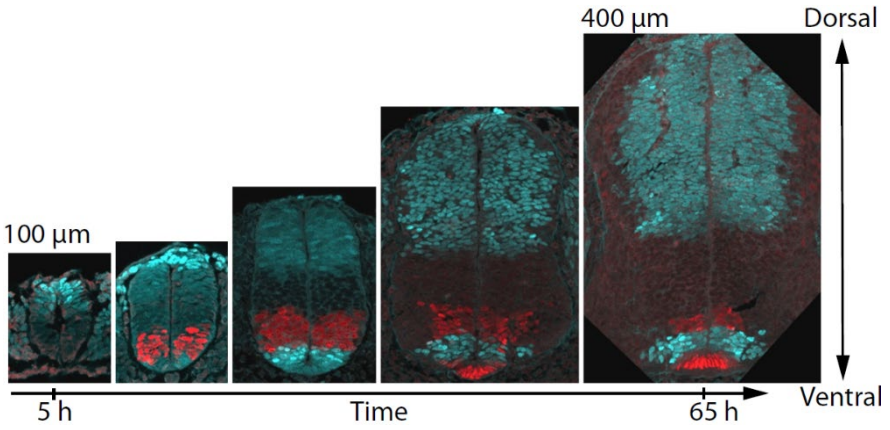

The morphogen signaling profiles do not scale with the embryo size

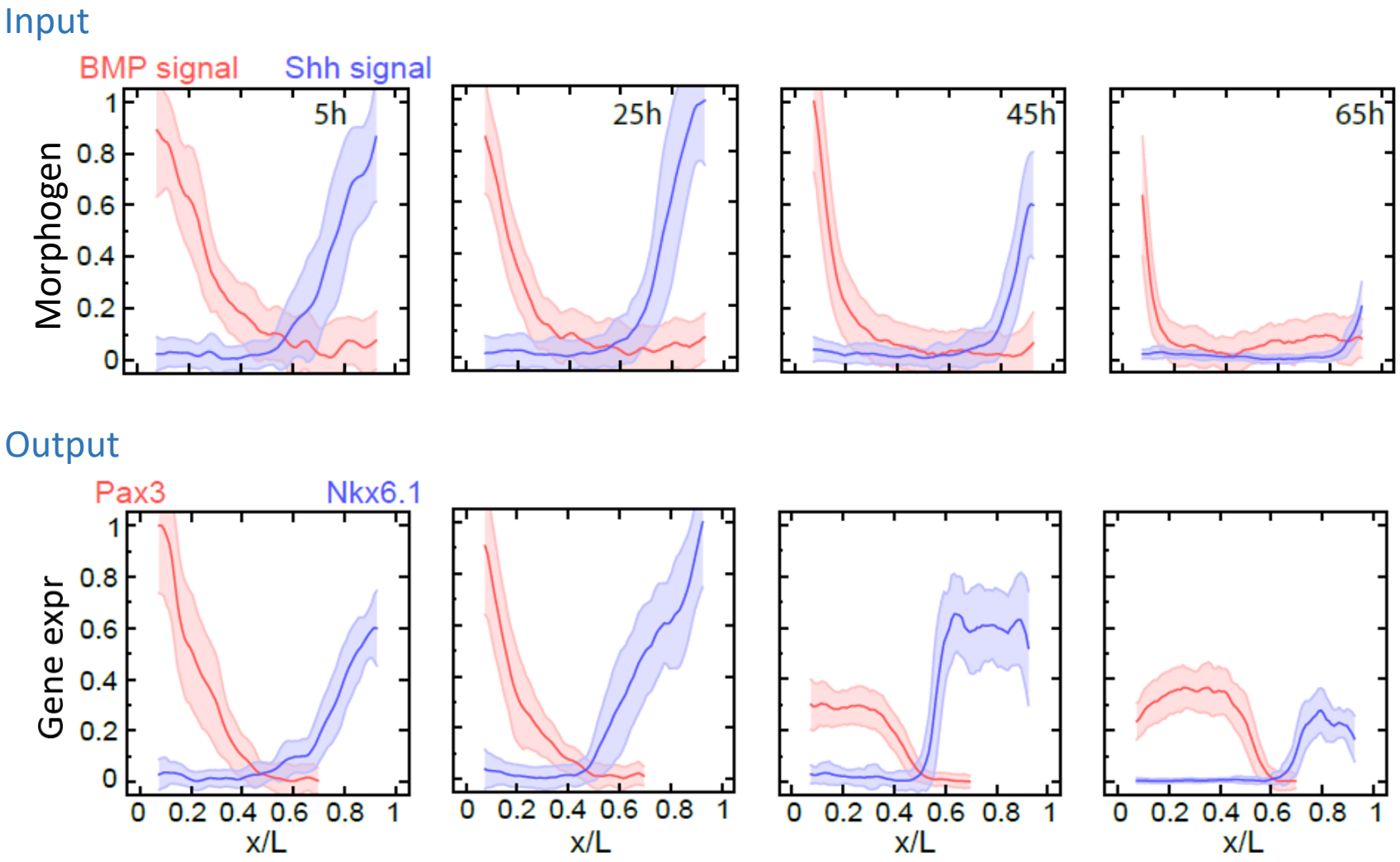

Zagorski et al., Science, 2017

The initial morphogen positional error corresponds to the boundary imprecision at later stages

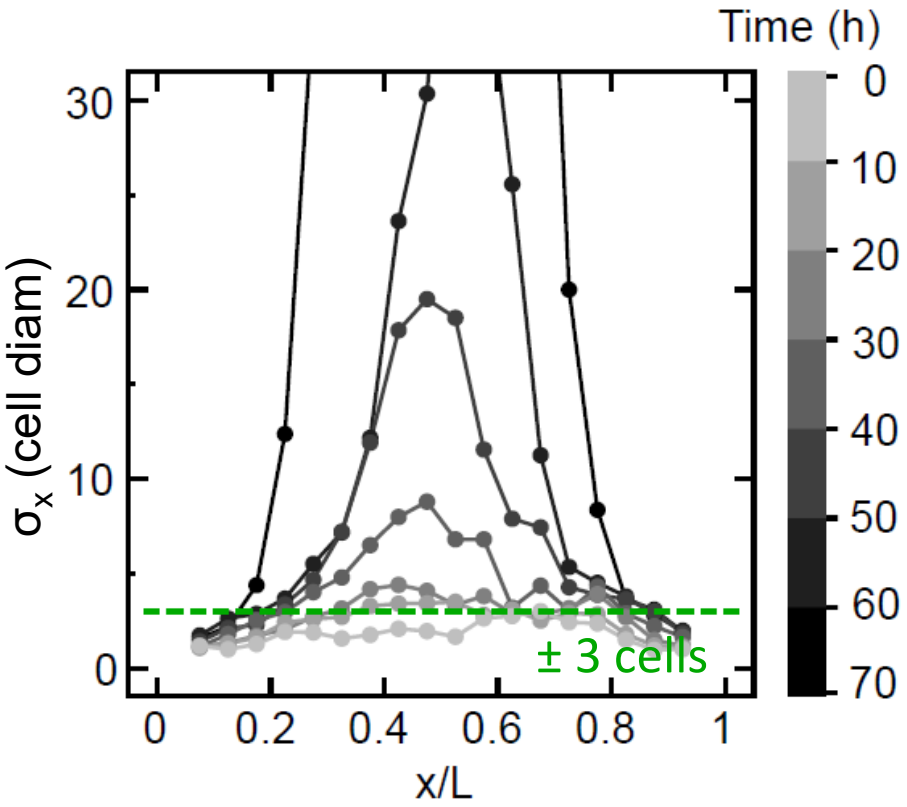

$$\sigma_x(x) = \left[\left(\frac{d[BMP]}{dx}\right)^2 \sigma_{BMP}^{-2} + \left(\frac{d[Shh]}{dx}\right)^2 \sigma_{Shh}^{-2}\right]^{-\frac{1}{2}}$$

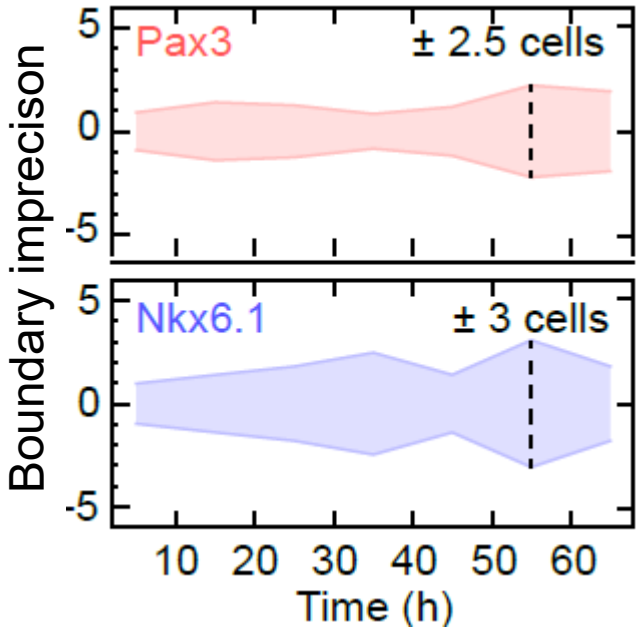

Zagorski et al., Science, 2017

Optimal decoder contains all the information that any cellular or computational mechanism could extract from input signals

Input signal

BMP Shh

$$\{g_i(x)\} = \{g_1(x), g_2(x)\}, \qquad K = 2$$

Signal distribution at every x

$$P(\{g_i\}|x) = \frac{1}{\sqrt{(2\pi)^K \det[\hat{C}(x)]}} \exp\left\{-\frac{1}{2}\sum_{i,j=1}^{K}(g_i - \bar{g}_i(x))(\hat{C}^{-1}(x))_{ij}(g_j - \bar{g}_j(x))\right\}$$

Optimal decoder from Bayes' rule

$$P(x^*|\{g_i\}) = \frac{1}{Z(\{g_i\})} P(\{g_i\}|x^*) P_X(x^*)$$

Tkacik et al., Genetics, 2015: formalism
Zagorski et al., Science, 2017: mouse spinal cord, K = 2
Petkova et al., Cell, 2019: fruit fly, K = 4
Tkacik & Gregor, Development 2021: review

Cells interpret the opposing morphogen signals using an optimal decoding strategy

$P(x^*|\{g_1, g_2\})$:

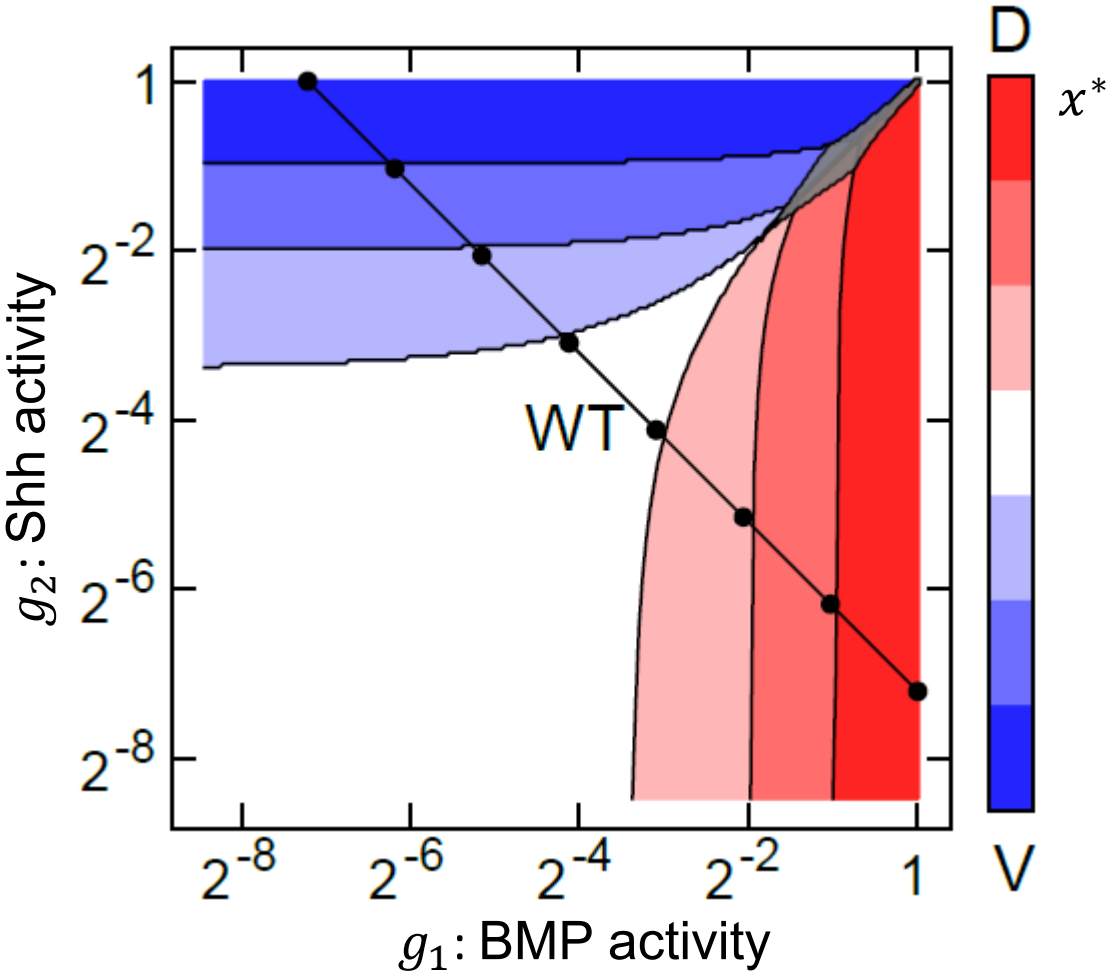

Zagorski et al., Science, 2017

The decoding map predicts the correct shifts of gene expression domains in mutant with reduced Shh

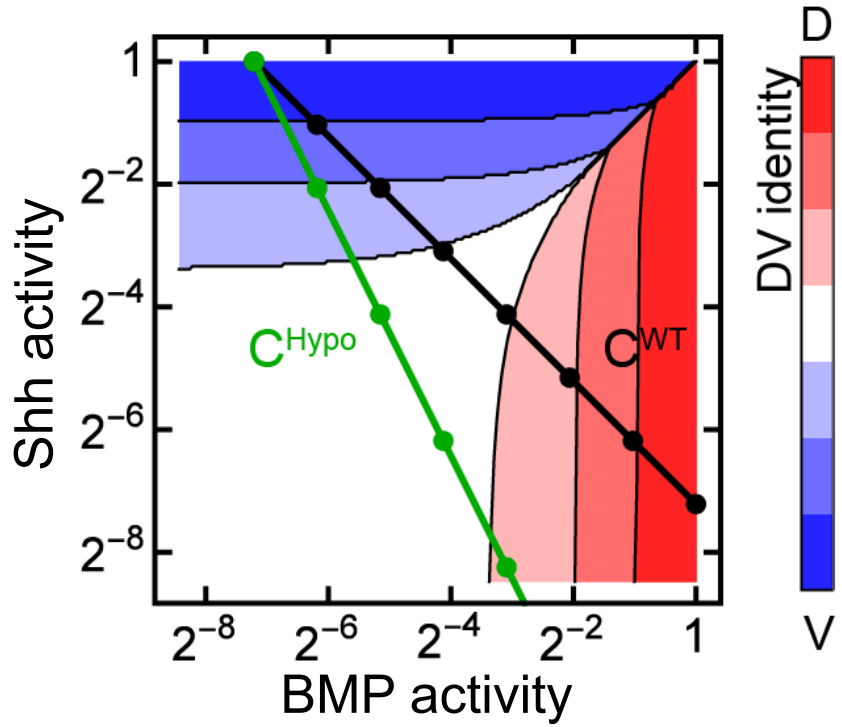

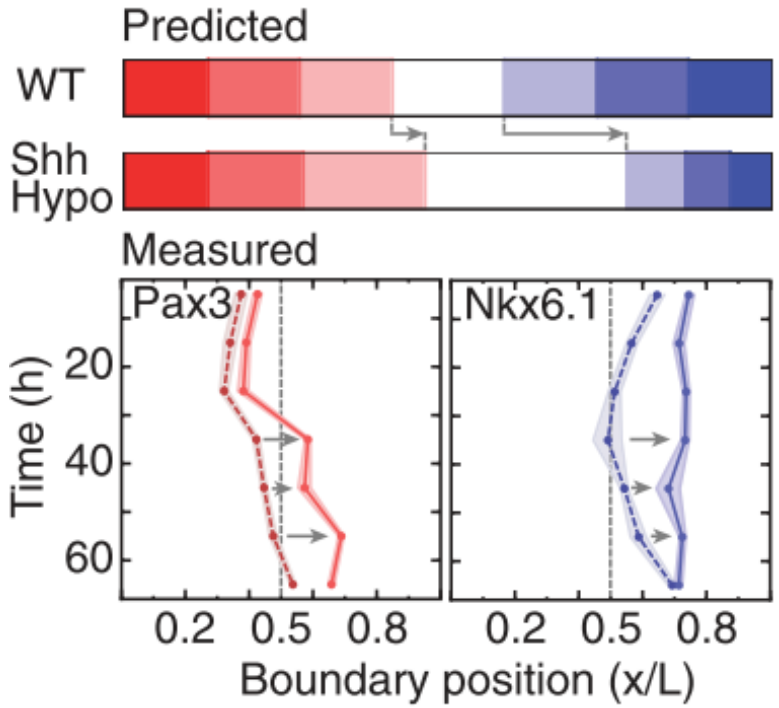

Zagorski et al., Science, 2017

Decoding map predicts bimodal *posterior* distribution of cell fates for high morphogen concentrations

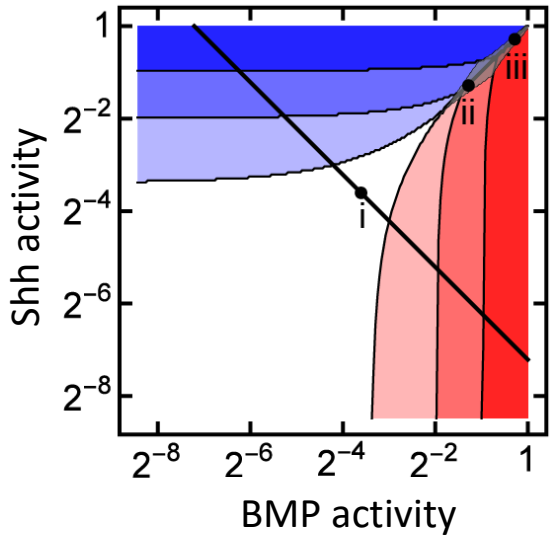

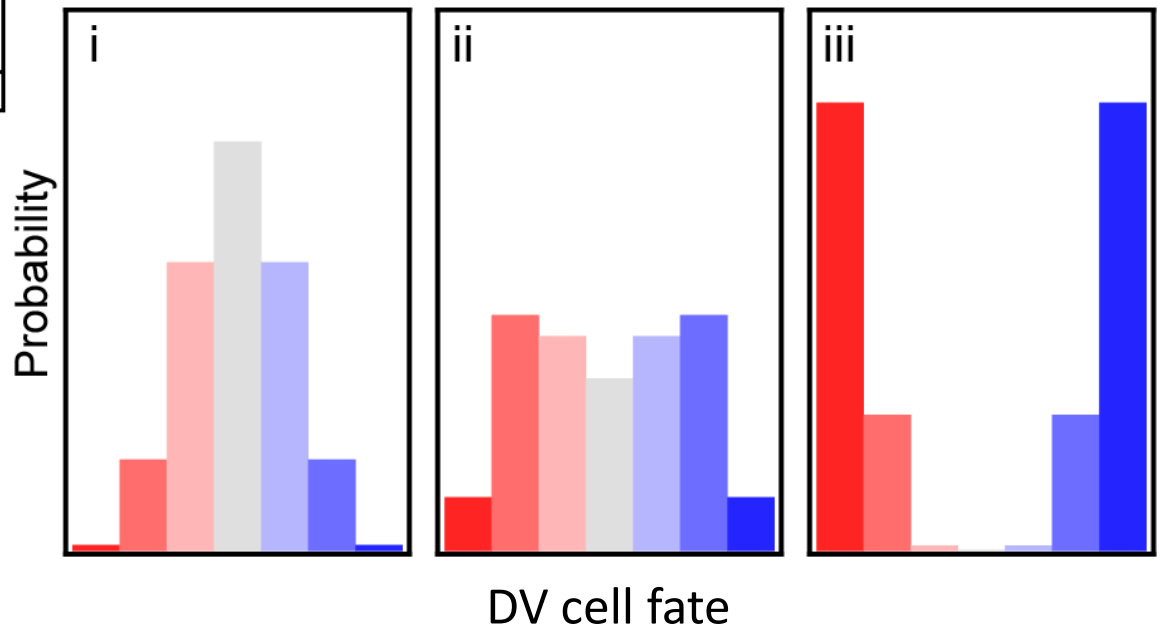

Zagorski et al., Science, 2017

The predicted bimodal distribution of cell fates is consistent with explant experiments

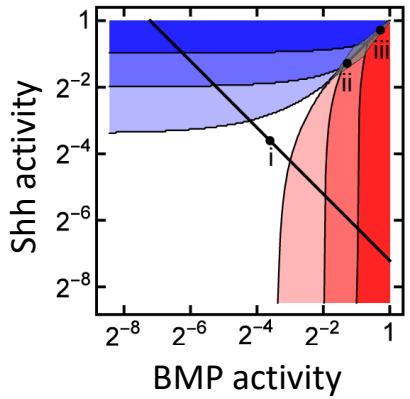

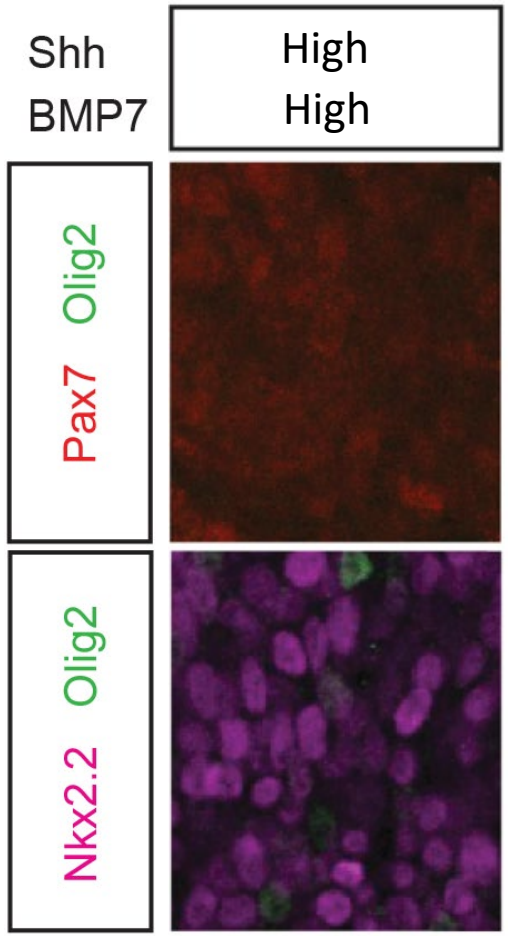

Red cells: Dorsal fates

Green cells: Intermediate fates

Violet cells: Ventral fates

Green cells: Intermediate fates

Zagorski et al., Science, 2017

The morphogens activate gene regulatory network to specify cell fate

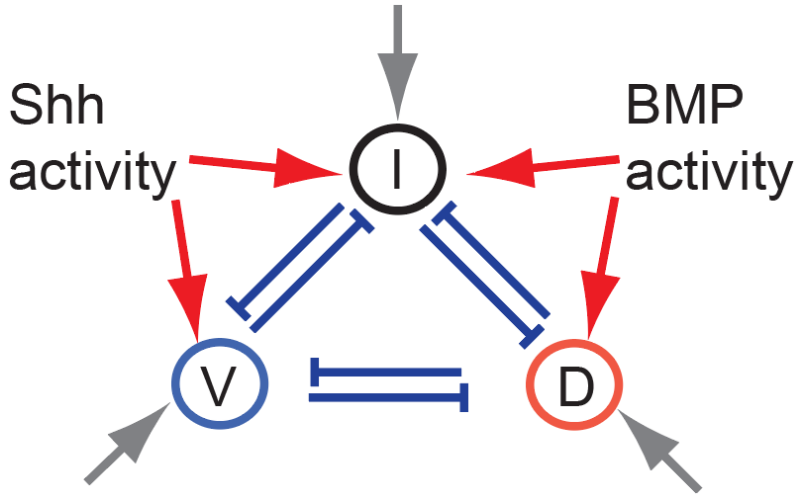

D: Pax3
I: Dbx2
V: Nkx6.1

$$\frac{d[D]}{dt} = \alpha_D \frac{\kappa_D + c_{B\to D}\kappa_D\,[BMP]}{(1 + K_{V\to D}[V])^{m_{V\to D}}(1 + K_{I\to D}[I])^{m_{I\to D}} + \kappa_D + c_{B\to D}\kappa_D\,[BMP]} - \gamma_D[D]$$

$$\frac{d[V]}{dt} = \alpha_V \frac{\kappa_V + c_{S\to V}\kappa_V\,[Shh]}{(1 + K_{D\to V}[D])^{m_{D\to V}}(1 + K_{I\to V}[I])^{m_{I\to V}} + \kappa_V + c_{S\to V}\kappa_V\,[Shh]} - \gamma_V[V]$$

$$\frac{d[I]}{dt} = \alpha_I \frac{\kappa_I + c_{S\to I}\kappa_I\,[Shh] + c_{B\to I}\kappa_I\,[BMP]}{(1 + K_{D\to I}[D])^{m_{D\to I}}(1 + K_{V\to I}[I])^{m_{V\to I}} + \kappa_I + c_{S\to I}\kappa_I\,[Shh] + c_{B\to I}\kappa_I\,[BMP]} - \gamma_I[I]$$

Zagorski et al., Science, 2017

Computational screen resulted in a set of successful GRNs consistent with experimental observations

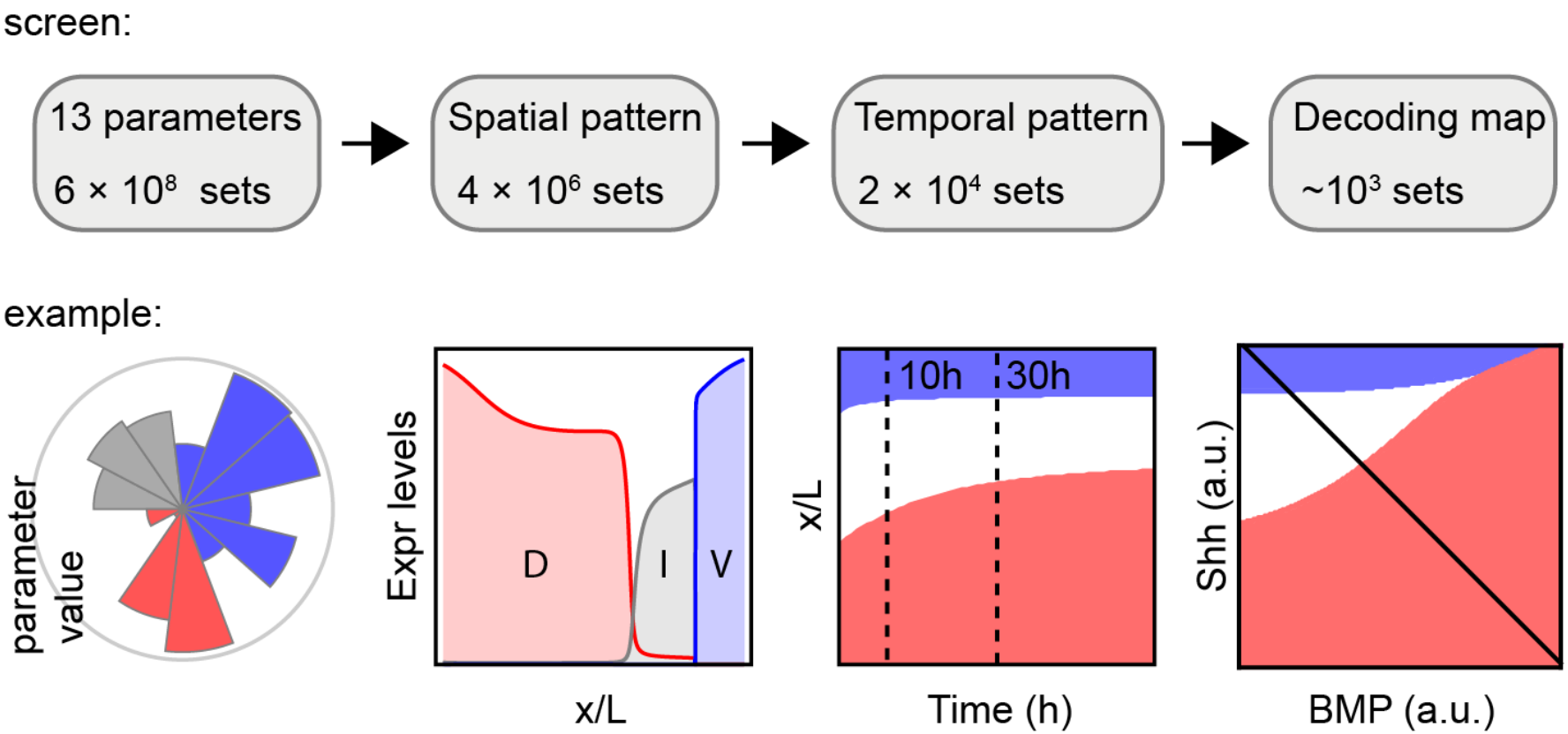

Zagorski et al., Science, 2017

The target gene pattern established by GRNs resulted in a wide range of boundary imprecision

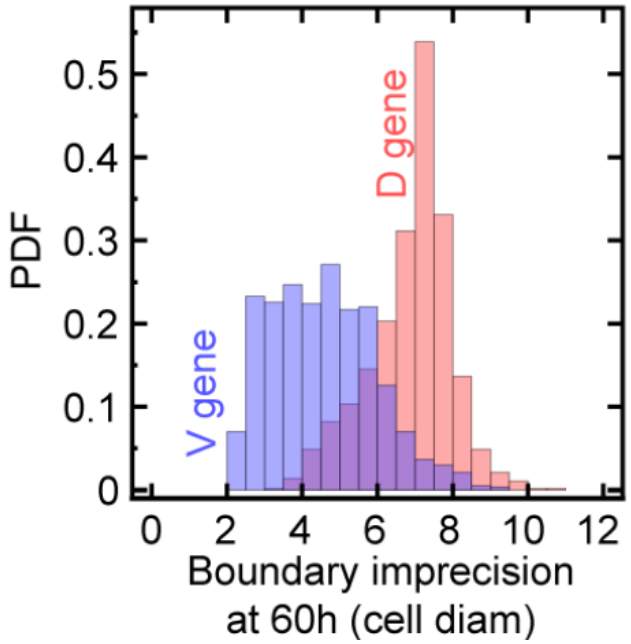

Zagorski et al., Science, 2017

Research questions

- How are morphogens interpreted to result in precise and reproducible patterns?
- How is pattern formation affected by tissue mechanical properties, cellular dynamics, and growth?
- How is morphogen source formed in growing tissue?
- What are conditions for emergence of stable patterns in tissues?

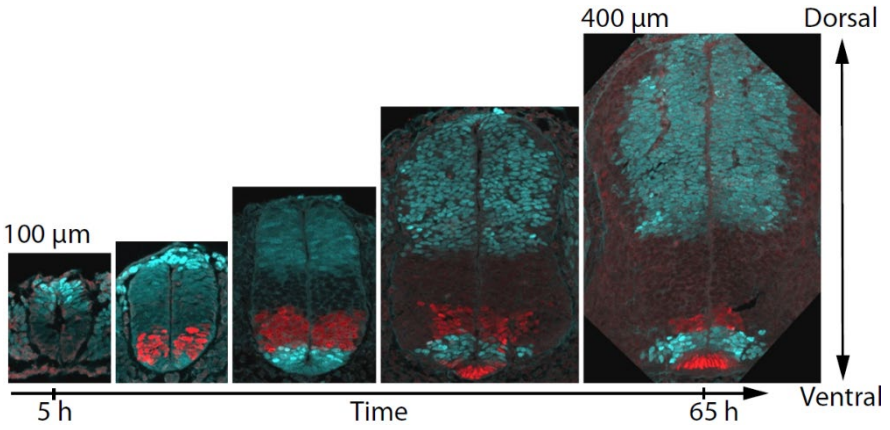

Clonal cell populations disperse differently at different developmental stages

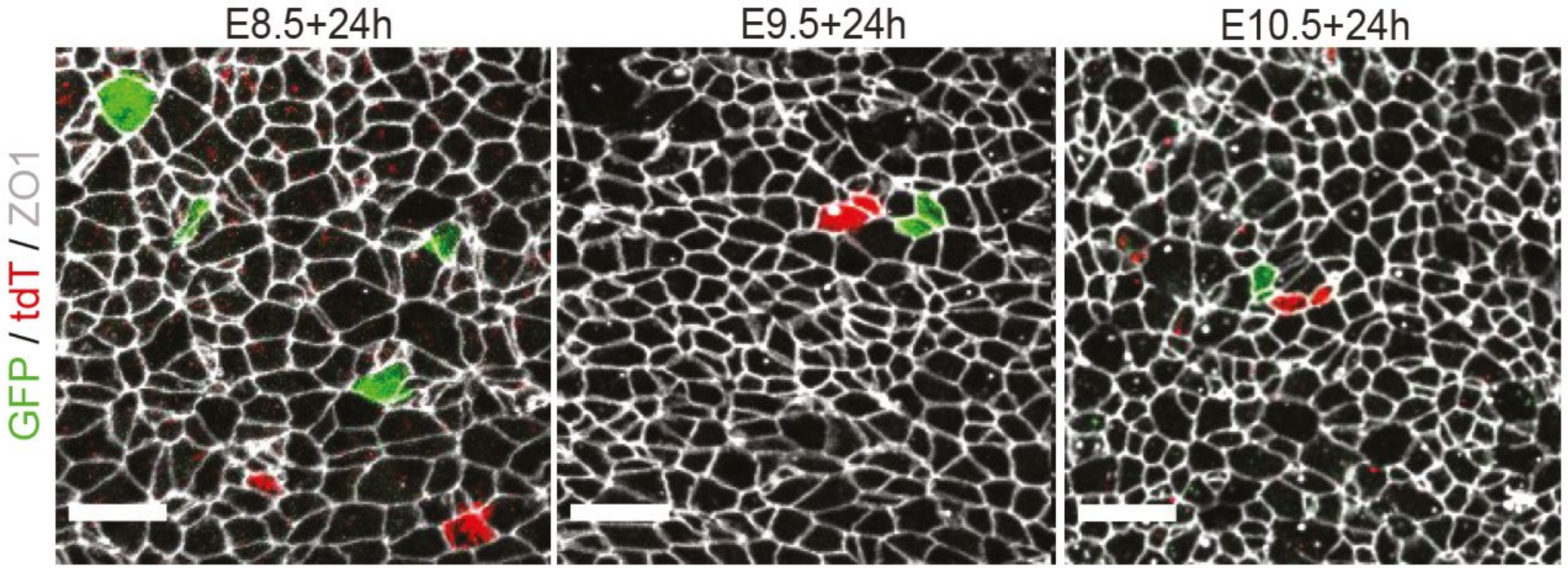

Bocanegra-Moreno et al., Nature Physics, 2023

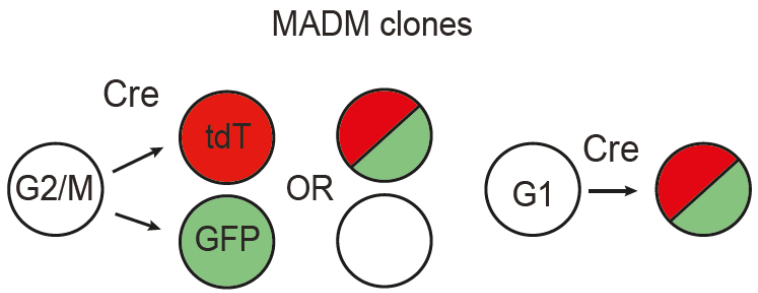

Hippenmeyer et al., Neuron 2010

Green and red cells – single clone

The number of clone fragments is higher at early developmental stages than at later stages

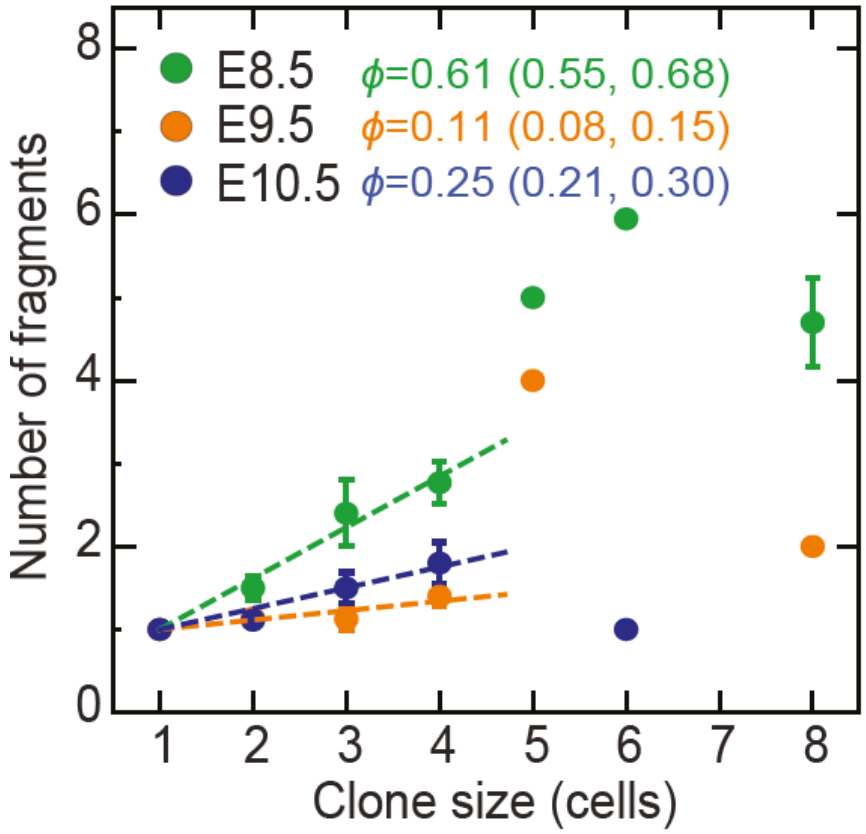

E8.5

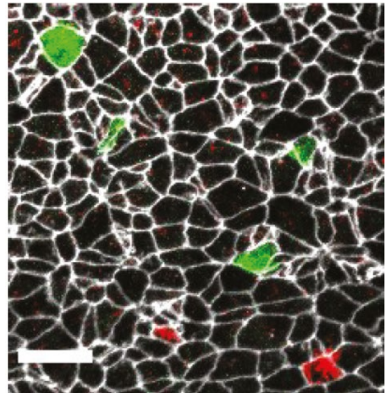

E10.5

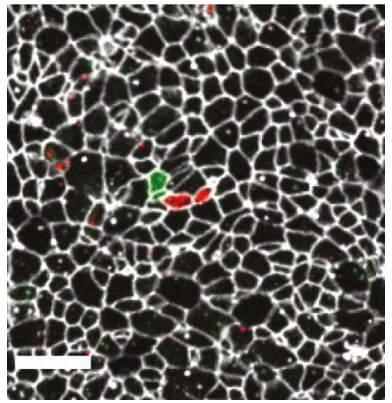

Bocanegra-Moreno et al., Nature Physics, 2023

Vertex model: movement of each cell is governed by movement of its vertices

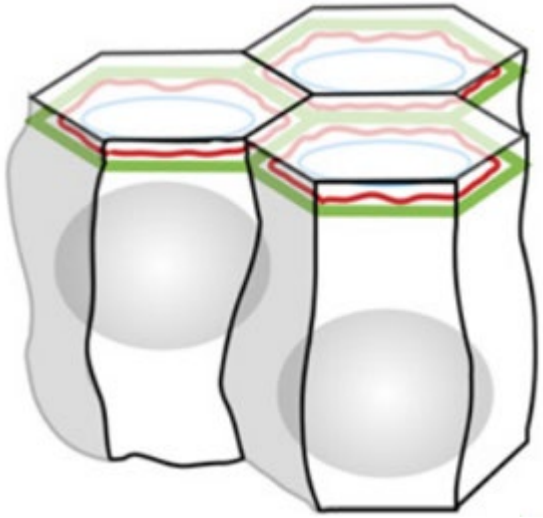

Actin
Cadherin
Myosin

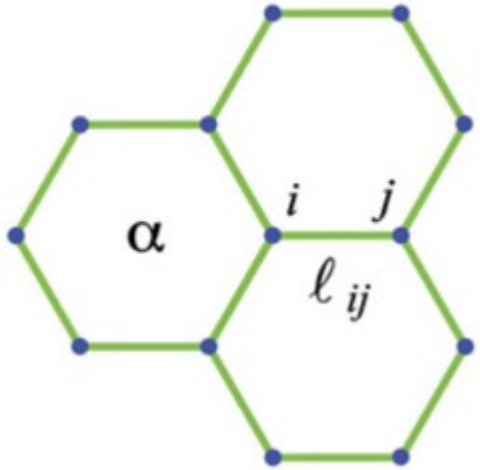

$$E(\boldsymbol{r_i}) = \sum_{\alpha} \frac{K_\alpha}{2}(A_\alpha - A_\alpha^0(t))^2 + \sum_{<i,j>} \Lambda_{ij} l_{ij} + \sum_{\alpha} \frac{\Gamma_\alpha}{2} L_\alpha^2$$

Elastic term | Line tension | Contractility

$$\boldsymbol{F_i} = -\frac{\partial E}{\partial \boldsymbol{r_i}}$$

$$\mu \frac{d\boldsymbol{r_i}}{dt} = \boldsymbol{F_i}$$

Farhadifar et al., Current Biology, 2007
Guerrero et al., Development 2019
Bocanegra-Moreno et al., Nature Physics, 2023

Vertex model ground state changes from fluid-like to solid-like with increasing tension and contractility

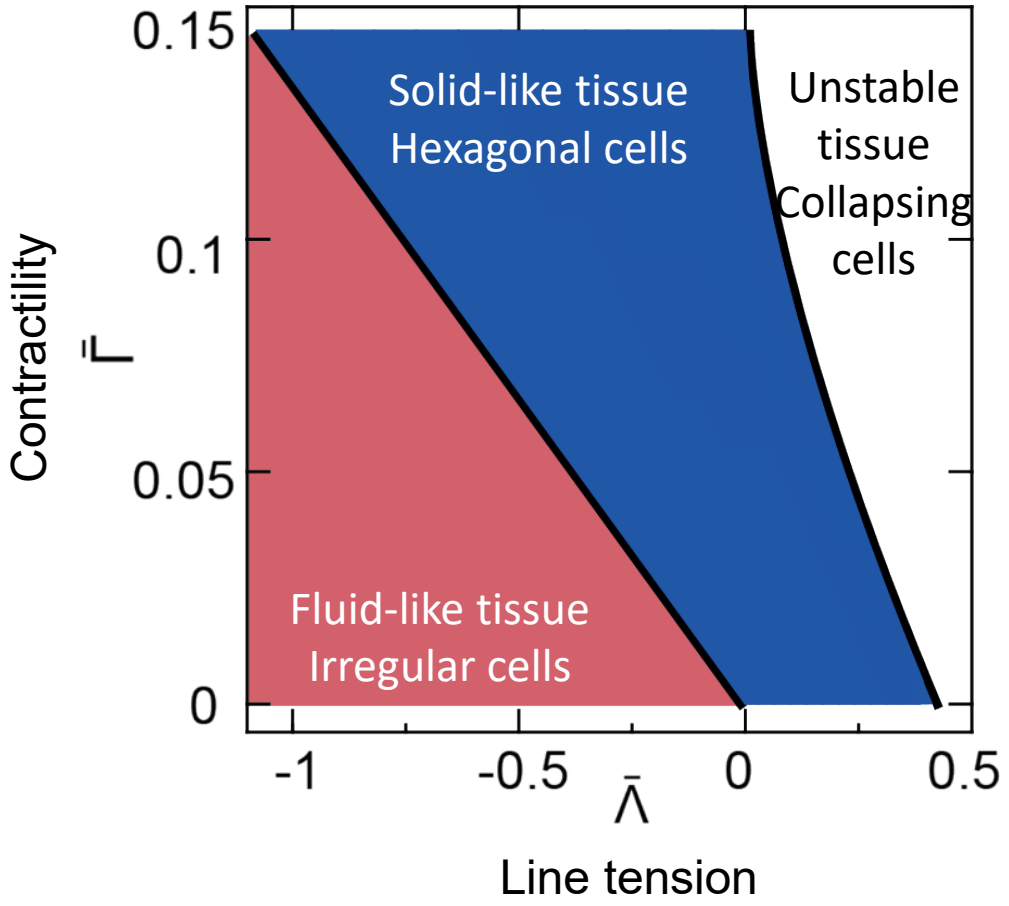

$$K_\alpha = K$$
$$\Lambda_{ij} = \Lambda$$
$$\Gamma_\alpha = \Gamma$$

$$A_\alpha^0(t) = A^0$$

$$\bar{\Lambda} = \Lambda K^{-1}(A^0)^{-3/2}$$
$$\bar{\Gamma} = \Gamma K^{-1}(A^0)^{-1}$$

Farhadifar et al., Current Biology, 2007

The classic formulation of vertex model could not reproduce experimental fragmentation

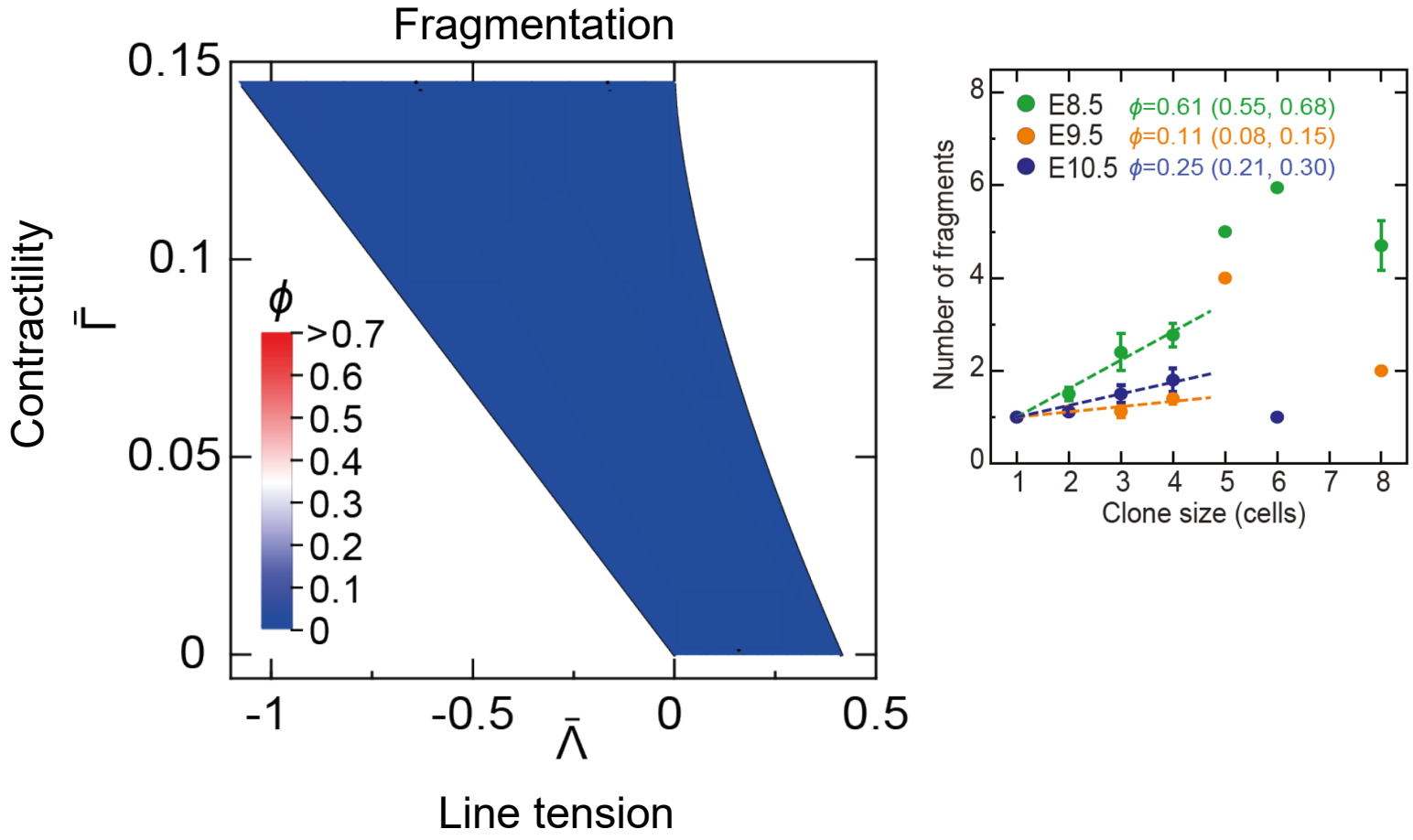

Bocanegra-Moreno et al., Nature Physics, 2023

Including noise in the line tension and interkinetic nuclear movement (IKNM) increased fragmentation

+ noise in Λ_{ij}
+ cell area kinetics by $A_\alpha^0(t)$

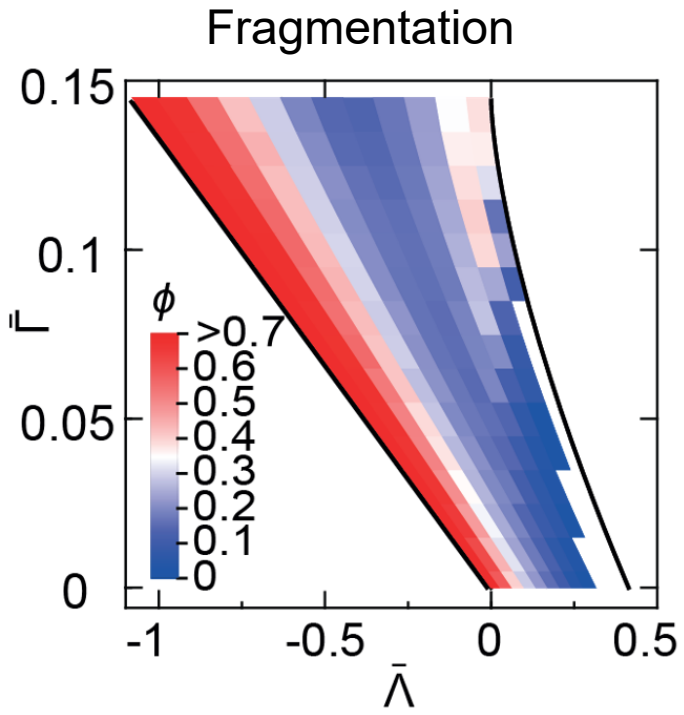

Bocanegra-Moreno et al., Nature Physics, 2023

Different levels of clone fragmentation were associated with different levels of cellular rearrangements (T1 transitions)

+ noise in Λ_{ij}
+ cell area kinetics by $A_\alpha^0(t)$

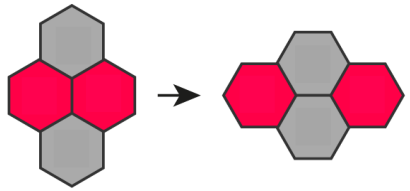

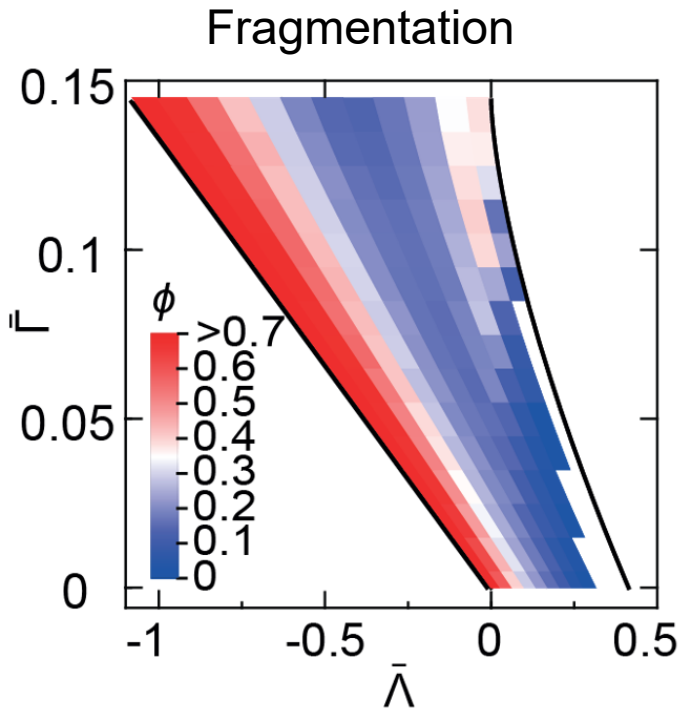

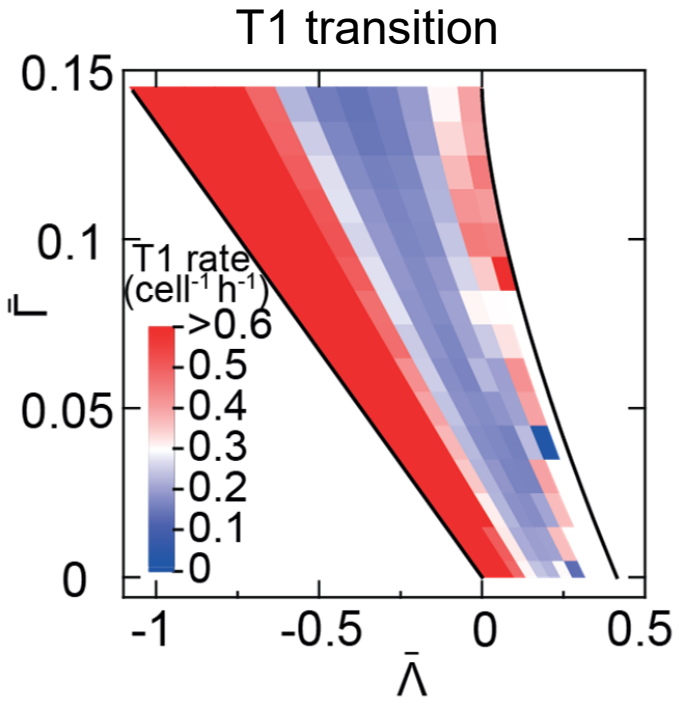

Bocanegra-Moreno et al., Nature Physics, 2023

Sub-region C is a novel region characterized by high levels of cell rearrangements

+ noise in Λ_{ij}
+ cell area kinetics by $A_\alpha^0(t)$

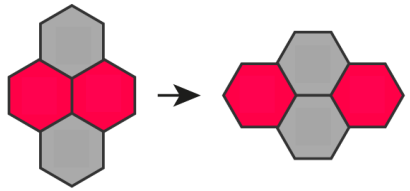

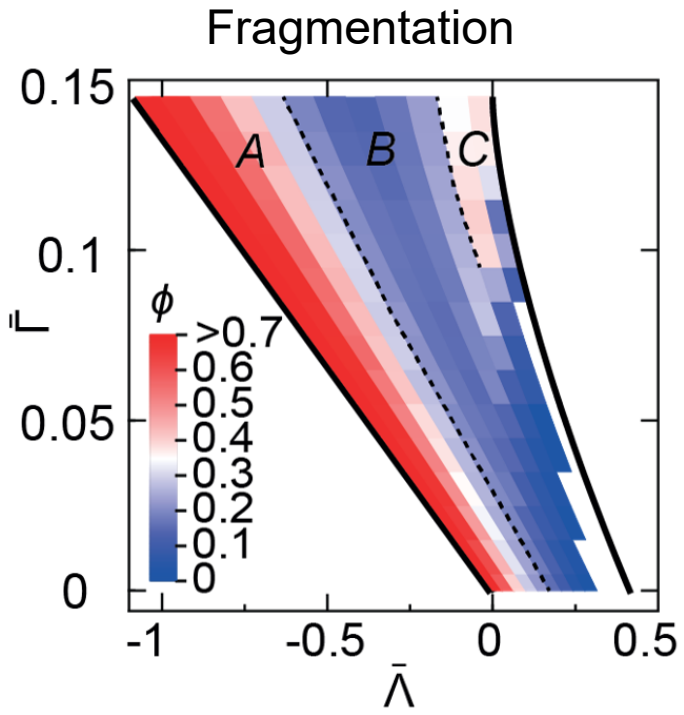

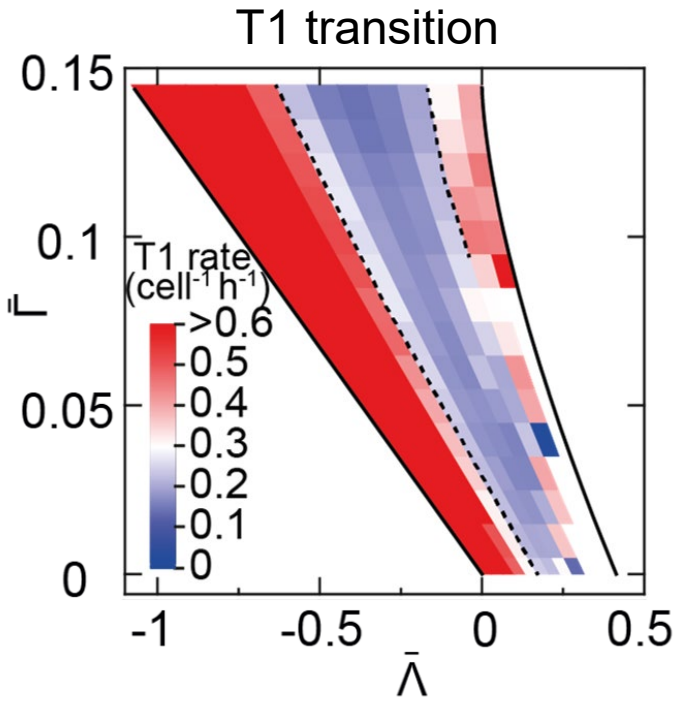

Bocanegra-Moreno et al., Nature Physics, 2023

Vertex model simulation of tissue in sub-region B

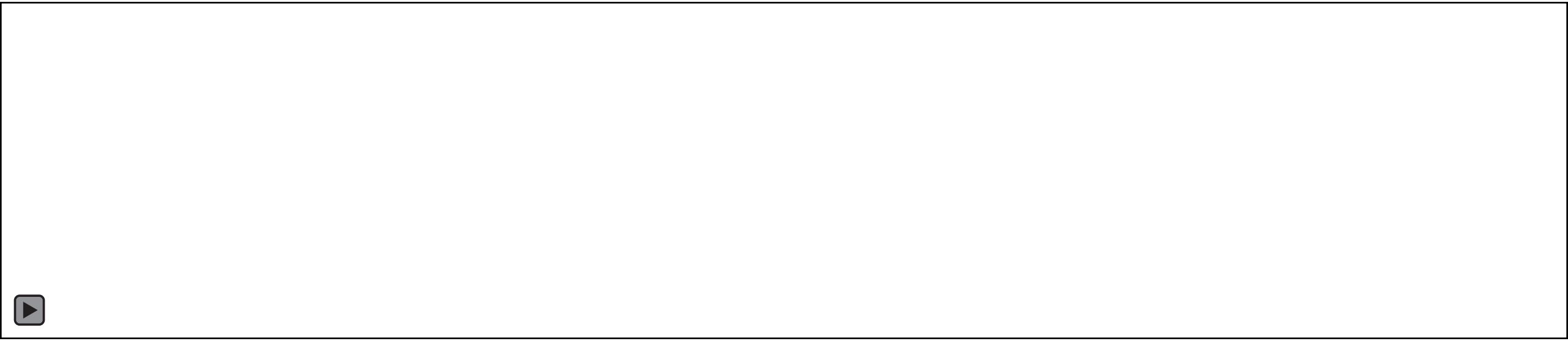

Bocanegra-Moreno et al., Nature Physics, 2023

Vertex model simulation of tissue in sub-region C

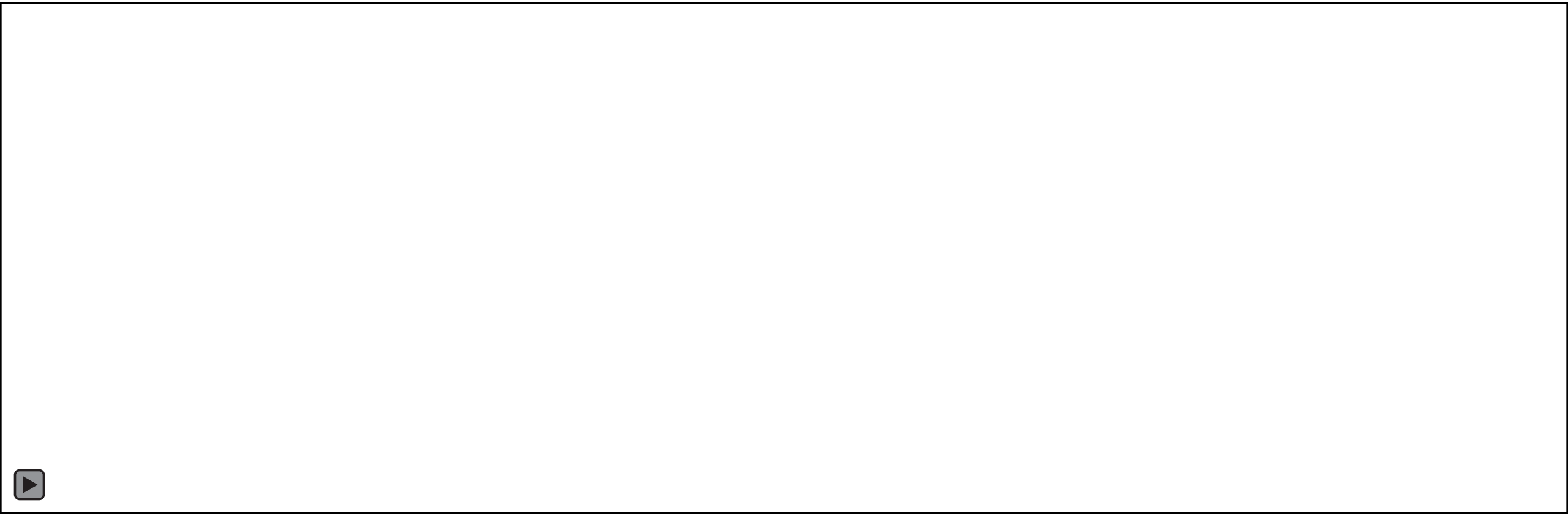

Bocanegra-Moreno et al., Nature Physics, 2023

Vertex model simulation of tissue in sub-region A

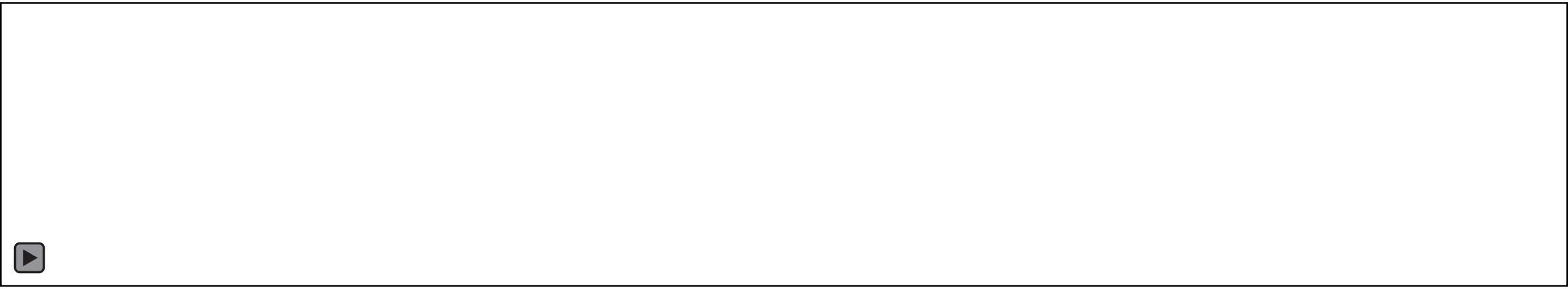

Bocanegra-Moreno et al., Nature Physics, 2023

Cell area variability is high only in sub-region C

Sub-region A

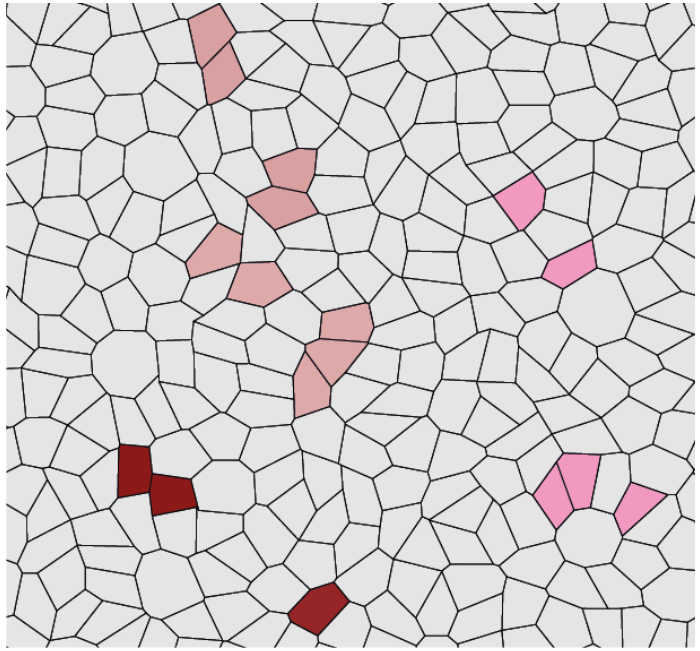

Sub-region B

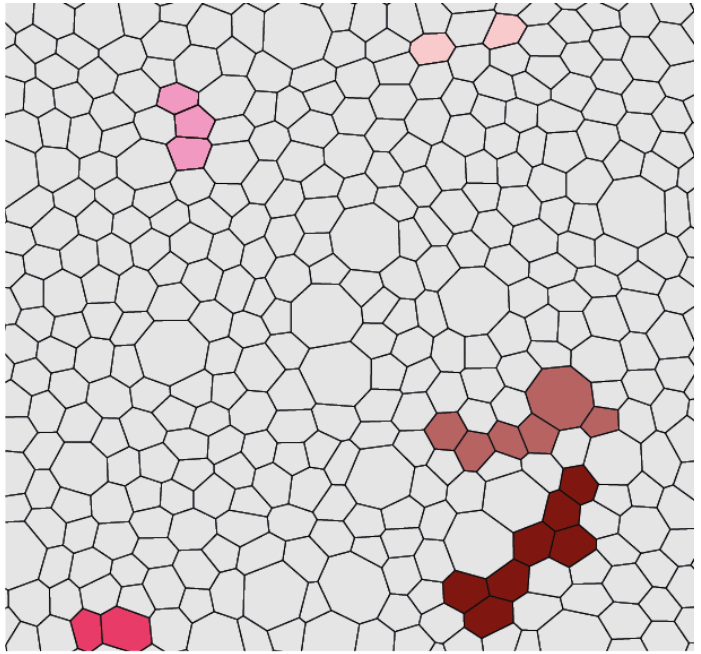

Sub-region C

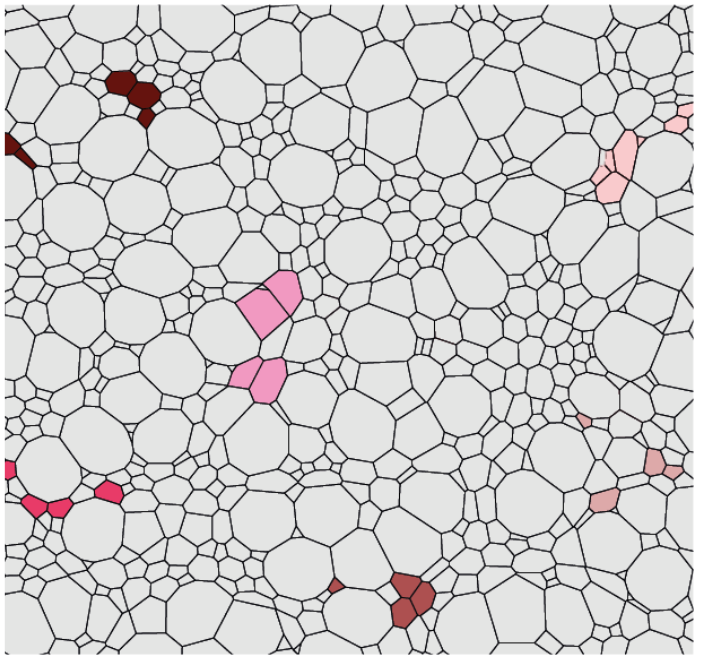

Bocanegra-Moreno et al., Nature Physics, 2023

Cell area variability is high only in sub-region C

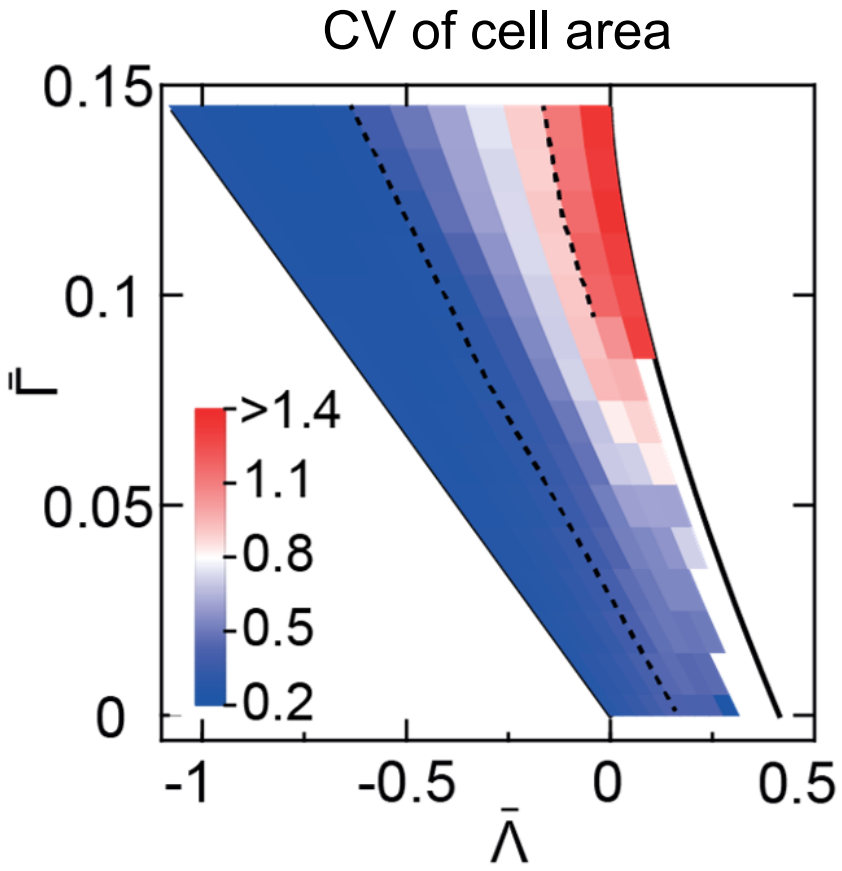

Bocanegra-Moreno et al., Nature Physics, 2023

Tissue simulated in sub-region C resembles the neural epithelium at E8.5

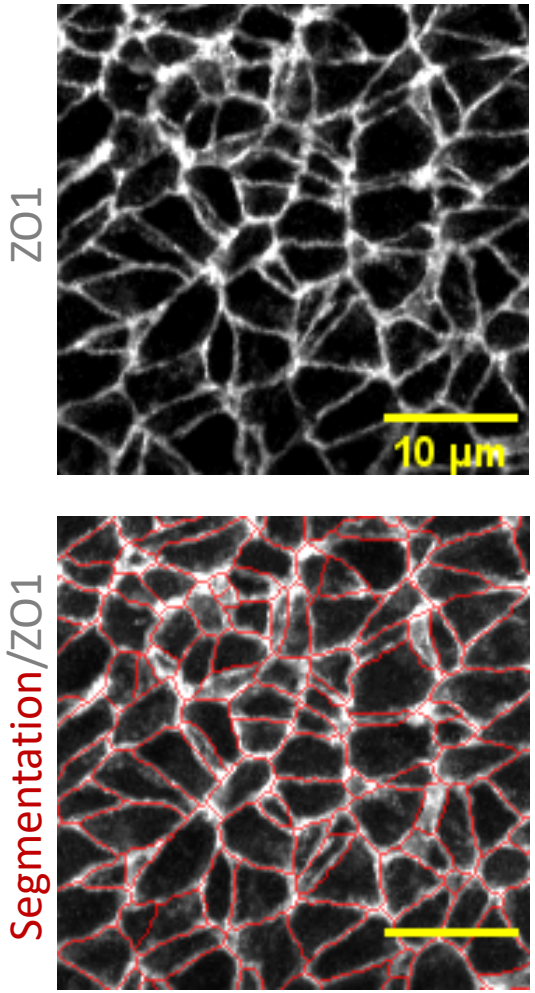

n= 6929 cells, 4 embryos

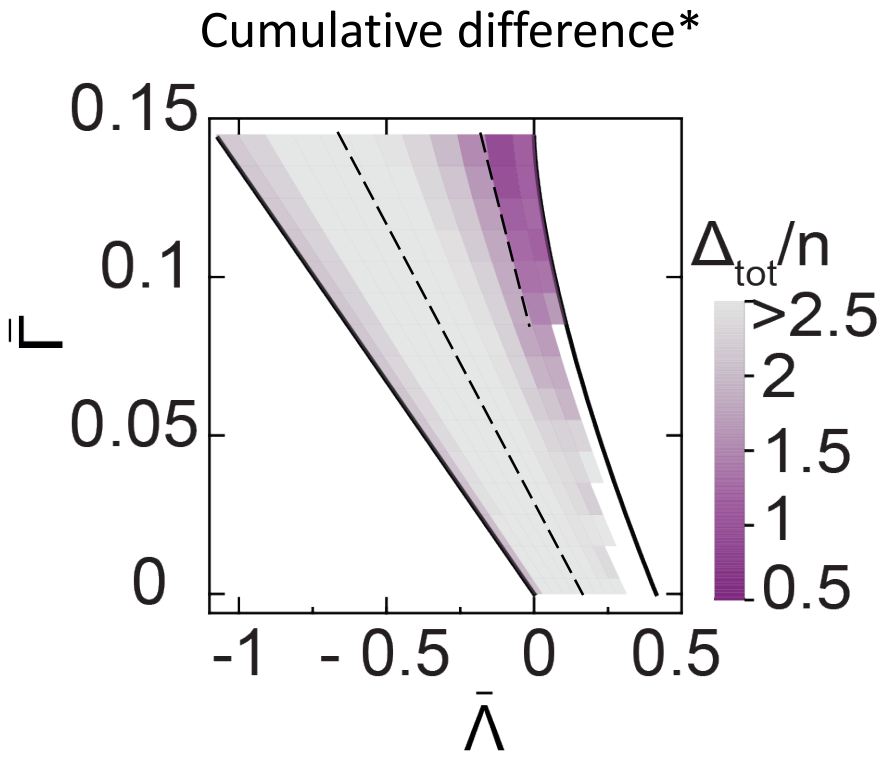

*Area CV, % Hexagons, normalized perimeter (p0), cell elongation, elongation CV, p0 CV, perimeter CV

Bocanegra-Moreno et al., Nature Physics, 2023

Dynamics of cell area affects the rate of cellular rearrangements and cellular heterogeneity in sub-region C

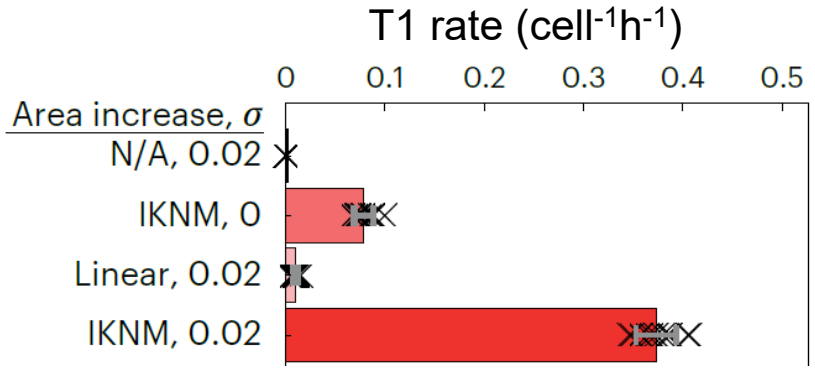

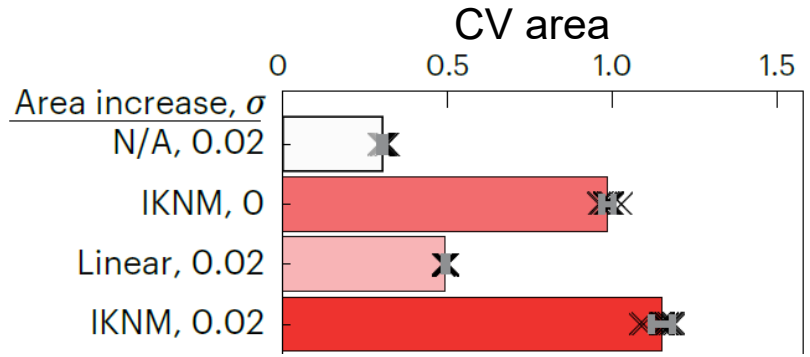

σ = magnitude of noise in Λ_{ij}

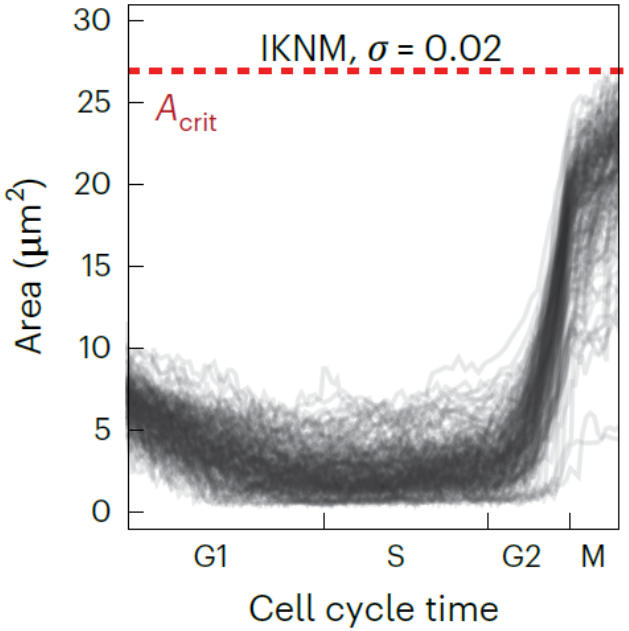

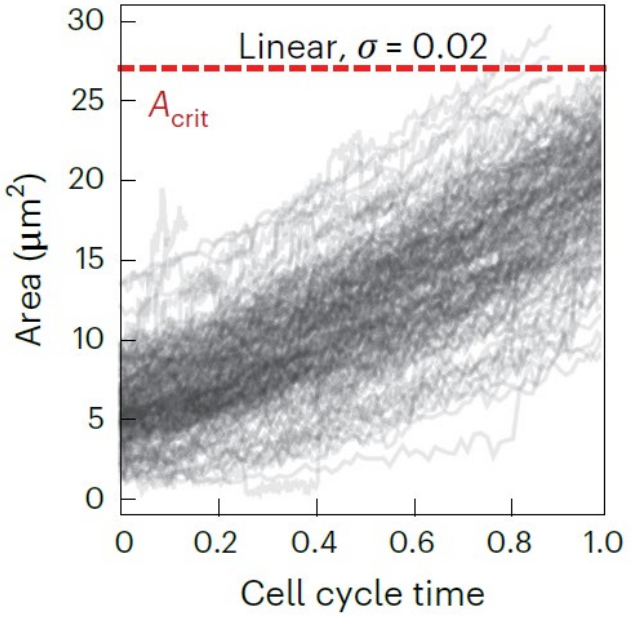

Bocanegra-Moreno et al., Nature Physics, 2023

Implementation of interkinetic nuclear movement (IKNM) in the vertex model

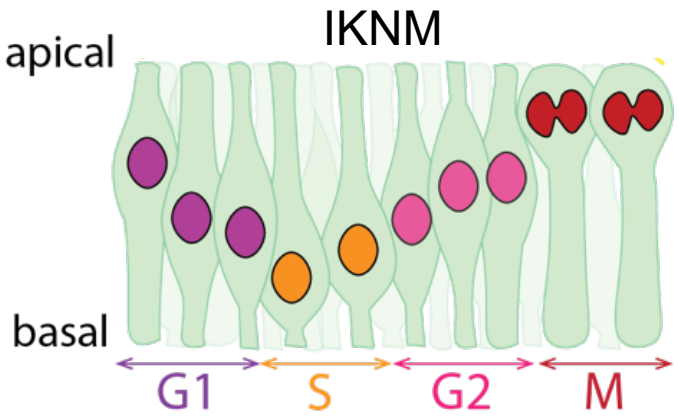

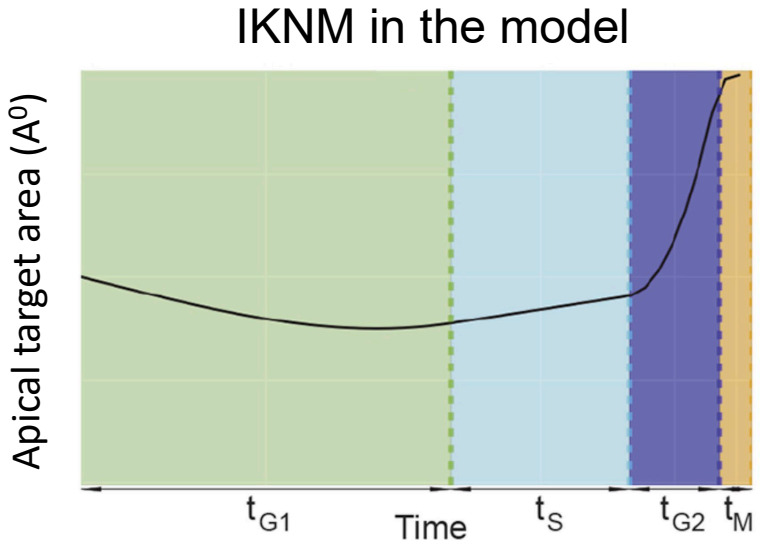

$$A^0_\alpha(\Delta t) = \tfrac{1}{2}(g_\alpha \Delta t + 1)(\rho_\alpha(\Delta t)^2 + 1)$$

g_α growth rate of the cell

$\rho_\alpha(\Delta t)$ piecewise linear function representing nucleus position

Guerrero et al., Development 2019

Bocanegra-Moreno et al., Nature Physics, 2023

Apical cell area rapidly increases before mitosis *in vivo*

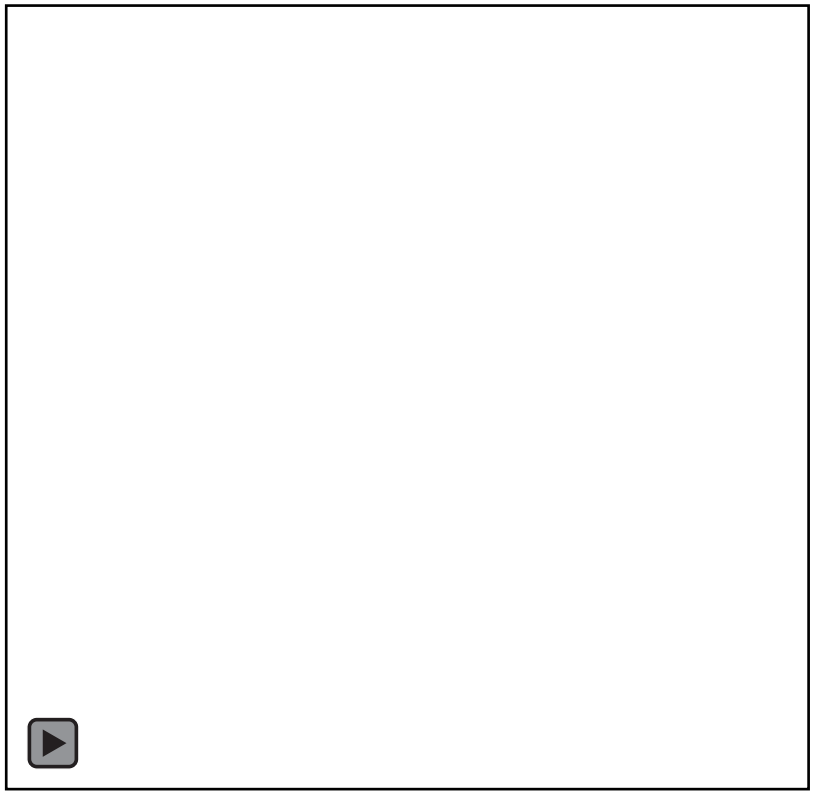

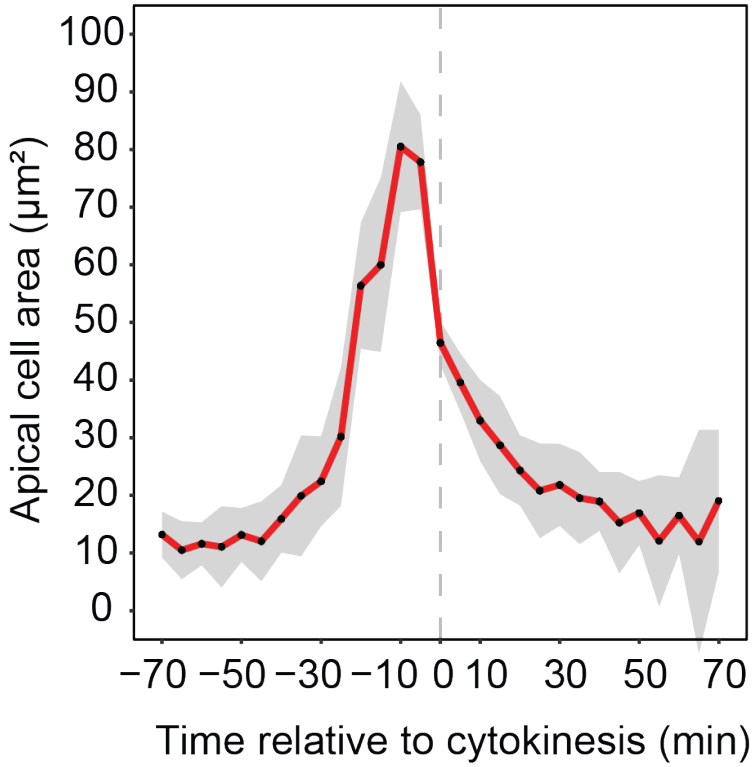

Bocanegra-Moreno et al., Nature Physics, 2023

Kinetics of apical cell area growth induces T1 transitions in sub-region C

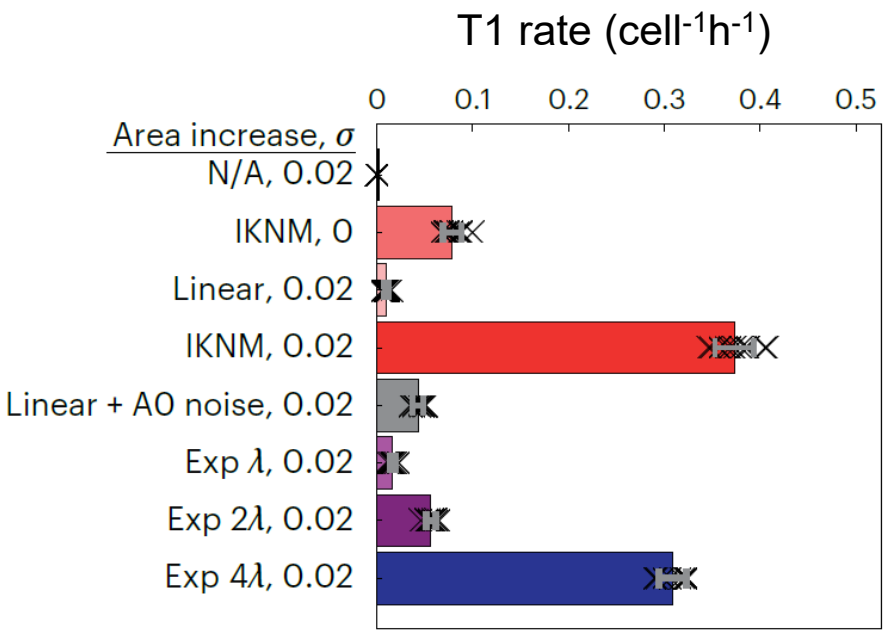

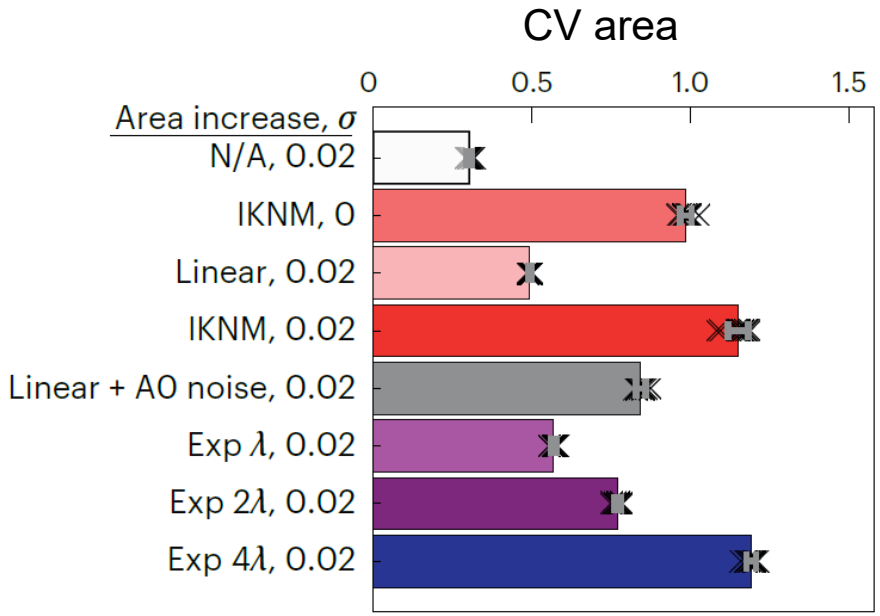

σ = magnitude of noise in Λ_{ij}

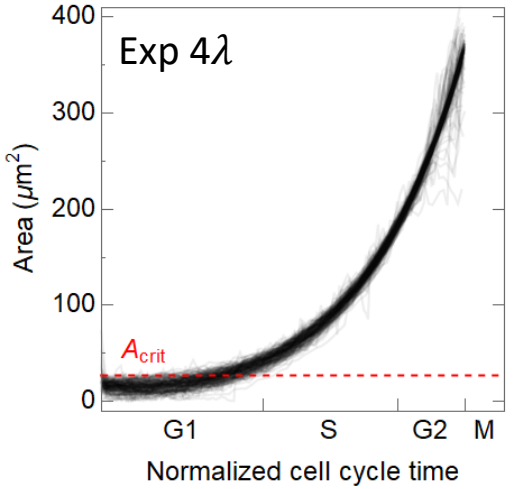

Bocanegra-Moreno et al., Nature Physics, 2023

The number of clone fragments is higher at early developmental stages than at later stages

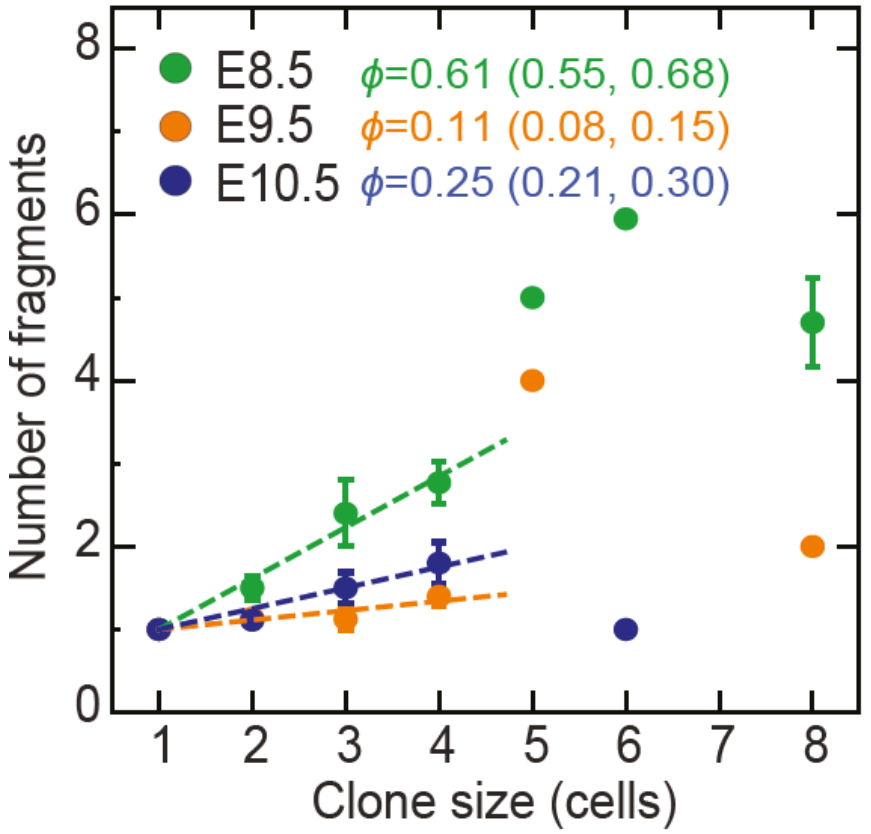

Bocanegra-Moreno et al., Nature Physics, 2023

The growth rate of neural epithelium goes down at later developmental stages

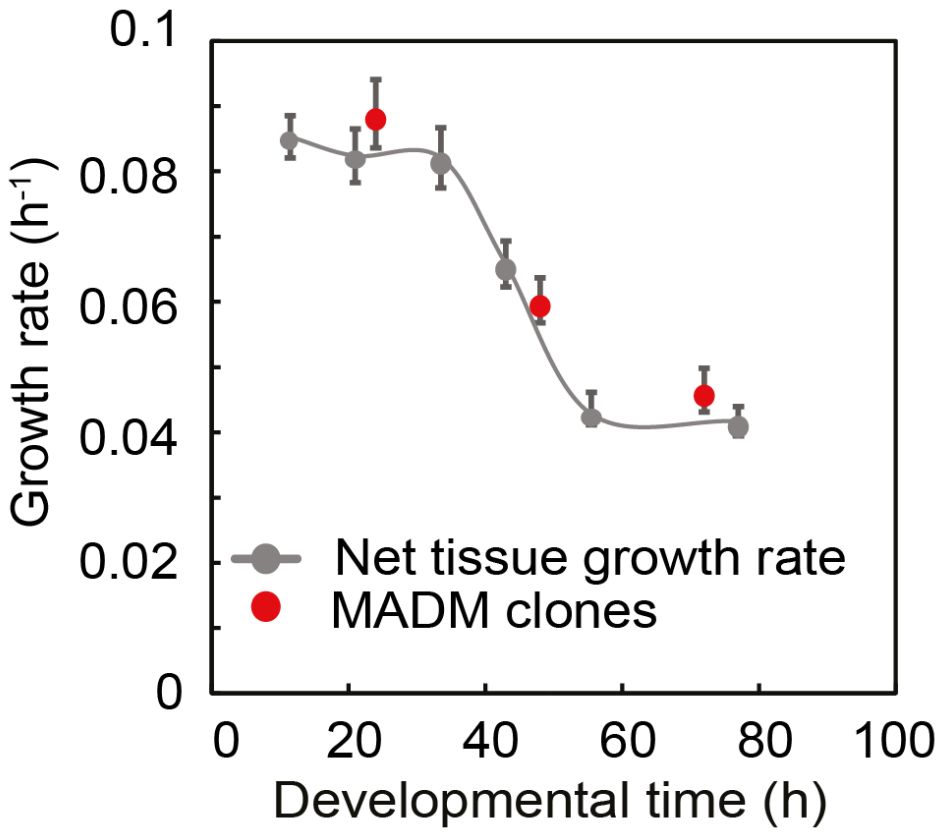

Kicheva et al., Science, 2014
Bocanegra-Moreno et al., Nature Physics, 2023

Lowering proliferation rate decreased fragmentation in vertex model simulation

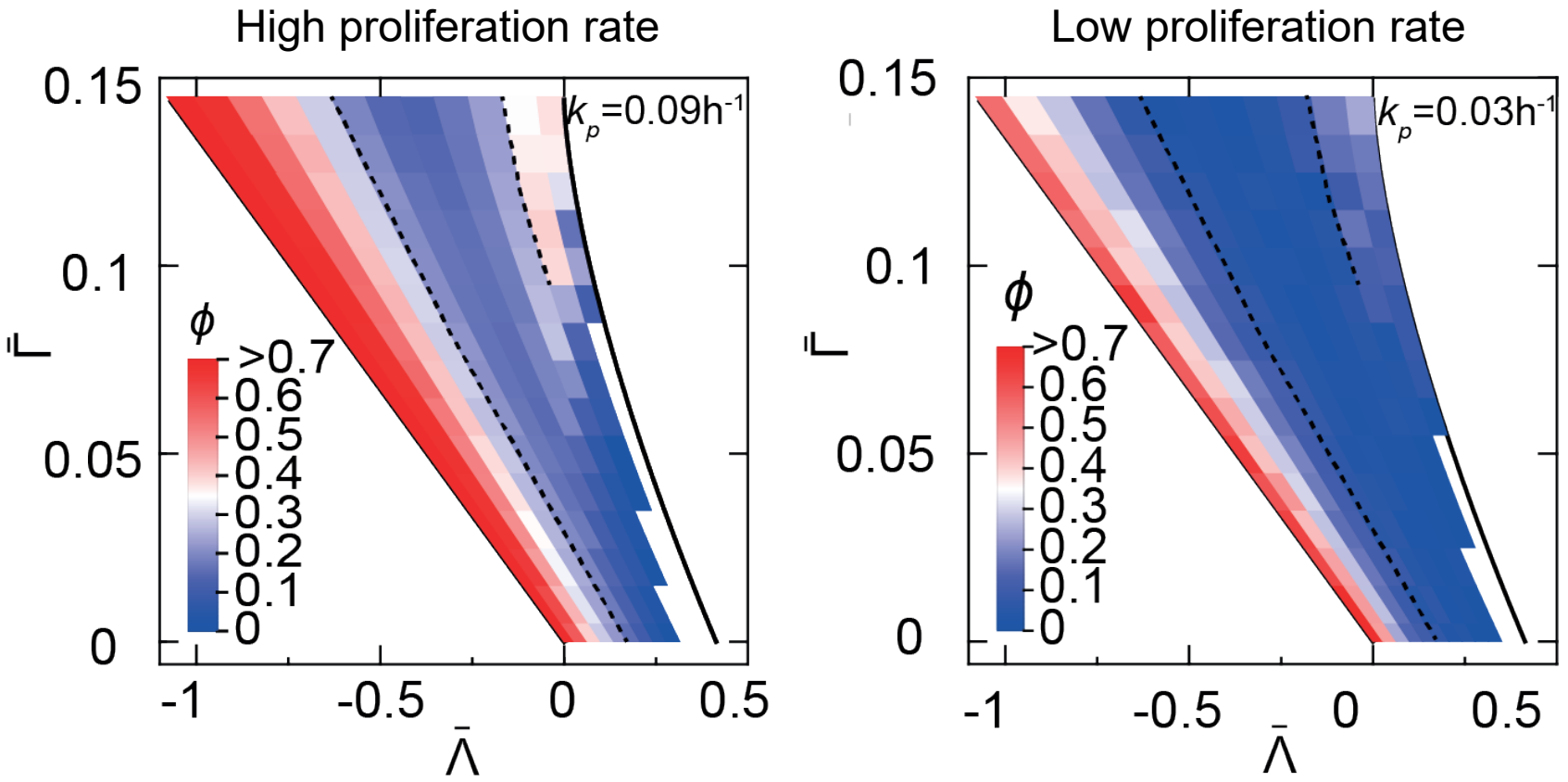

Bocanegra-Moreno et al., Nature Physics, 2023

The decrease in the proliferation rate decreased fragmentation in E8.5 embryos

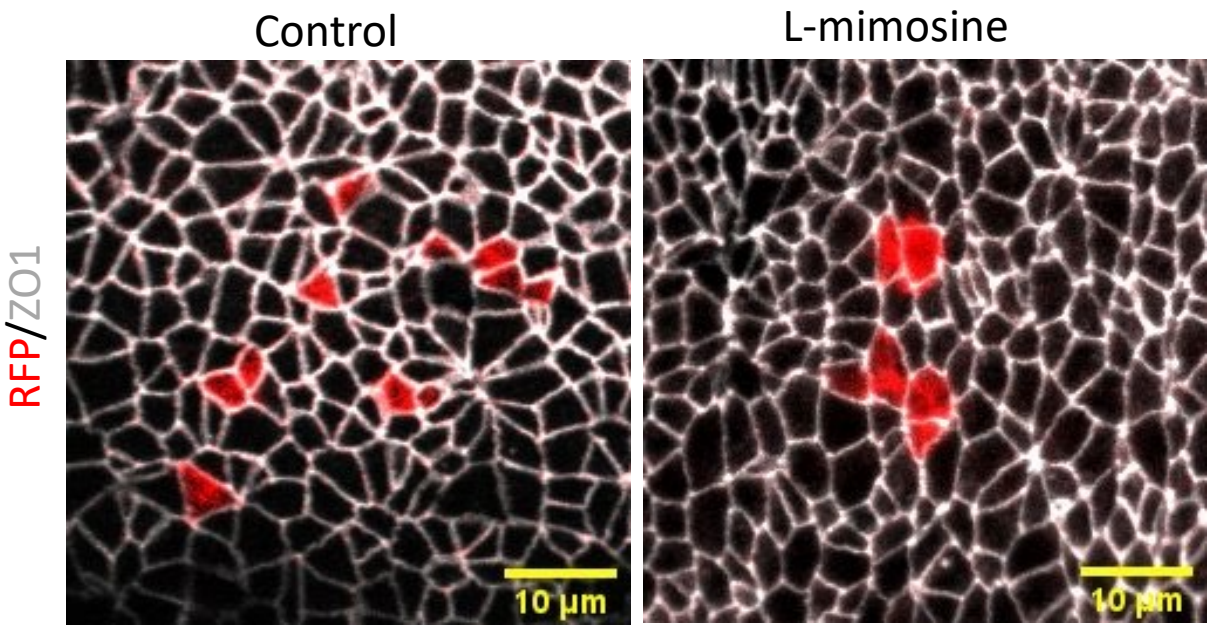

L-mimosine – cell cycle inhibitor

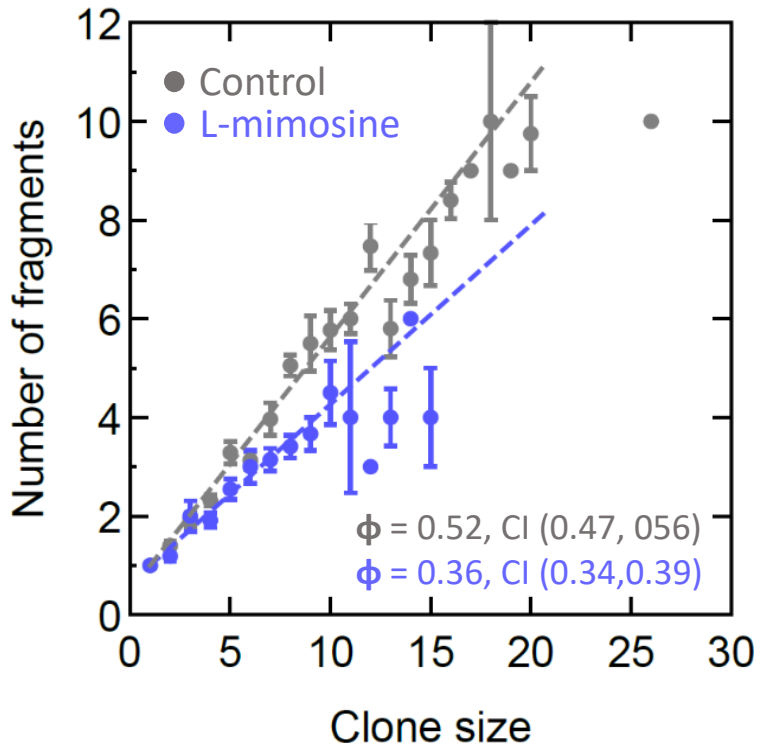

Bocanegra-Moreno et al., Nature Physics, 2023

Research questions

- How are morphogens interpreted to result in precise and reproducible patterns?
- How is pattern formation affected by tissue mechanical properties, cellular dynamics, and growth?
- How is morphogen source formed in a growing tissue?
- What are conditions for emergence of stable patterns in tissues?

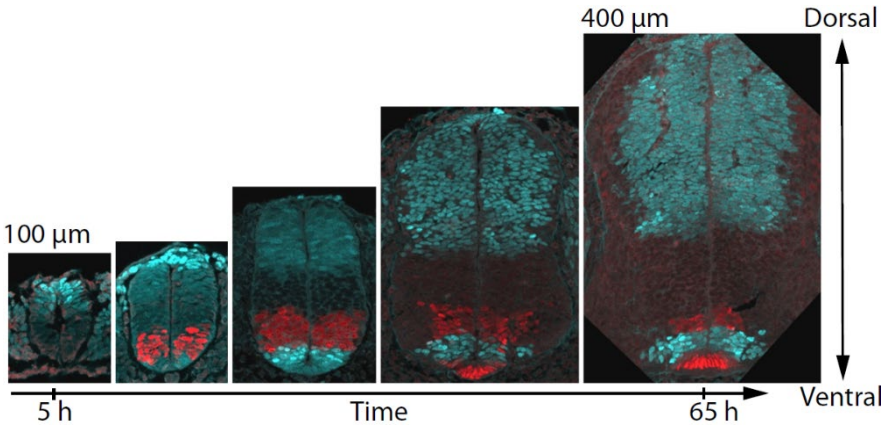

The GRN acts as an information decoder that specifies target pattern

Input signal

Information decoder

Output signal

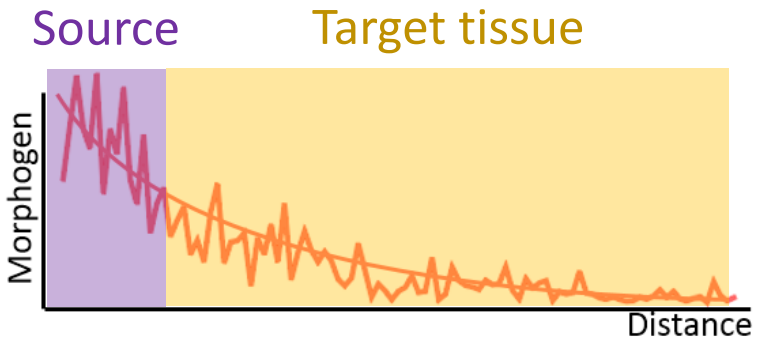

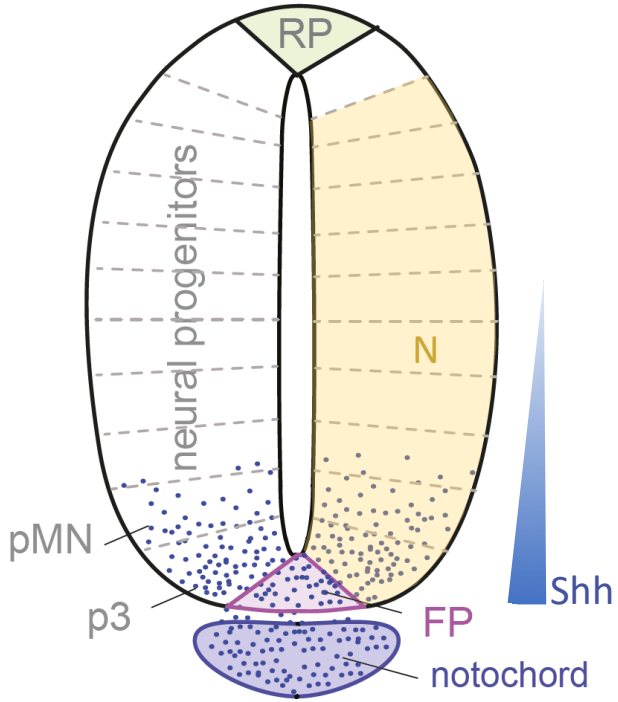

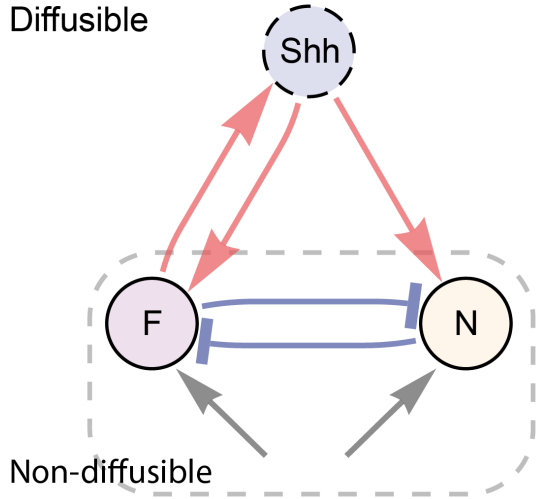

Ho et al., bioRxiv, 2024.03.01.582751

The GRN acts as an information decoder that specifies target pattern

Input signal

Information decoder

Output signal

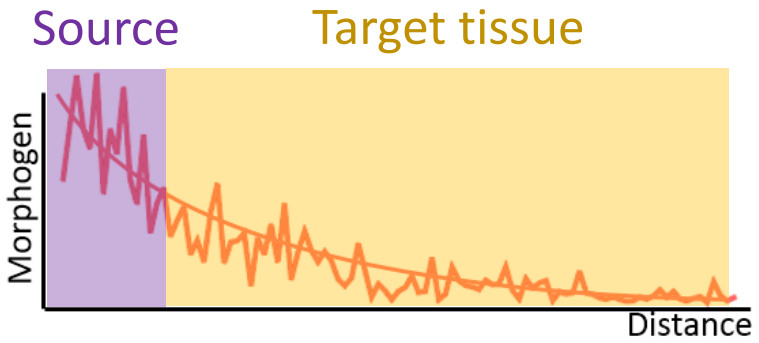

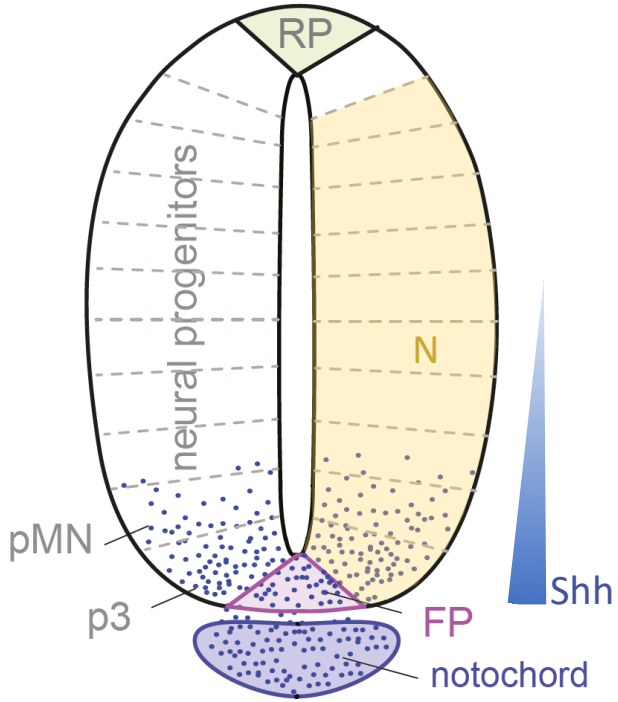

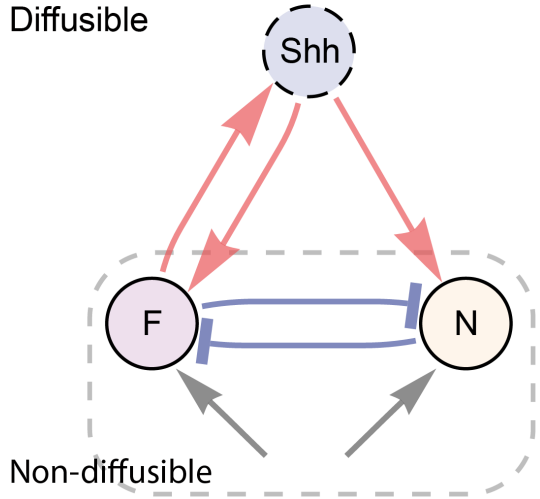

Ho et al., bioRxiv, 2024.03.01.582751

Thermodynamical model coupled with reaction-diffusion equation

$$\frac{\partial[F]}{\partial t} = \alpha_F \frac{\kappa_F + c_{S\to F}\kappa_F[Shh]}{(1 + K_{N\to F}[N])^{m_{N\to F}} + \kappa_F + c_{S\to F}\kappa_F[Shh]} - \gamma_F[F]$$

$$\frac{\partial[N]}{\partial t} = \alpha_N \frac{\kappa_N + c_{S\to N}\kappa_N[Shh]}{(1 + K_{F\to N}[F])^{m_{F\to N}} + \kappa_N + c_{S\to N}\kappa_N[Shh]} - \gamma_N[N]$$

$$\frac{\partial[Shh]}{\partial t} = D_S \frac{\partial^2[Shh]}{\partial x^2} + \alpha_S \frac{\kappa_{F\to S}[F]}{1 + \kappa_{F\to S}[F]} - \gamma_S[Shh]$$

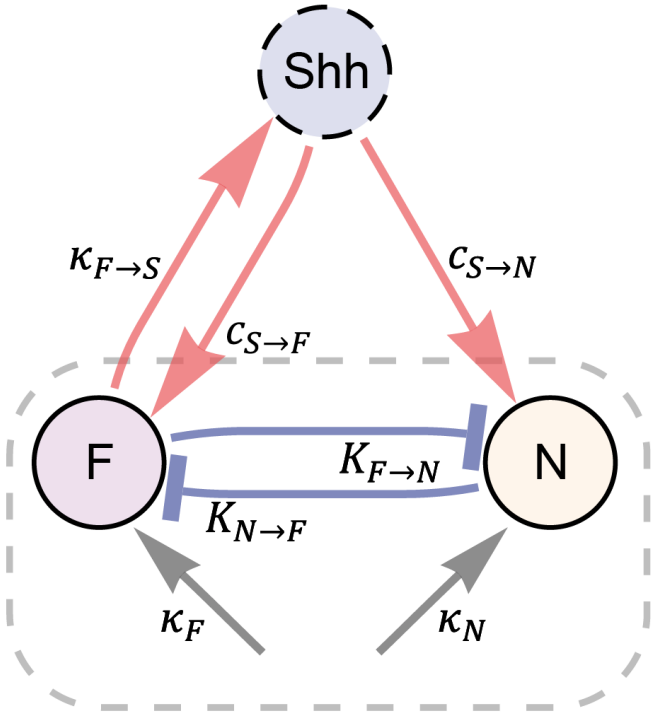

Ho et al., bioRxiv, 2024.03.01.582751

Spinal cord grows as pattern is established

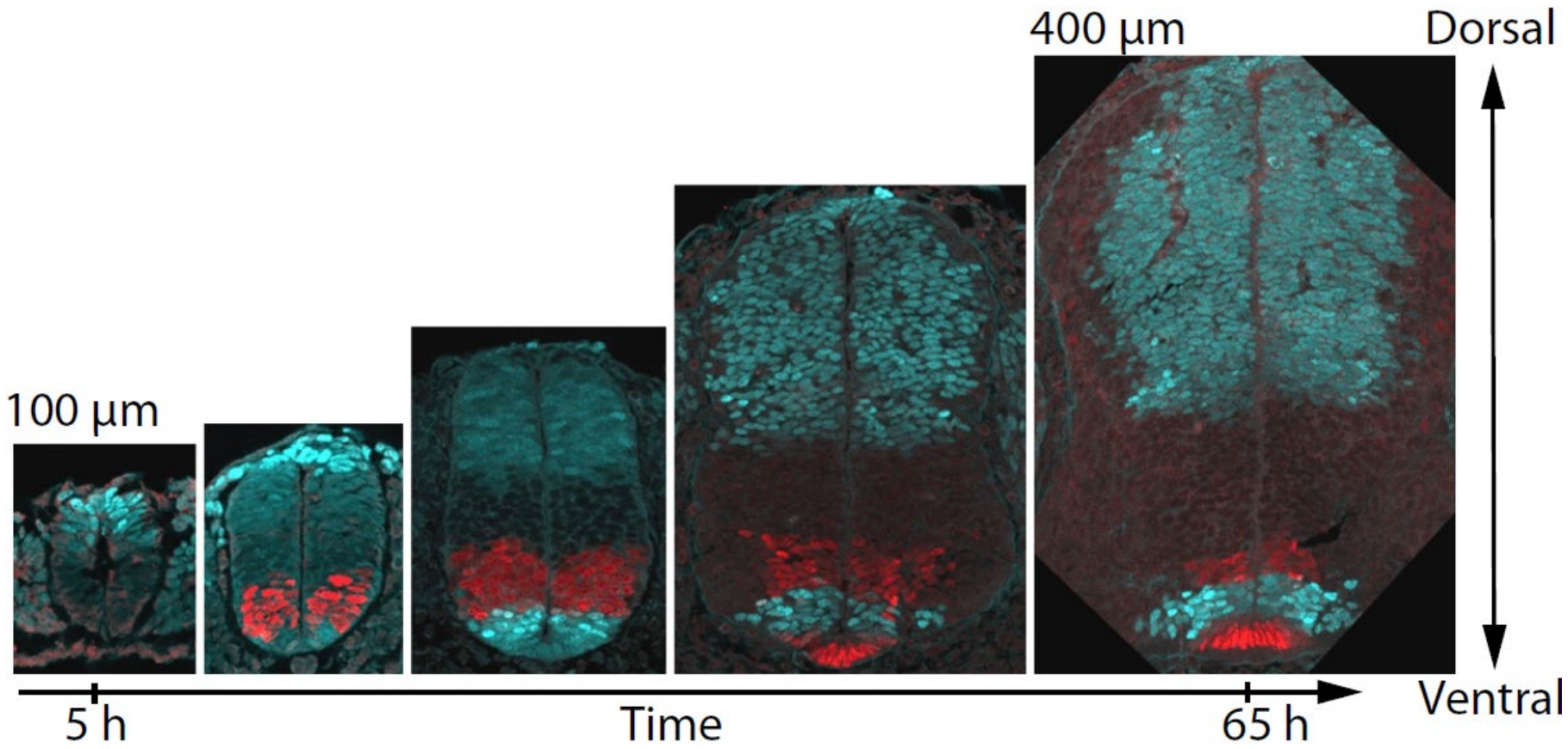

Kicheva et al., Science 2014
Zagorski et al., Science 2019
Bocanegra-Moreno et al., Nature Physics 2023

Computational screen: 169 979 successful solutions out of 400 000 visited

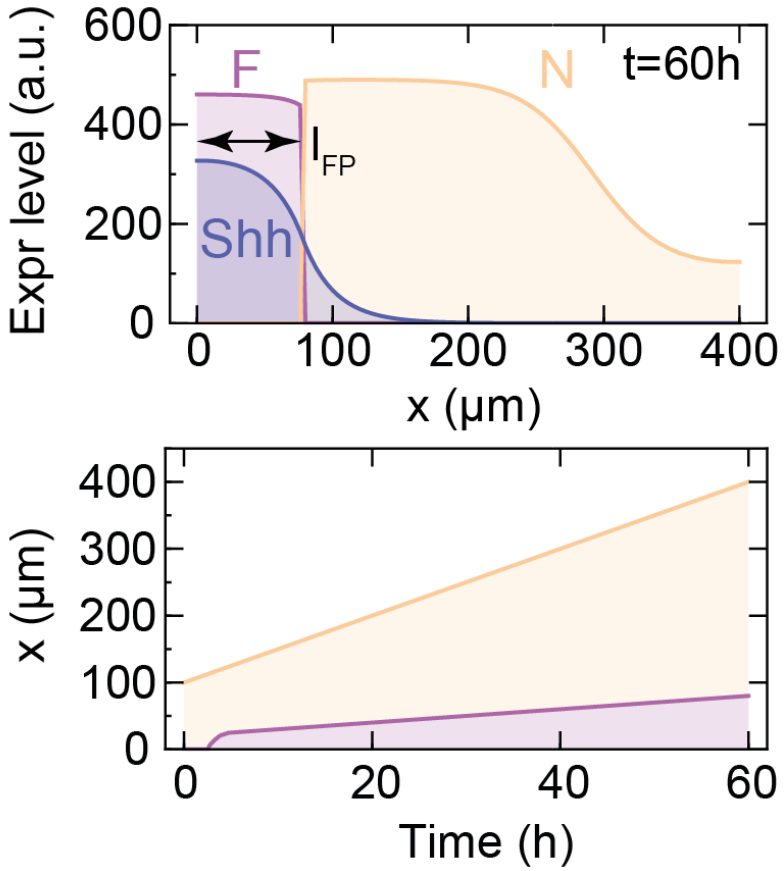

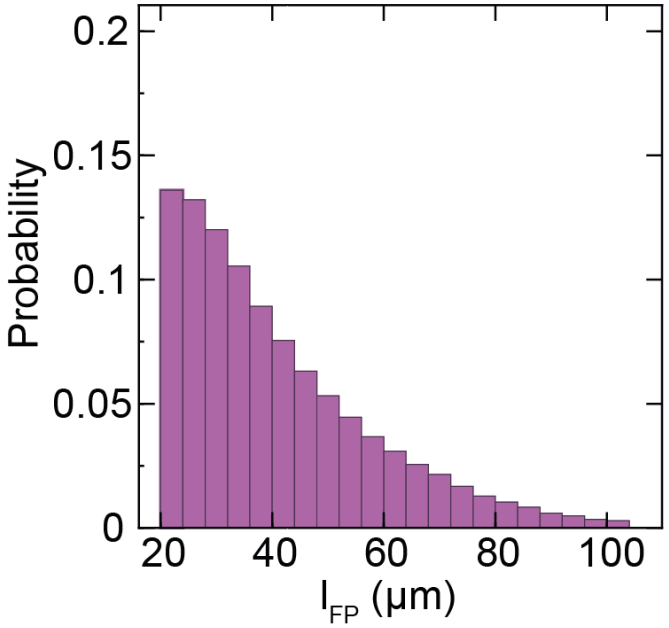

Success criteria:

- two domains, FP ventrally located
- FP size from 5% to 25% tissue length
- formed between 2.5 and 20h

Ho et al., bioRxiv, 2024.03.01.582751

Lack of clear dependence of FP size on parameter values

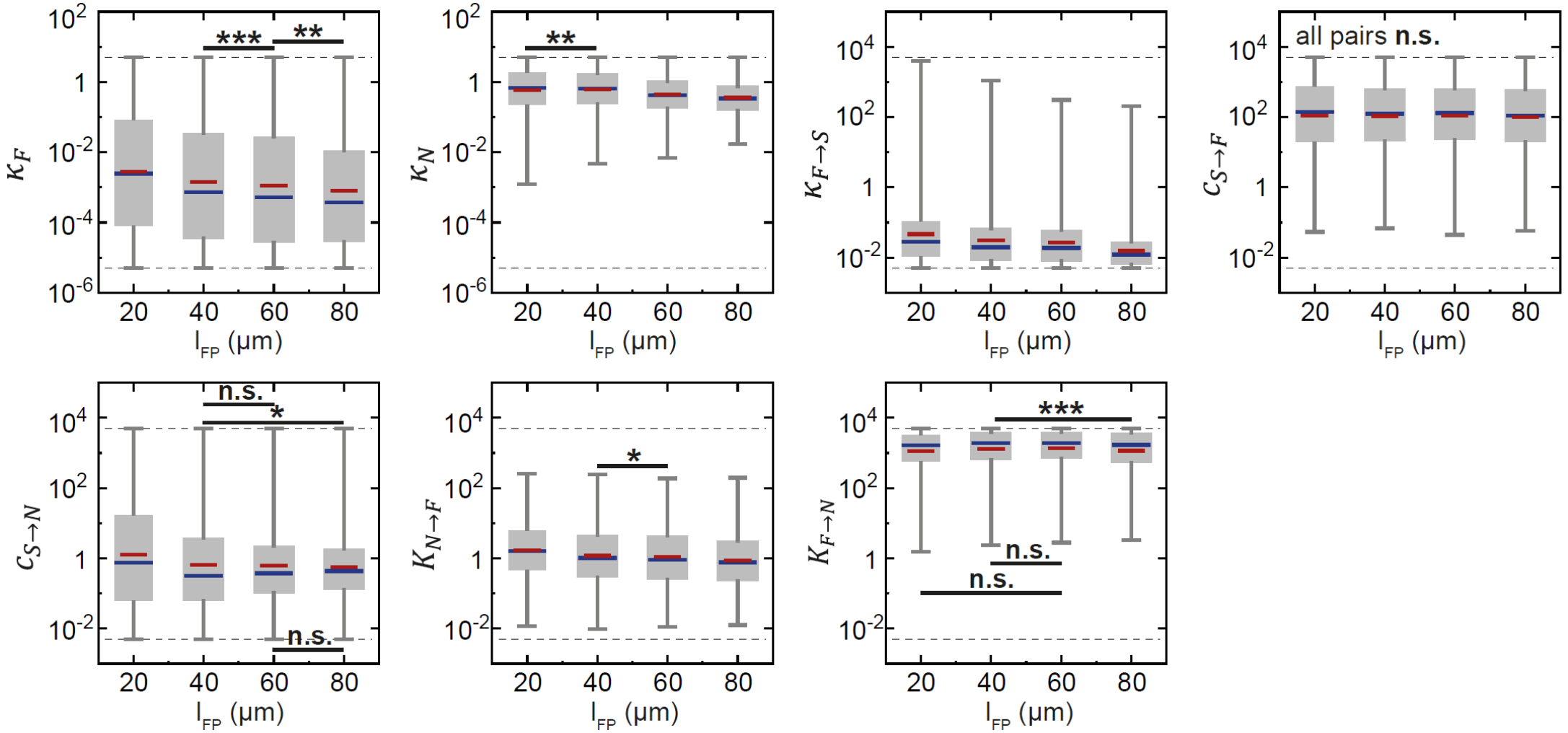

Ho et al., bioRxiv, 2024.03.01.582751

Perturbing most of the parameters strongly affects FP size

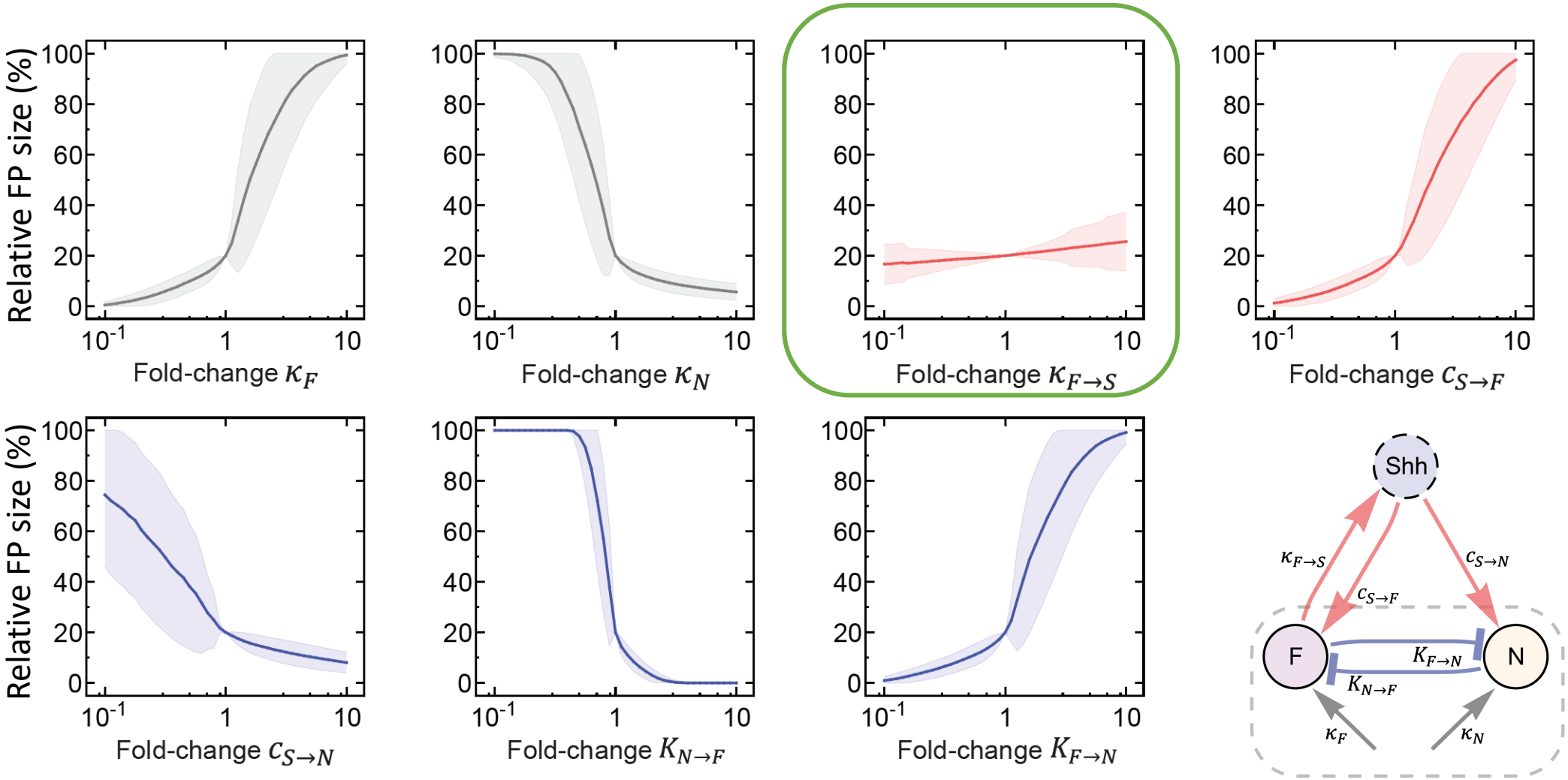

Ho et al., bioRxiv, 2024.03.01.582751

FP formation can occur by different mechanisms, dependent or independent of FP-derived Shh

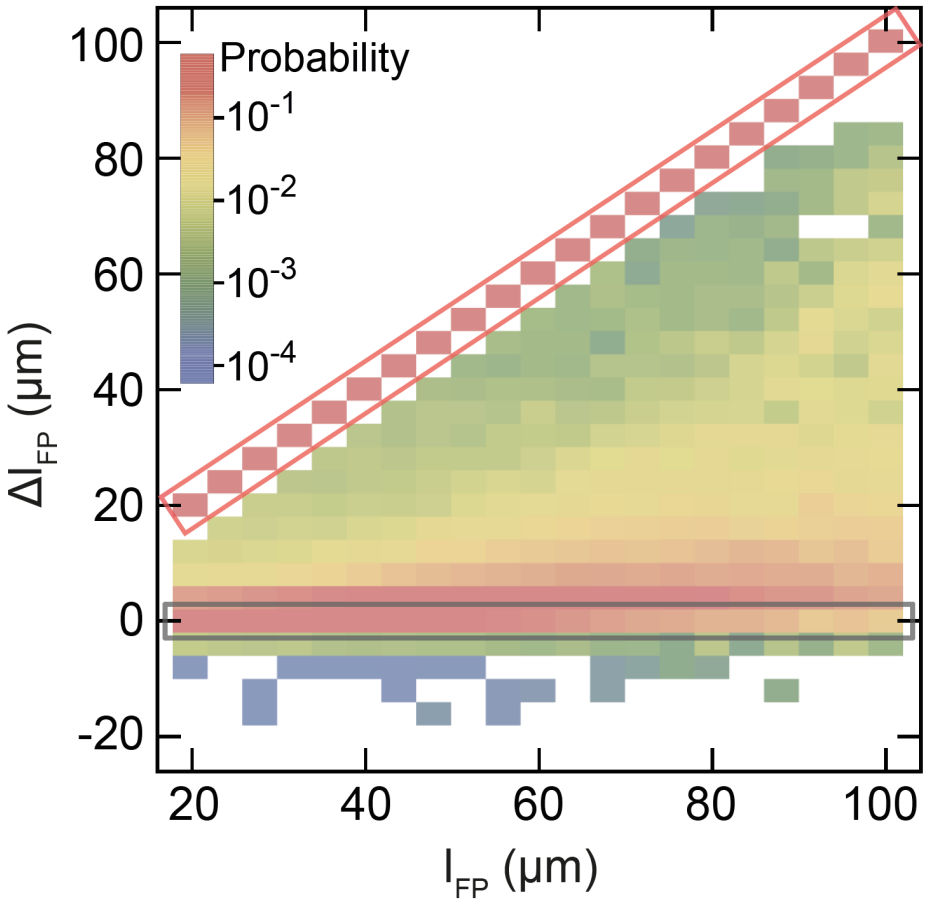

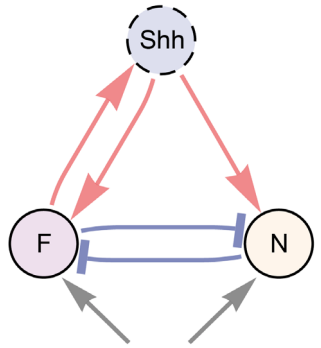

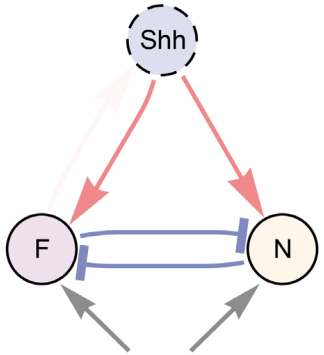

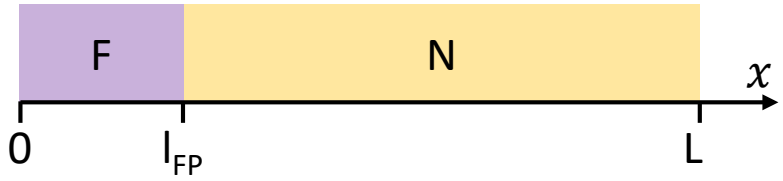

Shh **insensitive**, $\Delta l_{FP} = 0$

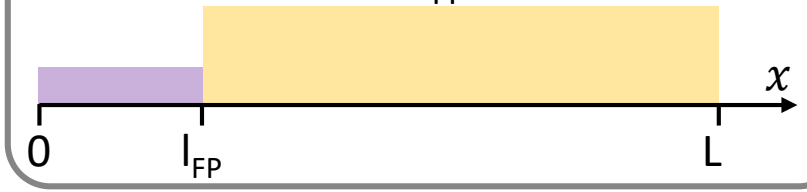

Shh **sensitive**, $\Delta l_{FP} = l_{FP}$

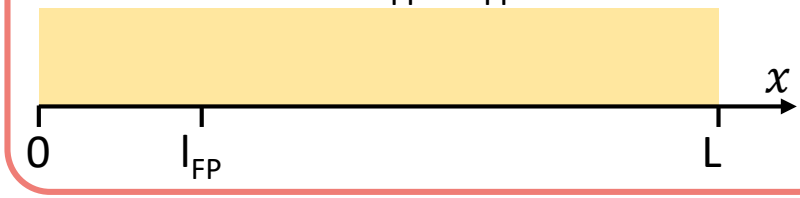

Ho et al., bioRxiv, 2024.03.01.582751

Distribution of parameters for Shh^{FP}-sensitive and insensitive classes of solutions

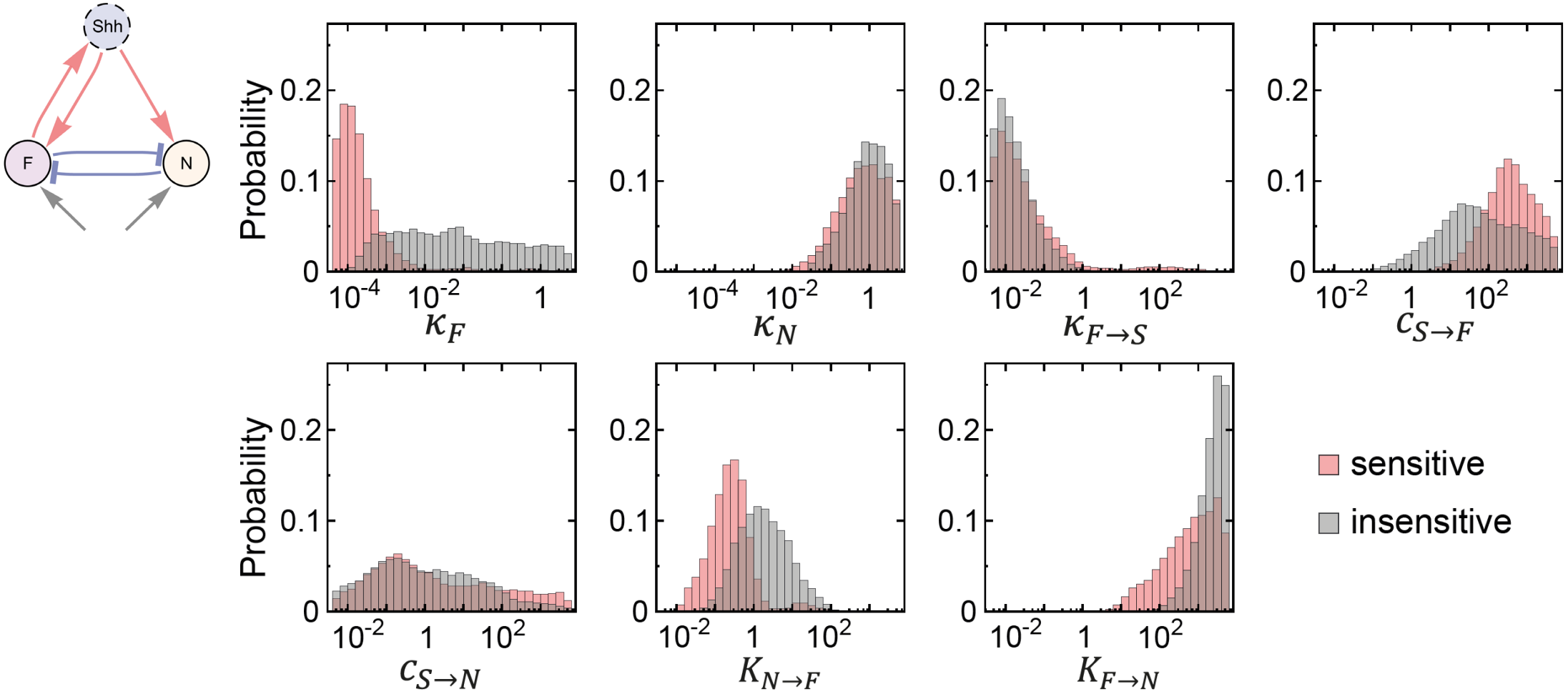

Ho et al., bioRxiv, 2024.03.01.582751

After formation the FP is scaling in size following tissue growth

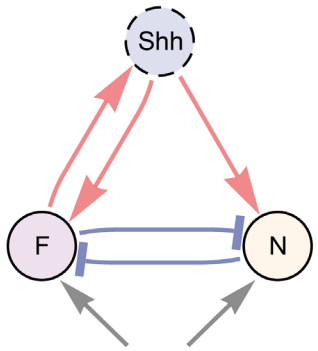

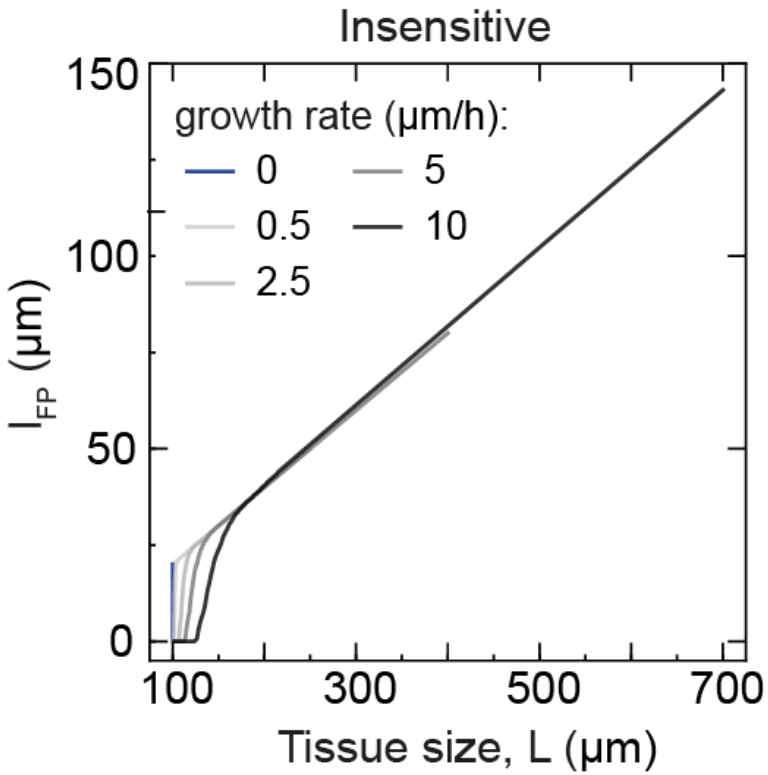

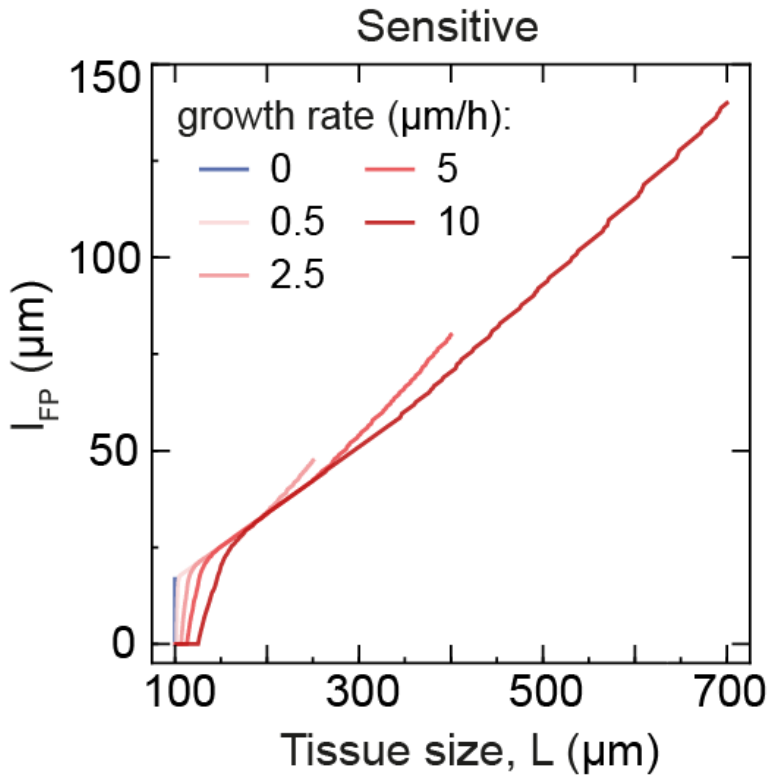

Ho et al., bioRxiv, 2024.03.01.582751

After formation the FP is scaling in size following tissue growth

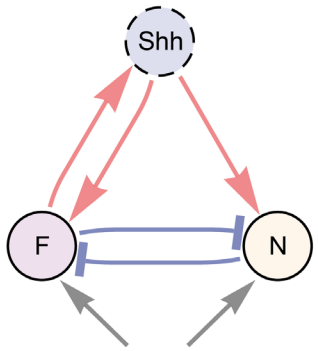

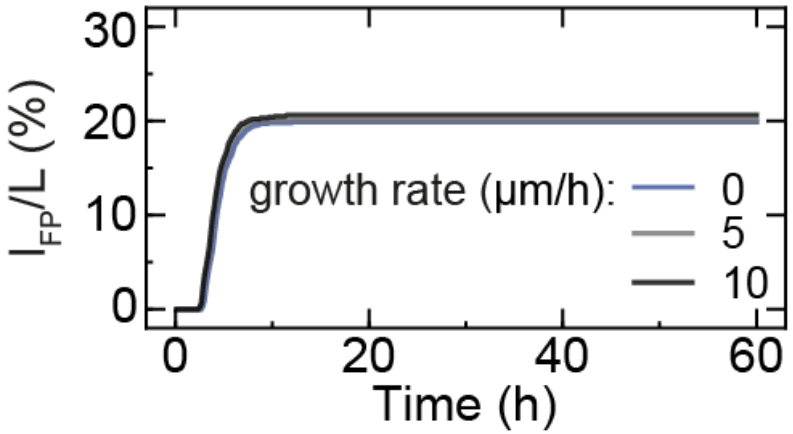

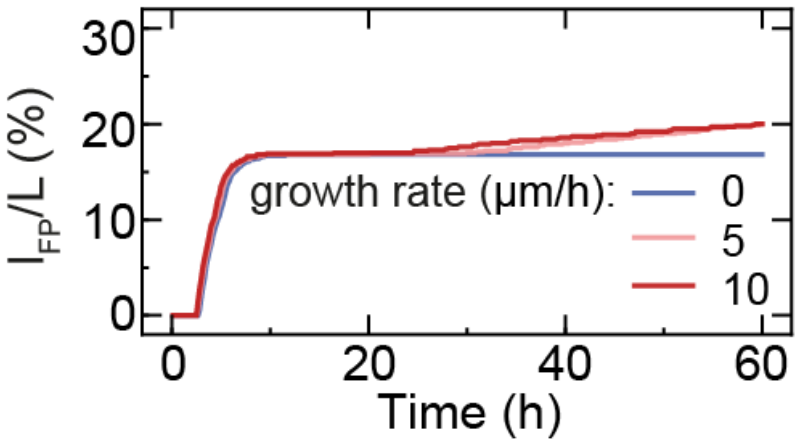

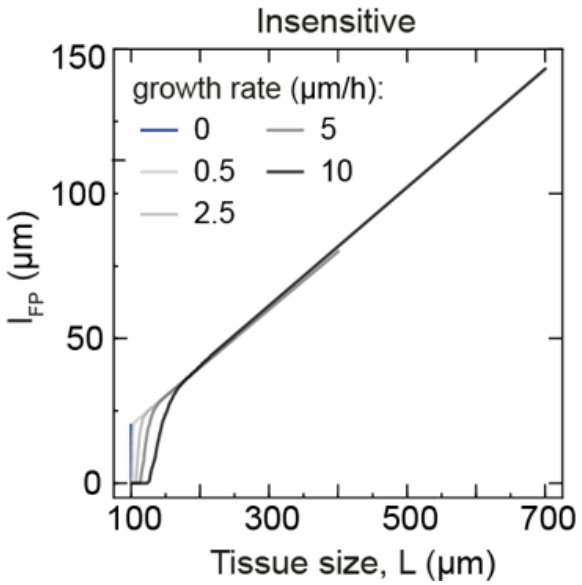

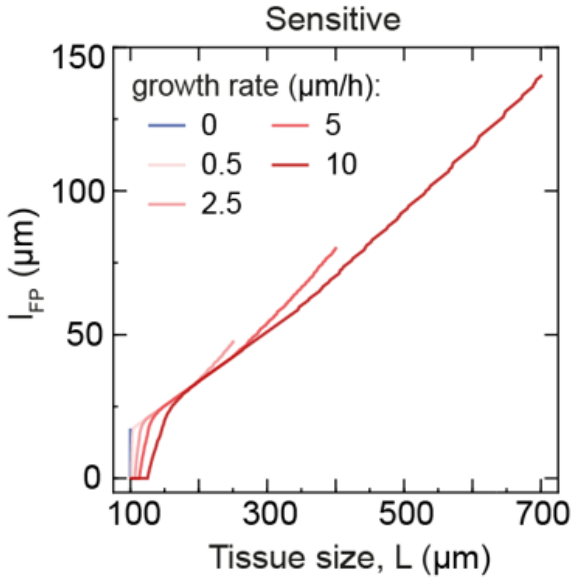

Ho et al., bioRxiv, 2024.03.01.582751

Removing Shh production by FP results in distinct solutions

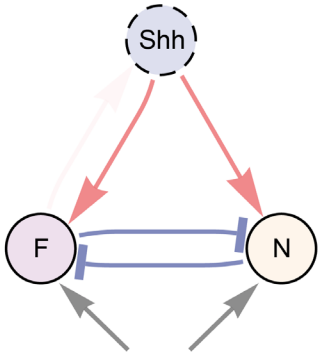

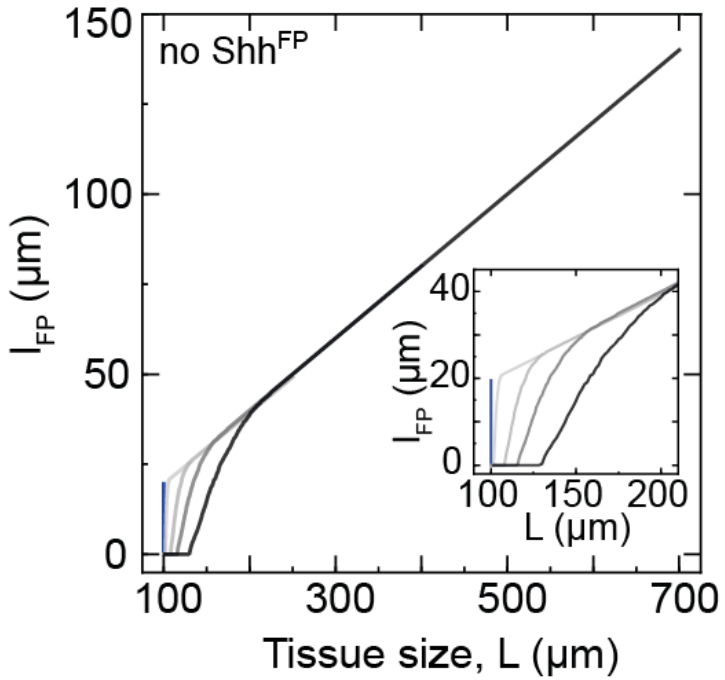

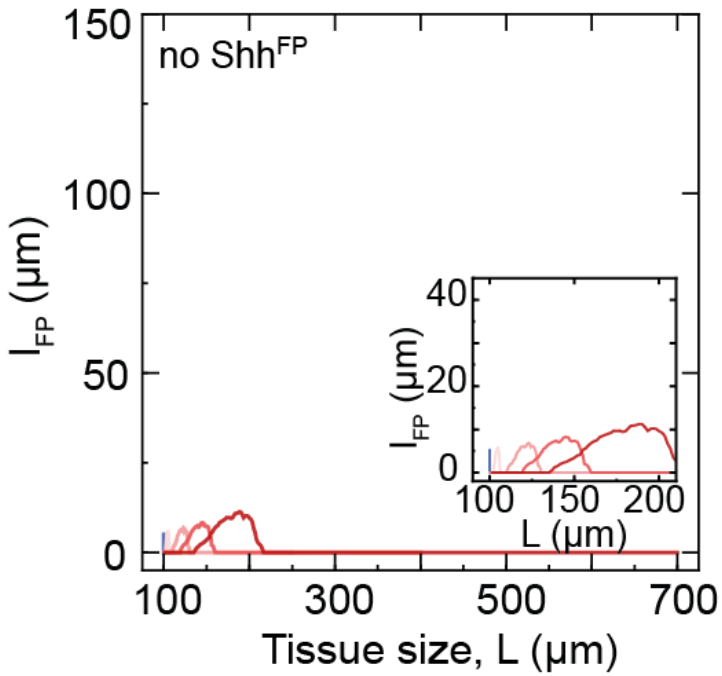

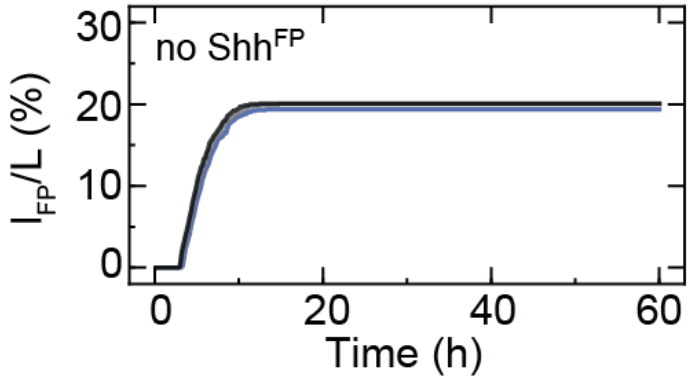

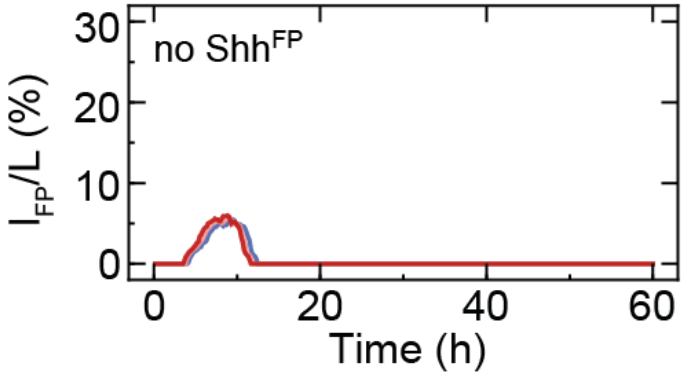

Ho et al., bioRxiv, 2024.03.01.582751

Two time scales of FP formation: establishment and scaling

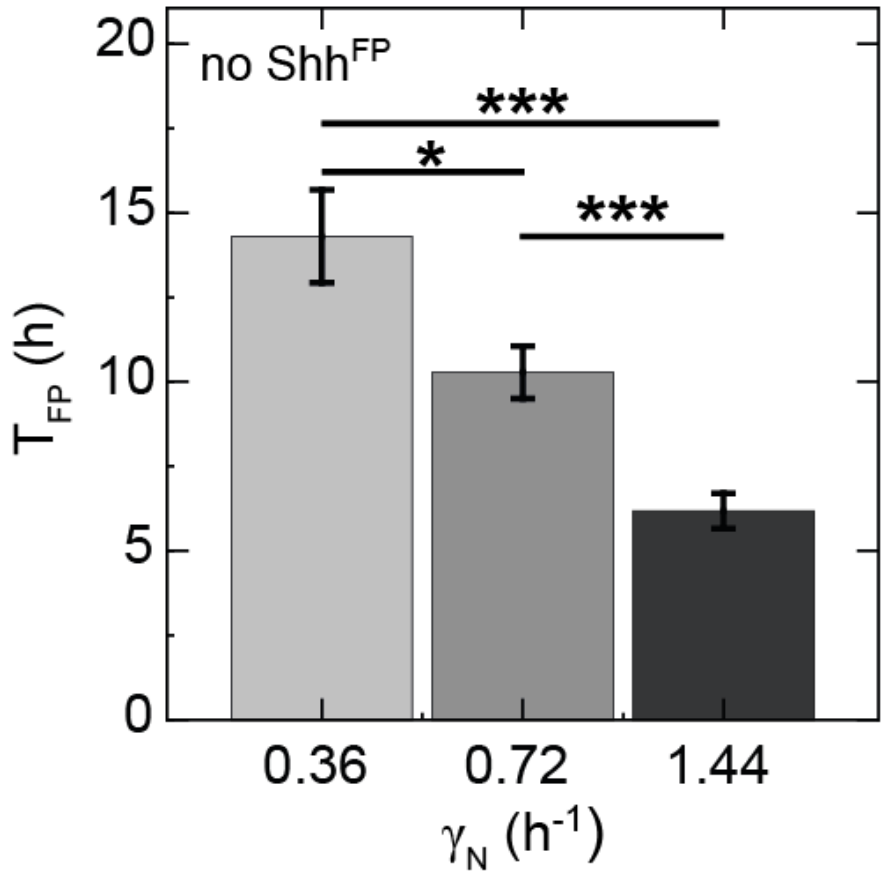

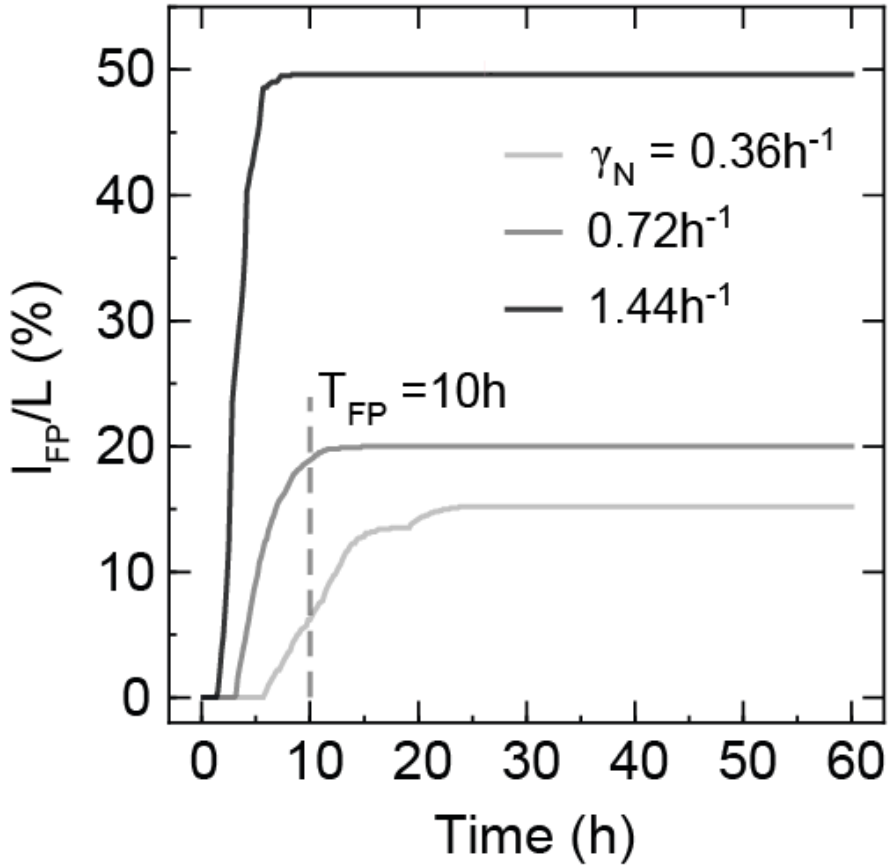

Ho et al., bioRxiv, 2024.03.01.582751

Initial flux regulates the size of FPs

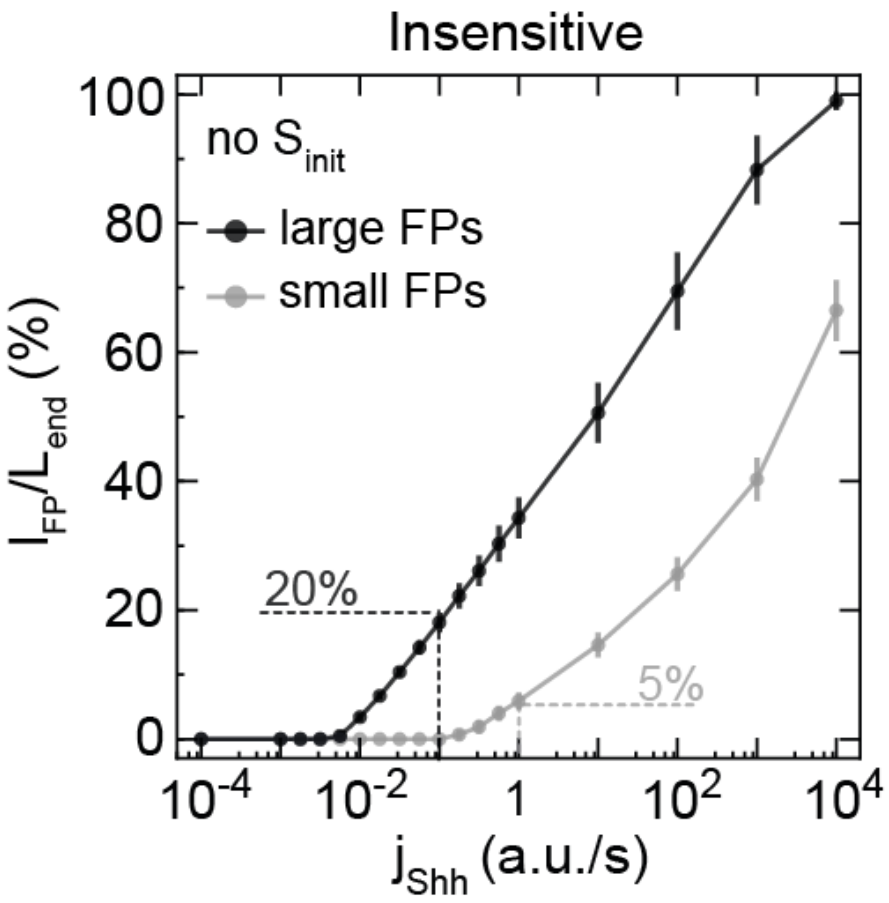

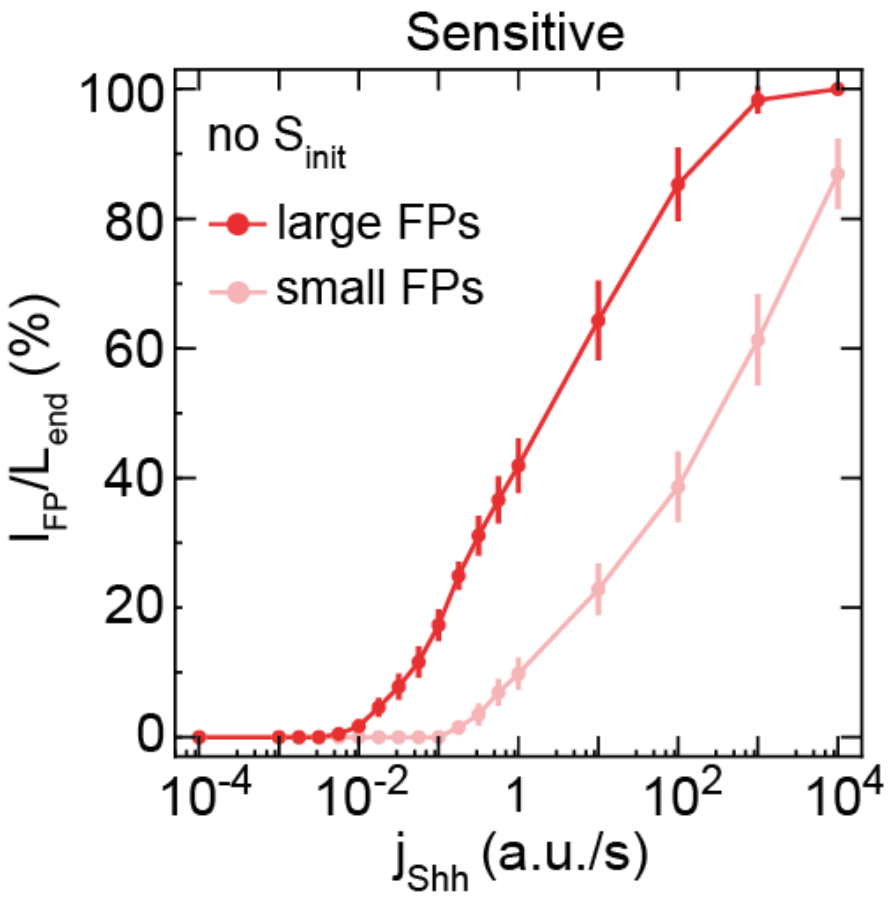

Ho et al., bioRxiv, 2024.03.01.582751

The increase in Shh amplitude over time depends on floor plate growth

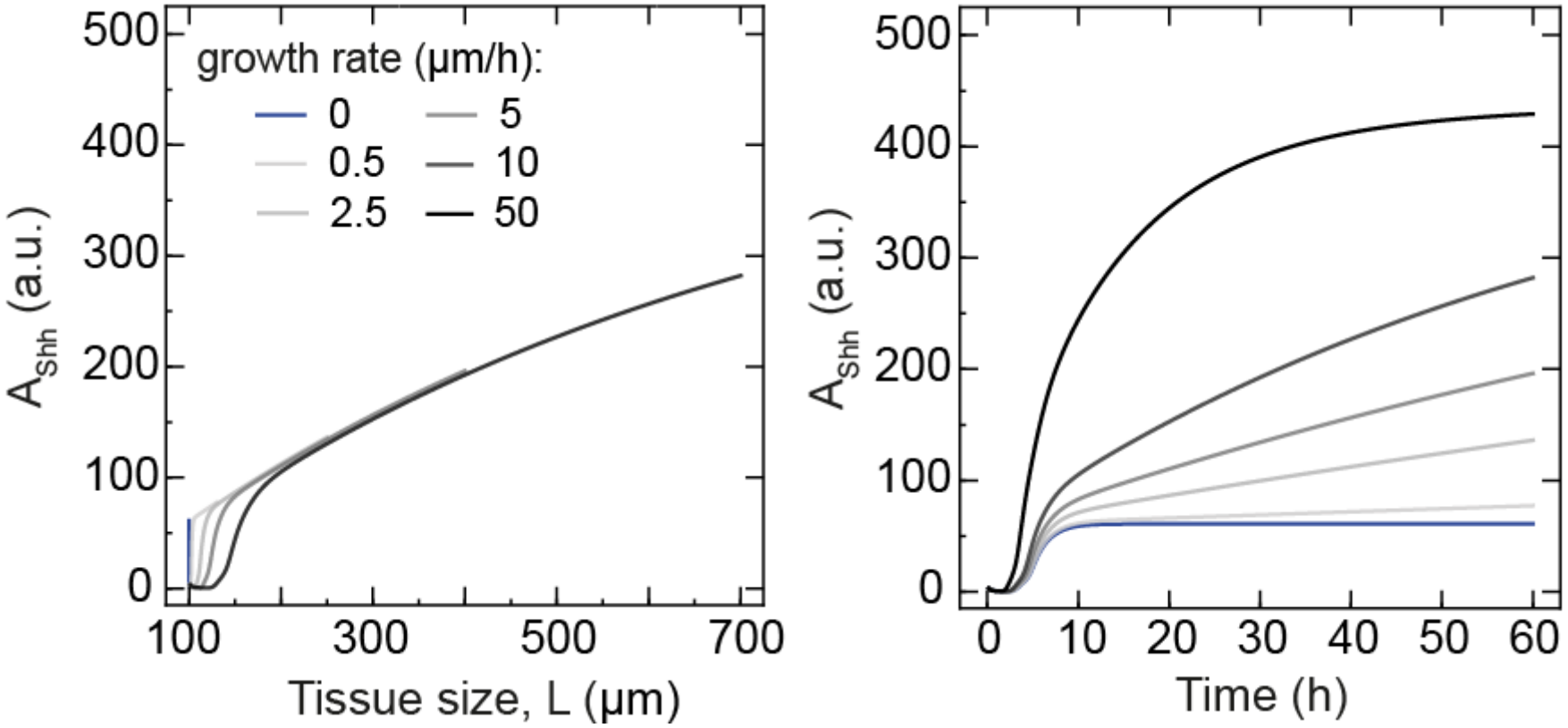

Ho et al., bioRxiv, 2024.03.01.582751

Removing Shh flux reduces Shh amplitude in the extent depending on the magnitude of flux

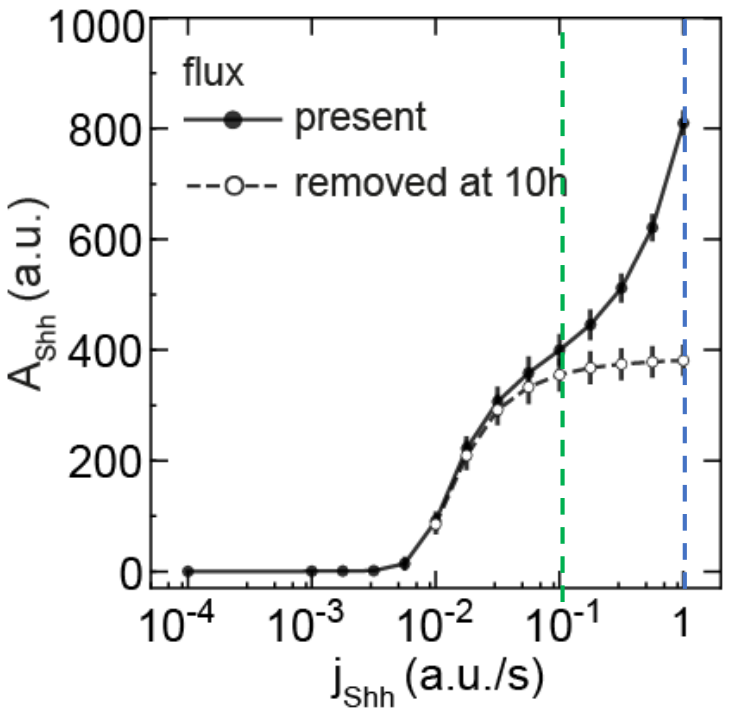

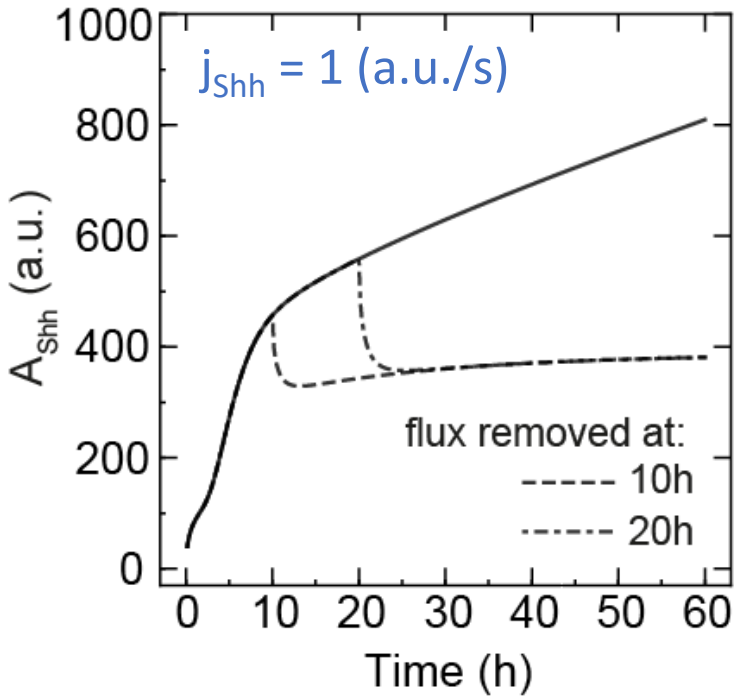

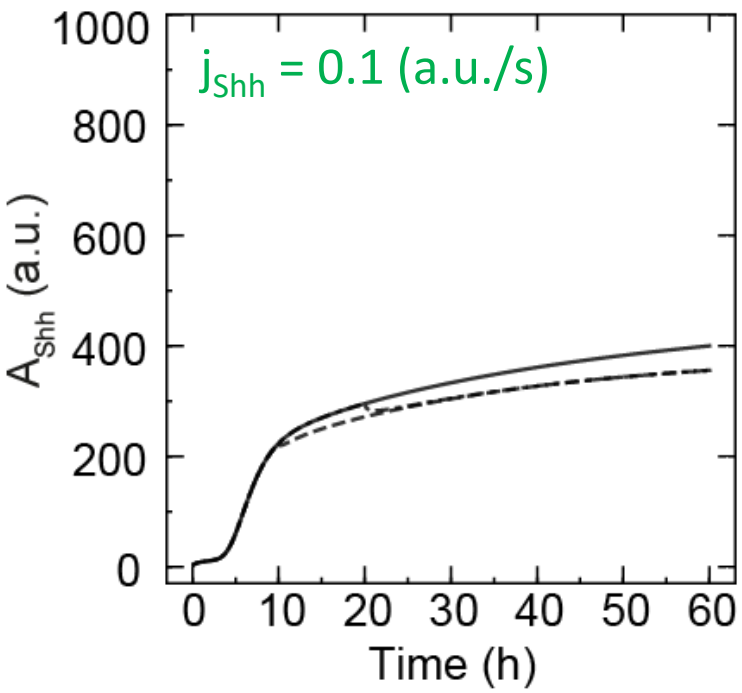

Ho et al., bioRxiv, 2024.03.01.582751

FP-derived Shh is not required for the formation of the floor plate

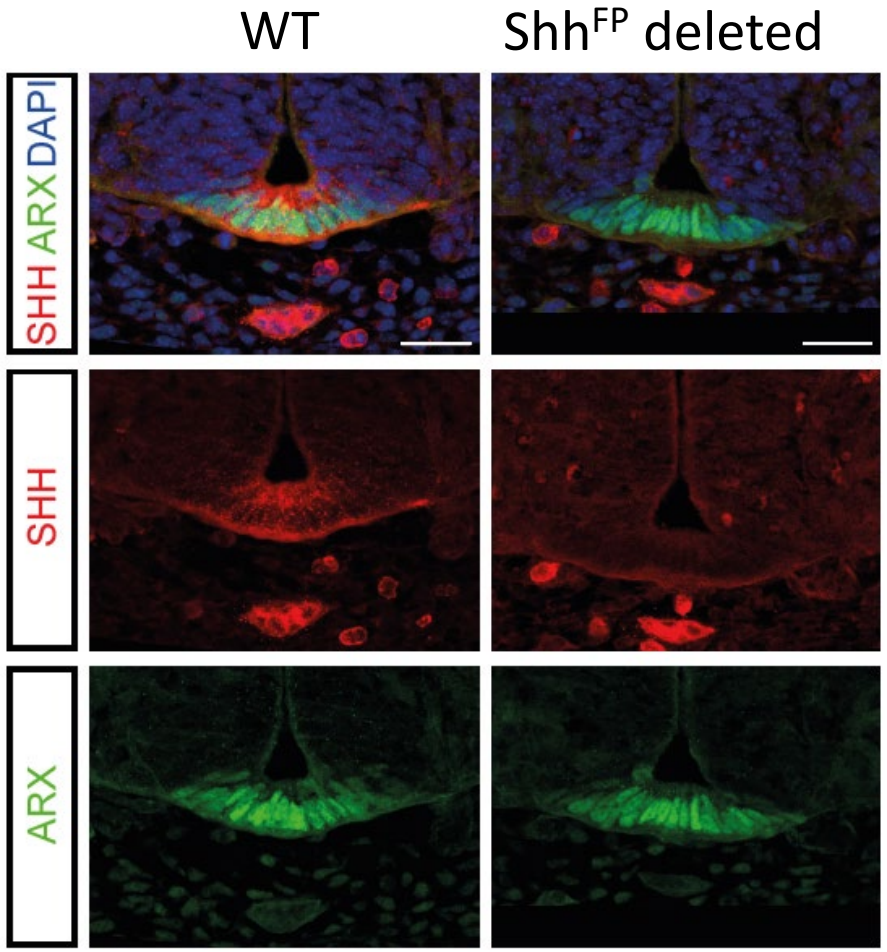

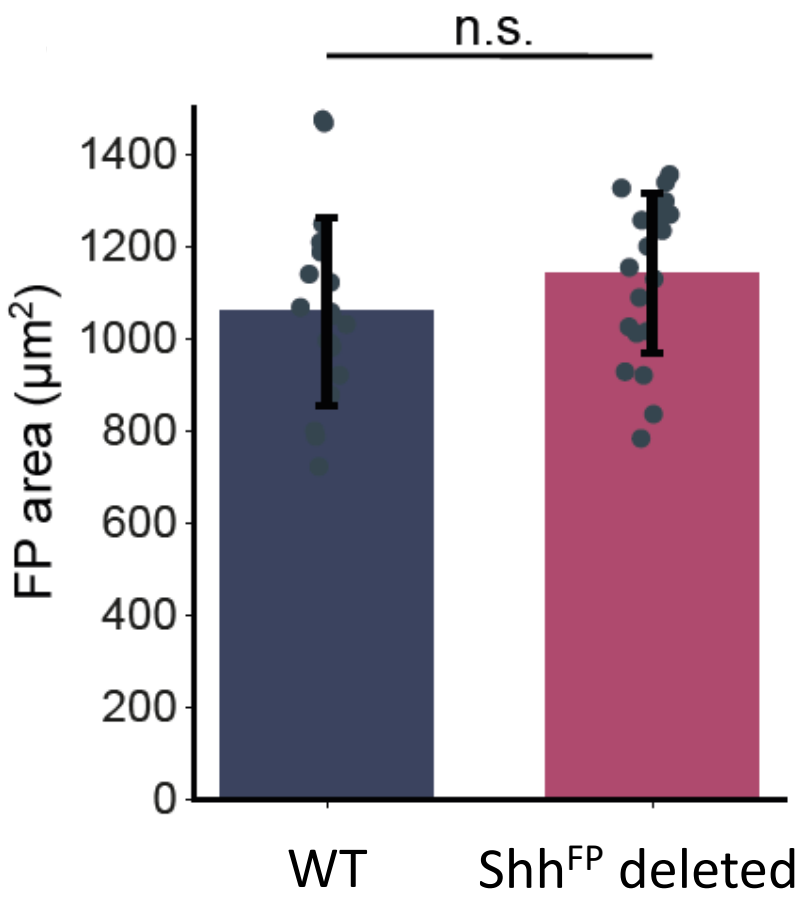

Ho et al., bioRxiv, 2024.03.01.582751

Early deletion of Shh results in a severe reduction of 85% of FP size

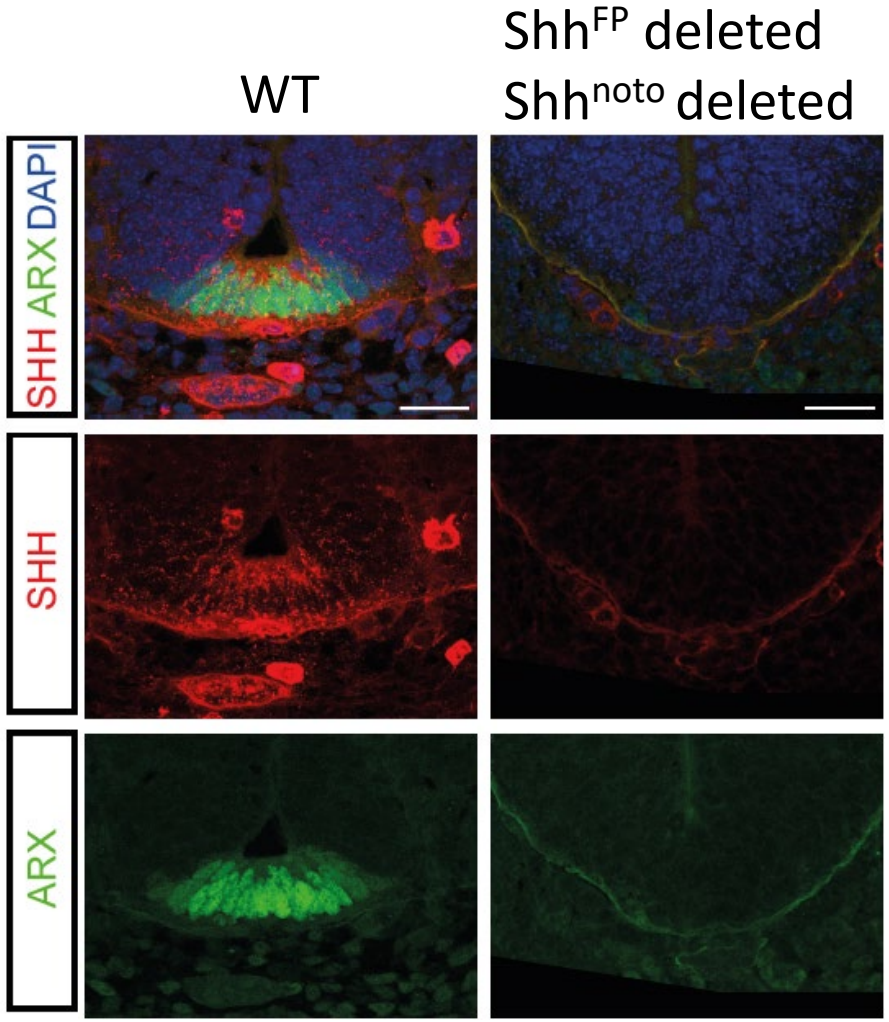

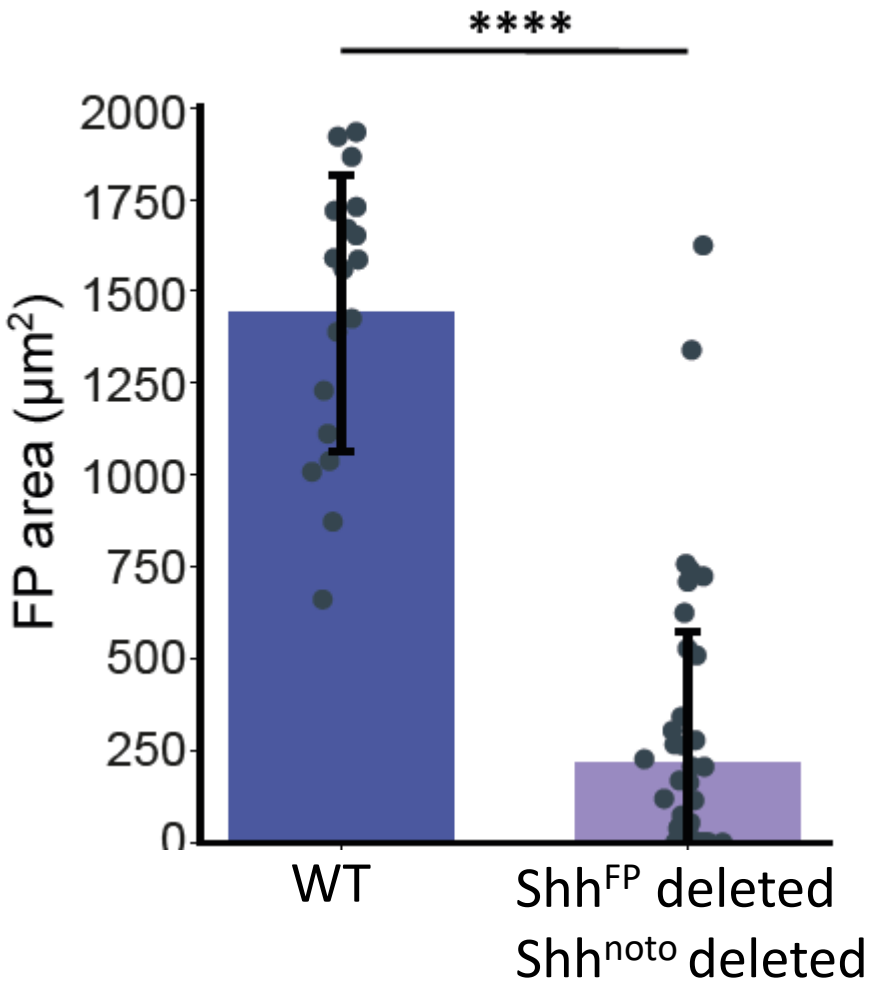

Ho et al., bioRxiv, 2024.03.01.582751

Late deletion of Shh does not alter FP size

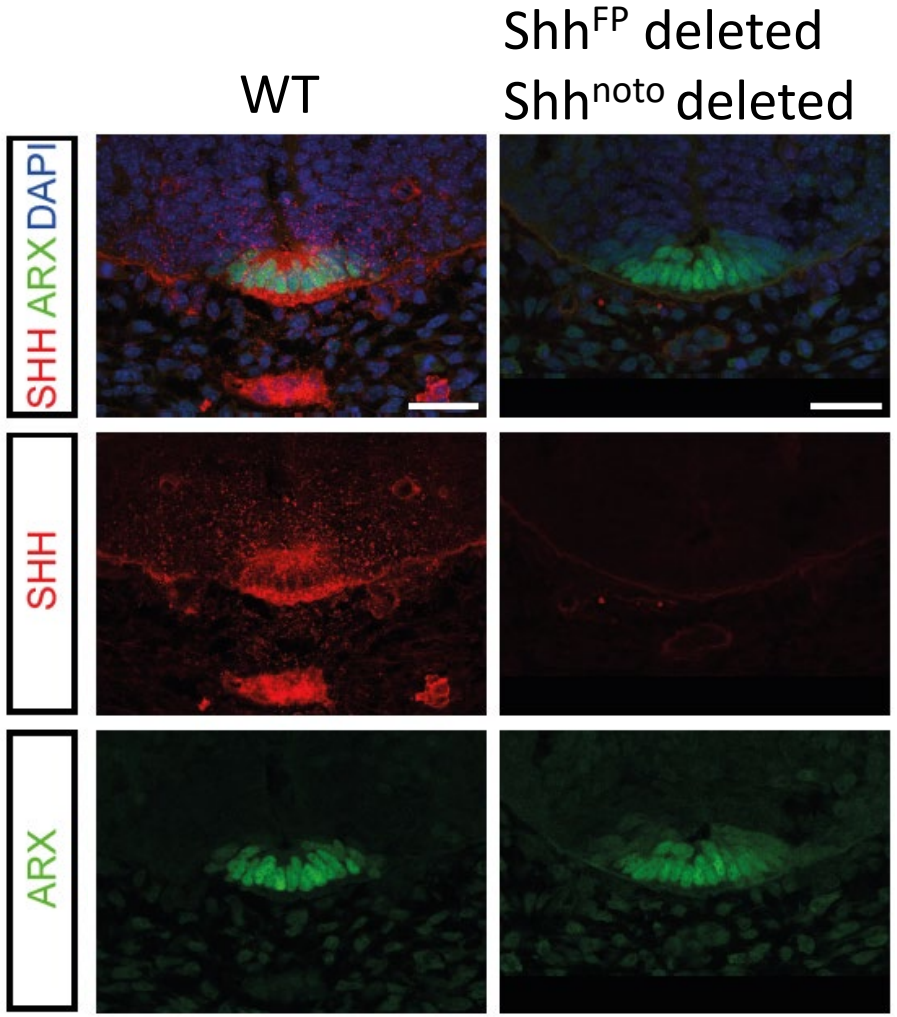

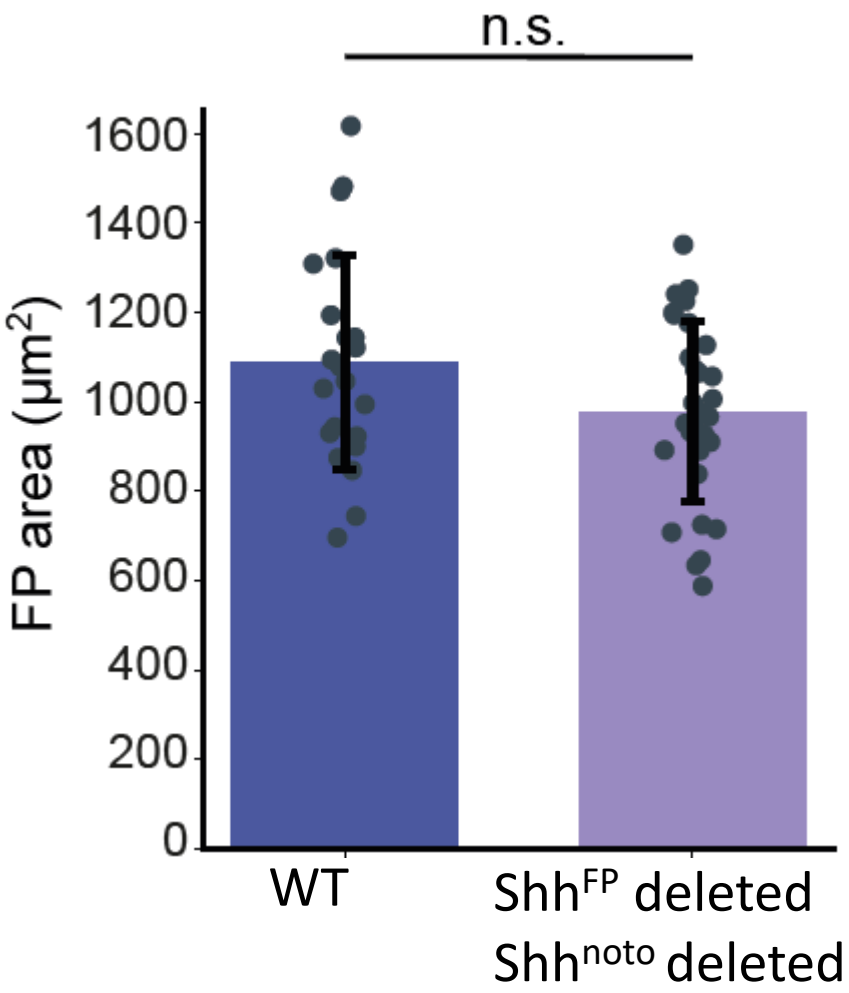

Ho et al., bioRxiv, 2024.03.01.582751

Research questions

- How are morphogens interpreted to result in precise and reproducible patterns?
- How is pattern formation affected by tissue mechanical properties, cellular dynamics, and growth?
- How is morphogen source formed in a growing tissue?
- What are conditions for emergence of stable patterns in tissues?

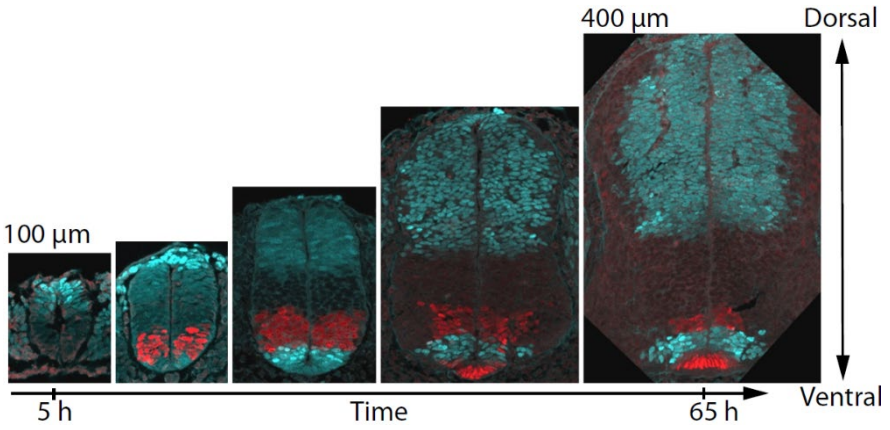

We explain the principles of gene expression pattern stabilization in systems of interacting, diffusible morphogens, with dynamically established source regions

PHYSICAL REVIEW LETTERS **130,** 098402 (2023)

Stability of Pattern Formation in Systems with Dynamic Source Regions

M. Majka,* R. D. J. G. Ho,† and M. Zagorski‡
Institute of Theoretical Physics and Mark Kac Center for Complex Systems Research, Jagiellonian University, Łojasiewicza 11, 30-348 Kraków, Poland

$$\partial_t \psi_i = D_i \partial_{xx} \psi_i - \gamma_i \psi_i + H_i \theta(F_i(\psi_1, \psi_2))$$

$$F_i(\psi_1, \psi_2) \simeq \epsilon_{ii} \psi_i + \epsilon_{ij} \psi_j - C_i$$

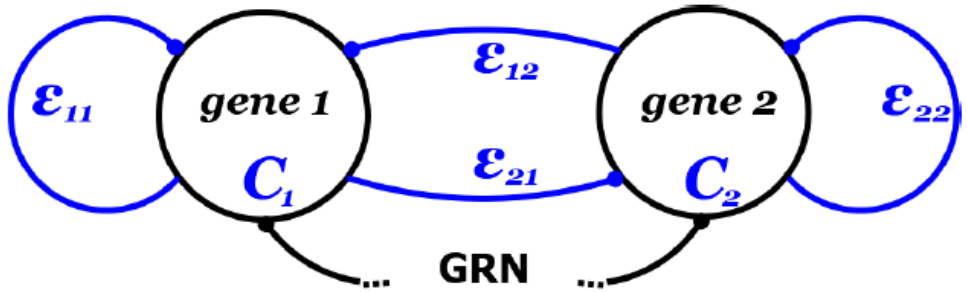

Majka et al., Physical Review Letters, 2023

Under specific conditions stable gene expression patterns (GEPs) are formed

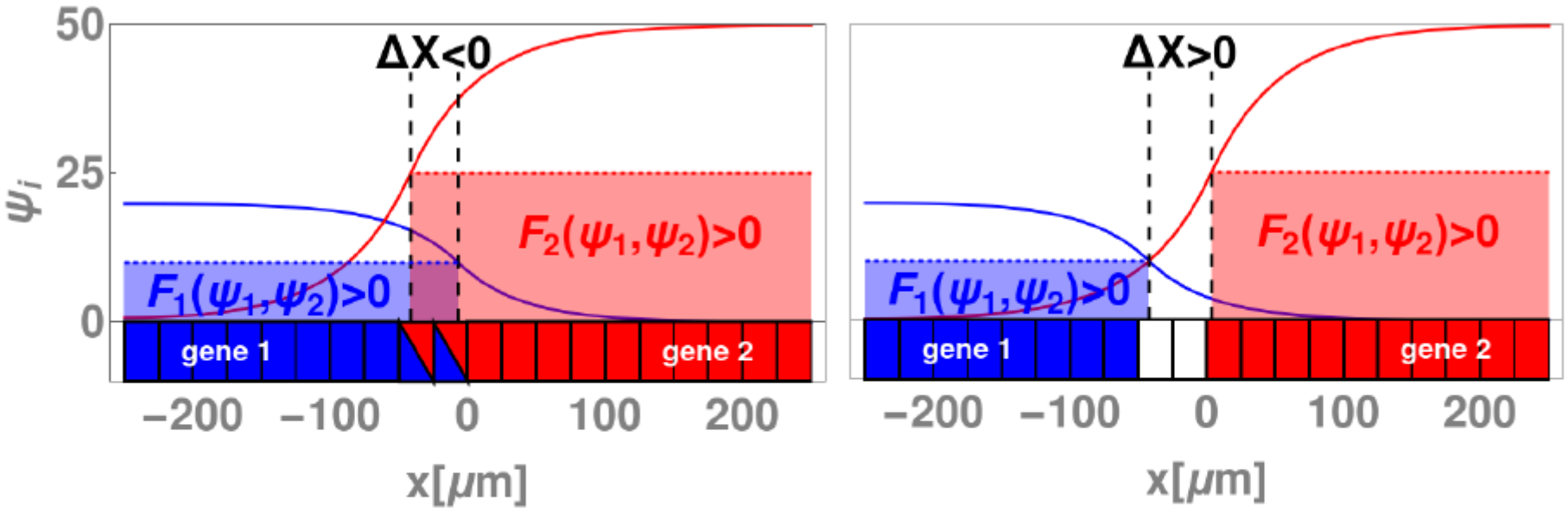

overlap = simultaneous gene expression or cell mixture (ΔX - precision)

gap = undifferentiated cells

Majka et al., Physical Review Letters, 2023

Indetermined GEP vs Travelling GEP vs Stable GEP

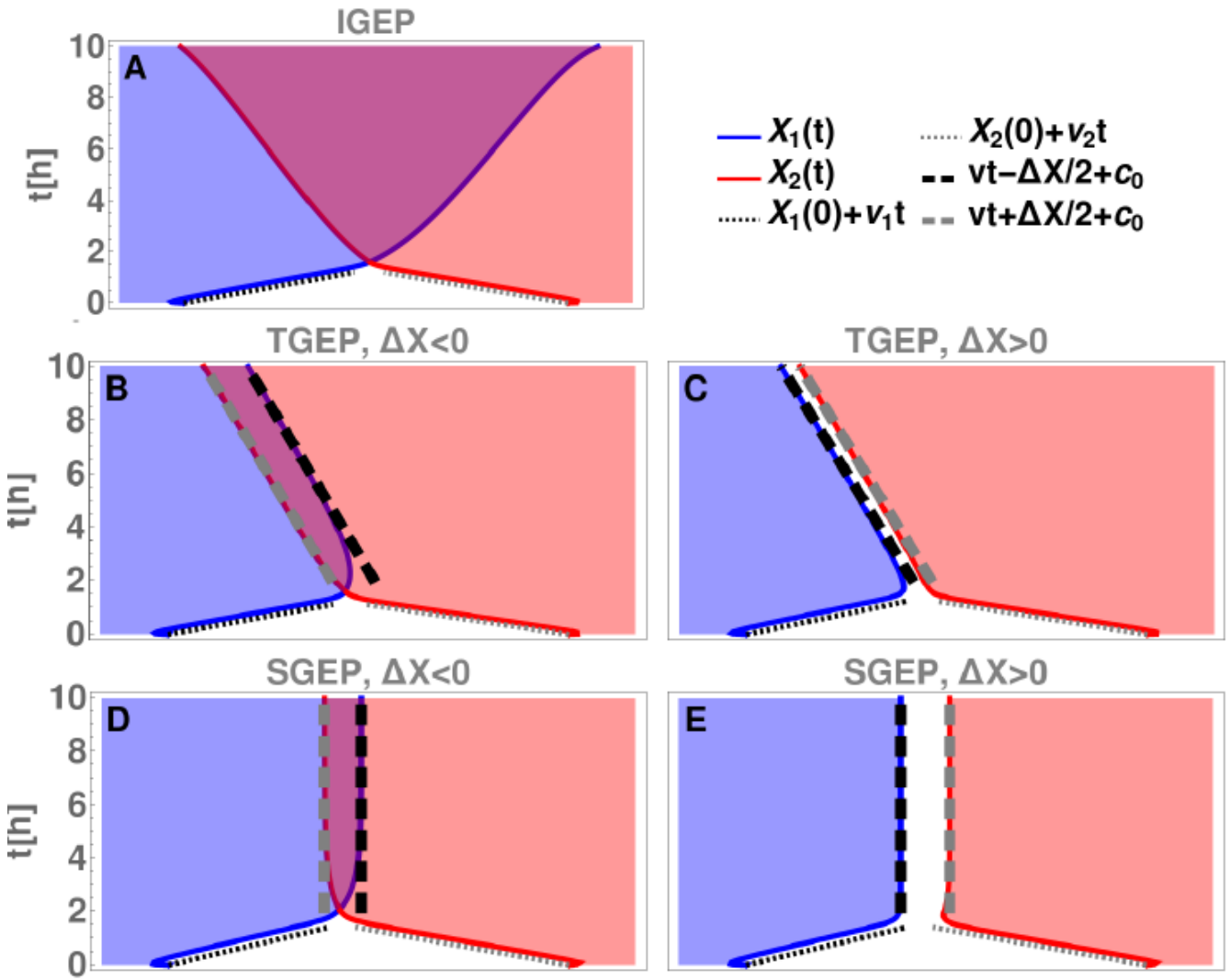

Majka et al., Physical Review Letters, 2023

GEP exhibit broad plateu of low-velocity drift

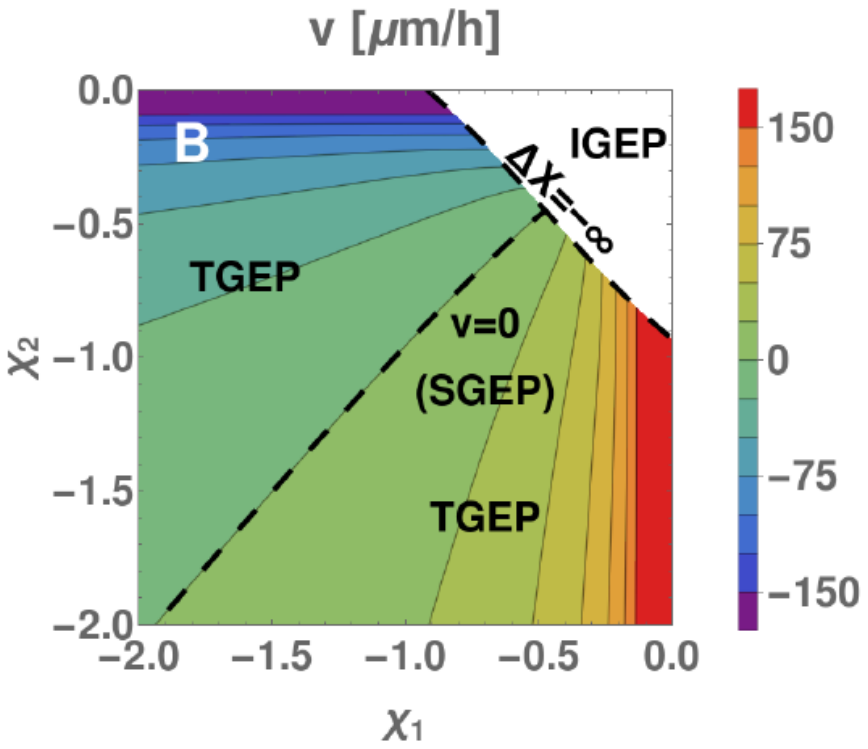

broad plateau of low-velocity drift, but $v = 0$ only for special combinations of χ_1 and χ_2

$\Rightarrow$ **stability requires fine-tuning of parameters**

$$\lambda_i = \sqrt{\frac{D_i}{\gamma_i}}, \qquad \tilde{\psi}_i = \frac{H_i}{\gamma_i}, \qquad S_i = \frac{2C_i}{\epsilon_{ii}\tilde{\psi}_i}, \qquad \chi_i = \frac{\epsilon_{ij}\tilde{\psi}_j}{\epsilon_{ii}\tilde{\psi}_i}$$

Majka et al., Physical Review Letters, 2023

Gap gene expression pattern exhibits shifts in the posterior part

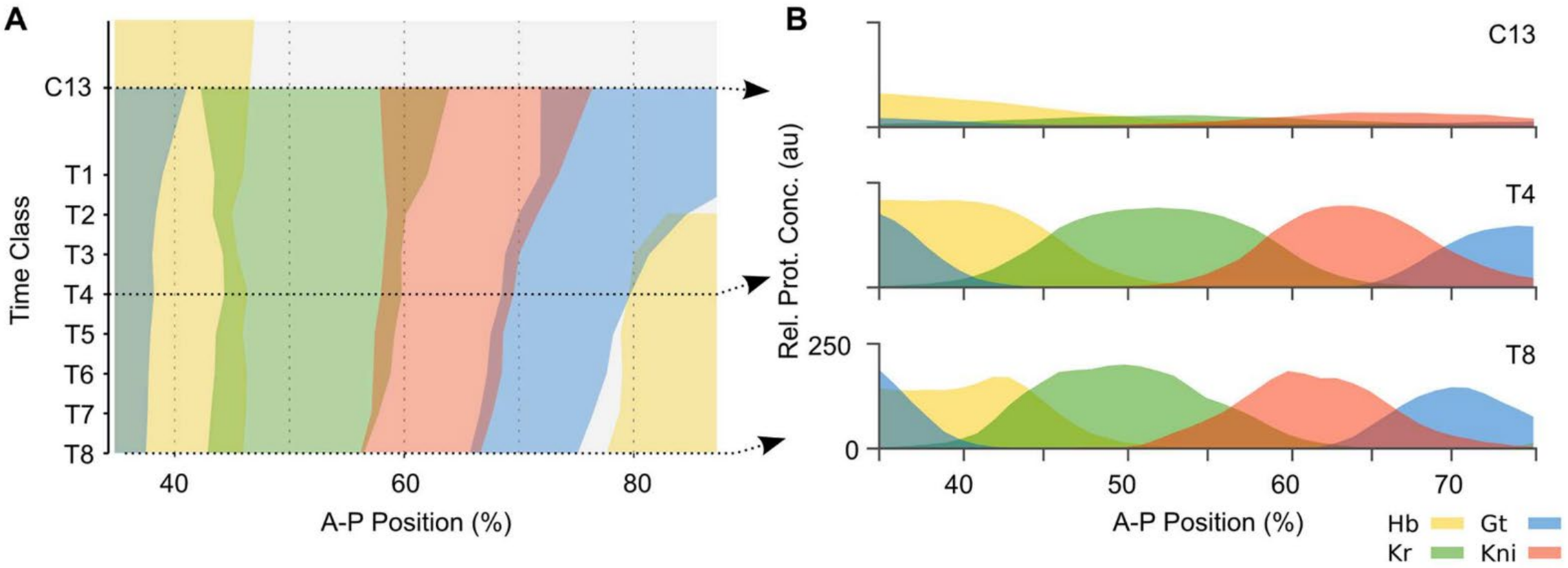

Estimated velocity of Kni-Gt is 17.5 µm over 44 minutes, that corresponds to v = 24 µm/h.

Verd et al., PLOS Comp Bio, 2017

Stability conditions for two-gene network motifs encountered in developmental GRNs

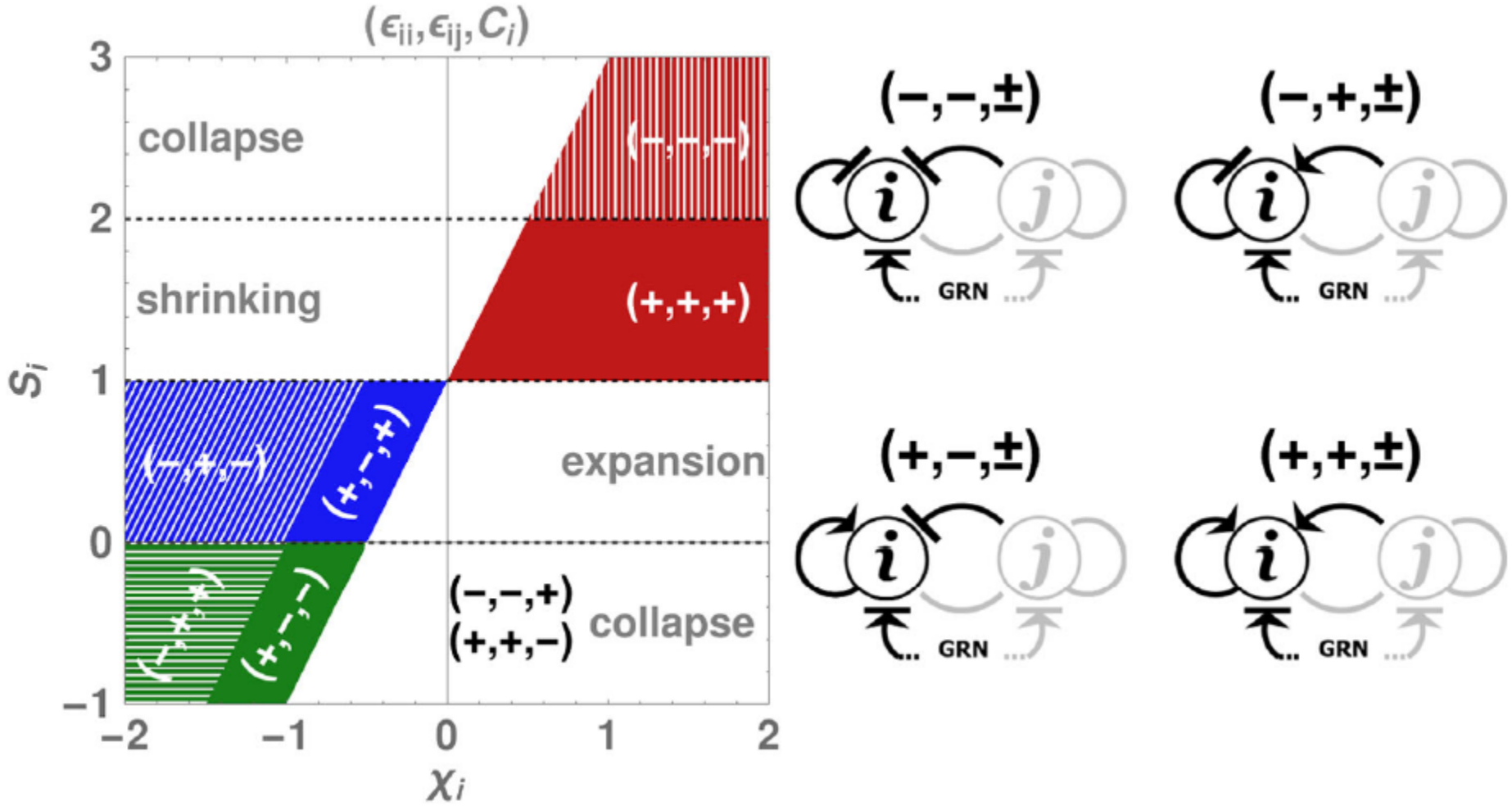

Majka et al., Physical Review Letters, 2023

Stable developmental patterns of gene expression without morphogen gradients in Drosophila-like system

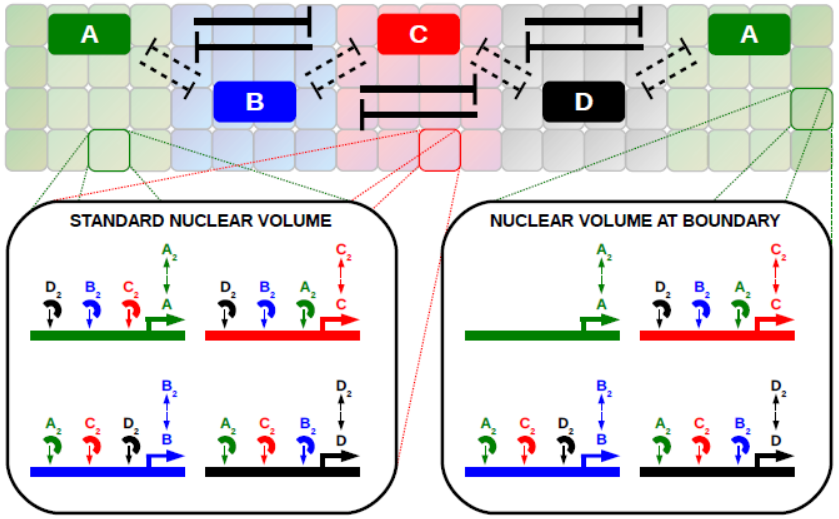

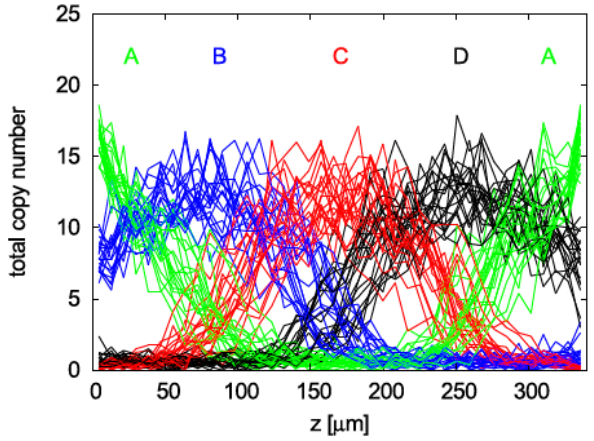

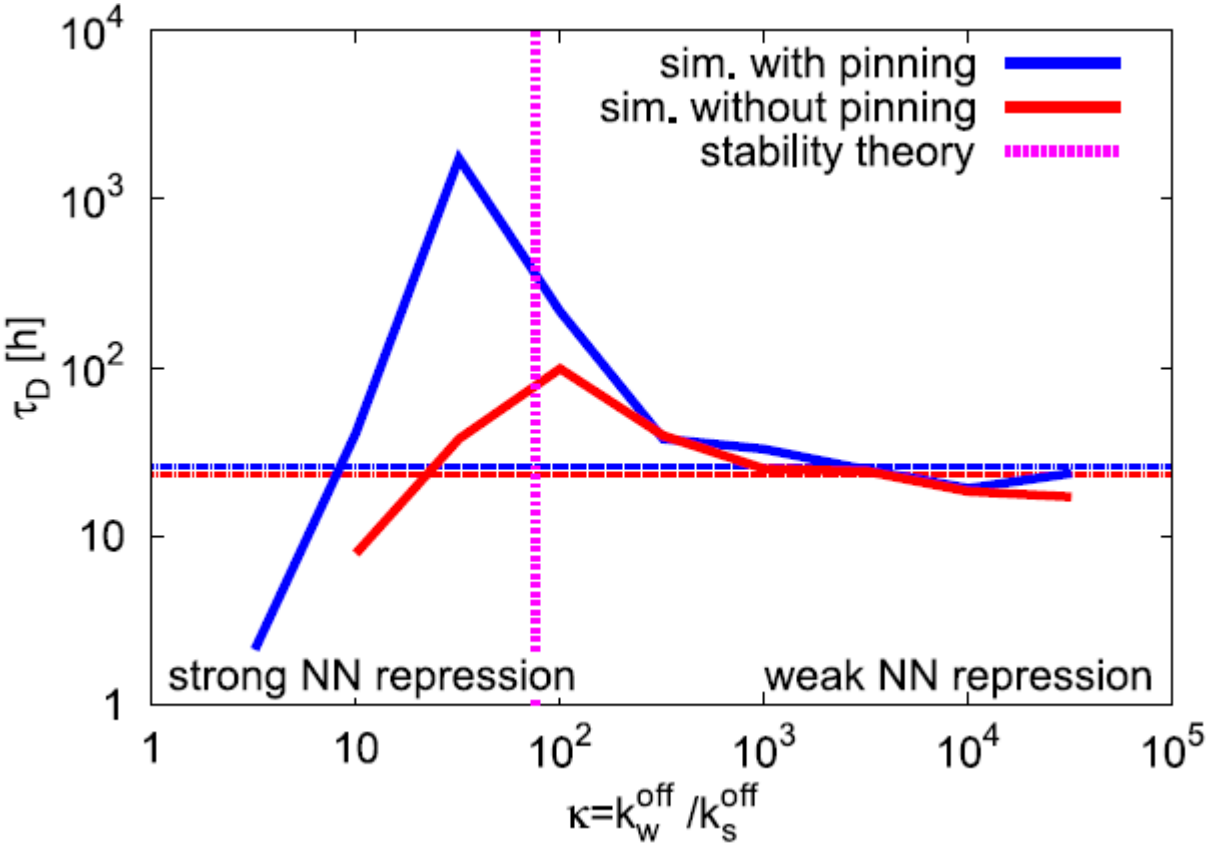

M Majka, NB Becker, PR ten Wolde, M Zagorski, TR Sokolowski,, *arXiv*: 2306.00537

Summary (part 1)

- Morphogens are interpreted close to optimal limit of processing of noisy signals

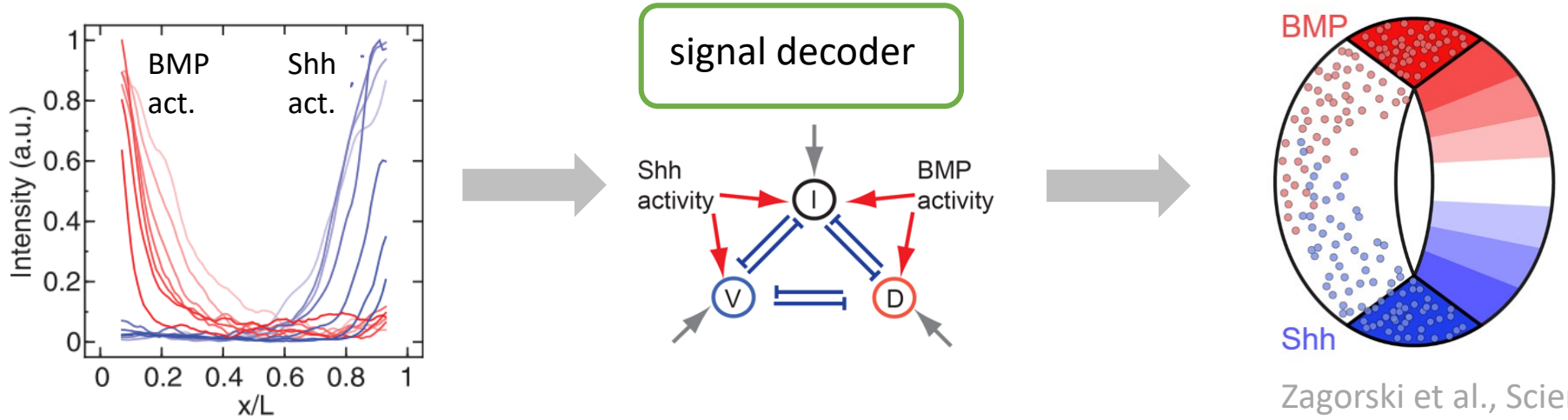

Zagorski et al., Science, 2017

- Patterning is affected by growth, cellular dynamics, and tissue properties

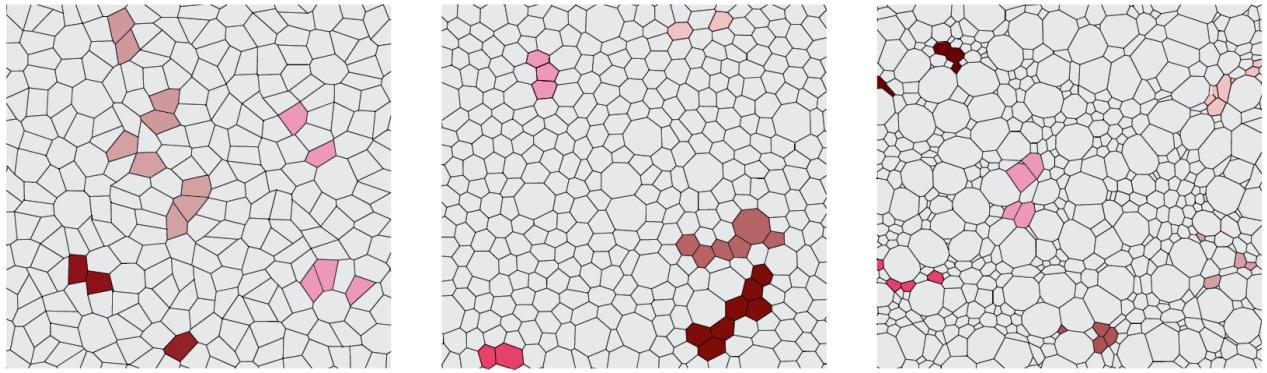

Bocanegra-Moreno et al., Nature Physics, 2023

Summary (part 2)

- Initial FP size is determined by GRN strengths, and later on it scales with the tissue size

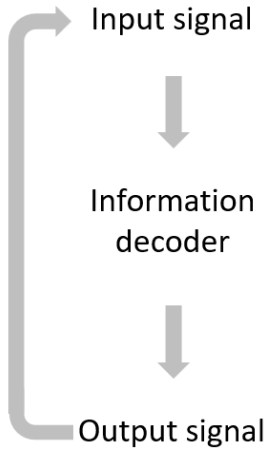

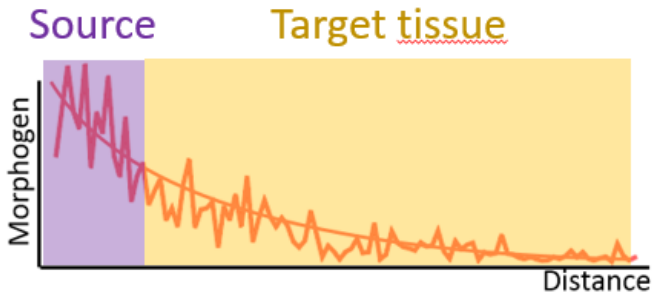

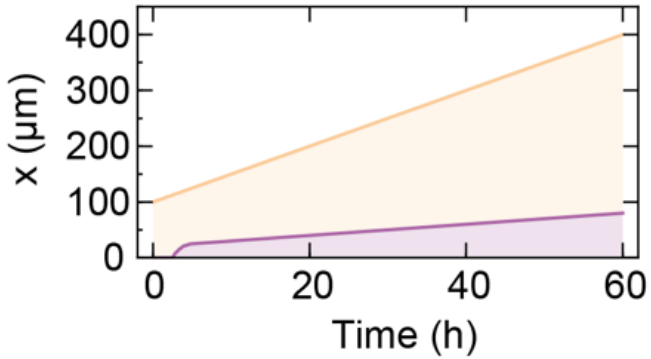

Ho et al., bioRxiv, 2024.03.01.582751

- Stable patterns of interacting domains emerge under specific conditions

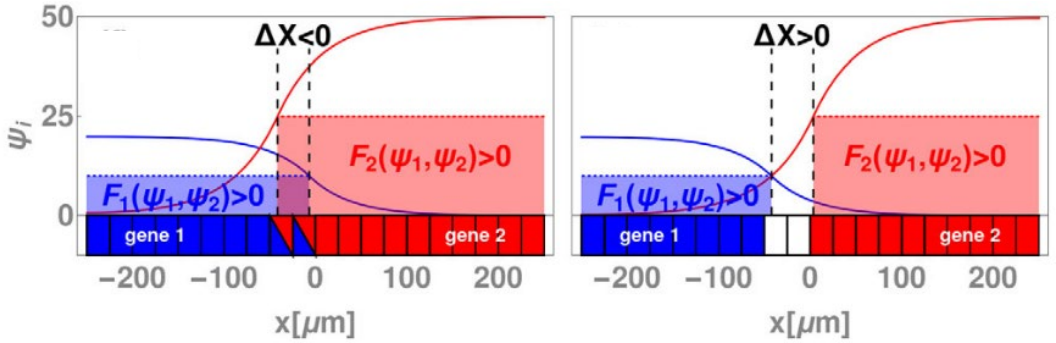

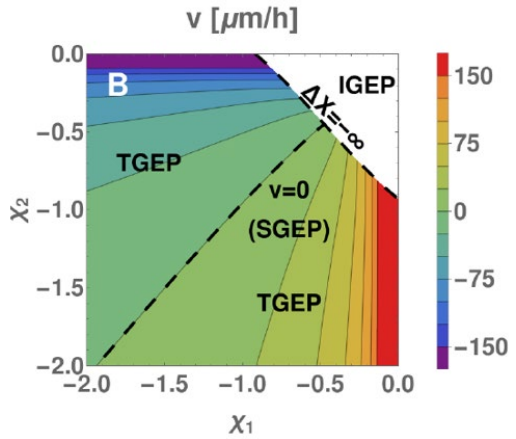

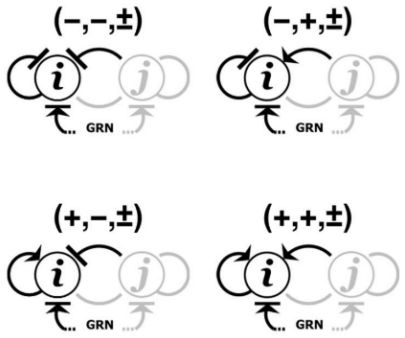

Majka et al., PRL, 2023

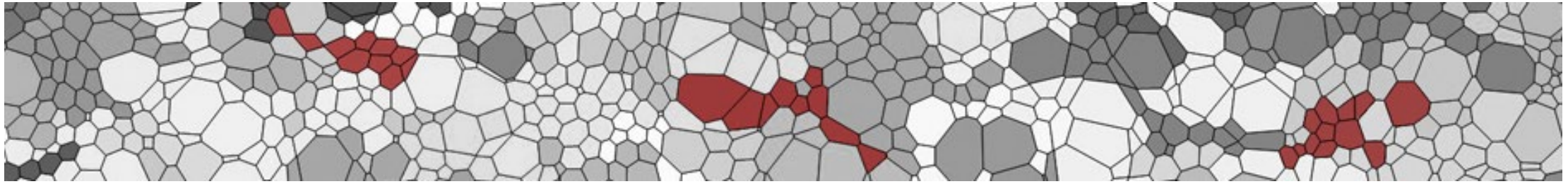

@zagorskigroup.com

IST Austria
Laura Bocanegra
Edouard Hannezo
Anna Kicheva
Kasumi Kishi
Amrita Singh
Gašper Tkačik

University of Cologne
Tobias Bollenbach

Francis Crick Institute
James Briscoe

AMOLF
Pieter Rein ten Wolde

FIAS, Germany
Thomas Sokolowski

GCRC Heidelberg
Nils Becker

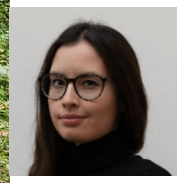

Group members (current and past)

Richard Ho
Maciej Majka
Adela Staszowska
Tomasz Kuliński
Hélder Larraguível
Salar Ghasemi Nasab
Joanna Doliwa

Funding

The project is financed by the National Science Centre, Poland, no. 2021/42/E/NZ2/00188

The project is financed by the Polish National Agency for Academic Exchange

Ministry of Science and Higher Education
Republic of Poland

RESEARCH UNIVERSITY
EXCELLENCE INITIATIVE

PhD research scholarship

JOIN US

JAGIELLONIAN UNIVERSITY
IN KRAKÓW

National
Science
Centre
Poland

RESEARCH
UNIVERSITY
EXCELLENCE INITIATIVE

http://zagorskigroup.com/